CHAPTER 4

Results and Discussion: Extraction of Phenols

CHAPTER 4

RESULTS AND DISCUSSION: EXTRACTION OF PHENOLS

4.1 INTRODUCTION

Systematic investigations on extraction of phenols using ELMs were conducted in this Study. Extraction of phenols is typical representative of Type I transport. Four phenols namely phenol, o-cresol, p-cresol and o-chlorophenol were extracted individually from their aqueous solutions using ELMs prepared using kerosene as the membrane phase, Span 80 as the surfactant (emulsifier) and NaOH as the stripping reagent in the inner phase of the W/O emulsions. The emulsions were prepared by the procedure described in Chapter 3. The W/O emulsions were characterized by internal phase droplet size distribution, specific gravity, viscosity and the interfacial tension between the emulsion phase and the external aqueous phase containing the solute.

Experiments were carried out to study the effects of various emulsion composition variables and process variables on the extraction of phenols. Emulsion composition variables studied included the effects of internal phase fraction (ϕ), surfactant concentration (W_{surf}) and NaOH concentration in the internal phase (C_{io}). Process variables studied included stirring speed, Treat ratio (TR) of emulsion to feed and the initial solute concentration in the feed. Selected runs were carried out to assess the effect of temperature and also other membrane materials on extraction. A set of extraction runs were also carried out using ELMs prepared with a proprietary surfactant.

All extraction results are presented as plots of solute concentration (normalized, using initial solute concentration) versus sampling time i.e. "C_e/C_{eo} versus t". All experimental runs were carried out for duration of thirty minutes inspite of the fact that in many runs the extraction was over in a time period of just 15 minutes.

Repeating certain crucial runs assessed reproducibility of the results. All data Tables for the various extraction runs are reported in Appendices B to E.

4.2 CHARACTERIZATION OF EXTRACTING EMULSIONS

4.2.1 Internal drop size distribution of W/O emulsion

The size distribution of inner phase droplets is the most important parameter in characterizing any emulsion. Two emulsions may have the same average drop diameter and yet exhibit quite dissimilar behaviour because of differences in their distribution of diameters. Stability and resistance to creaming, rheology, chemical reactivity and physiological efficiency are few of the phenomena influenced by both relative size and size distribution (Orr 1983)

Emulsions are seldom composed of droplets of uniform sizes; if droplet size exhibits a wide statistical distribution the emulsion is polydisperse in contrast to monodisperse systems. The ideal size depends on available methods of preparation and most emulsions are polydisperse. If droplet division takes place according to a geometrical series, a monodisperse system is approached. Polydisperse systems are due to formation of smaller fragments. Droplets begin to make close contact when internal phase volume of the emulsion ranges from 60-70 %; close contact begins to affect some of their sensible properties like viscosity, surface tension etc.

Internal droplet sizes of emulsions prepared using kerosene as the oil phase, Span 80 as the emulsifier and NaOH as the internal phase were measured as described in Chapter 3.3. Measurements were usually made at 600 magnification. However, when droplet sizes were very small, a magnification of 1500 was used. Changes in the internal drop size distribution of the emulsion with a change in internal volume fraction (ϕ), and also internal reagent concentration (C_{io}) were measured and the results are presented as histograms in Fig. 4.1.

It is seen from Fig. 4.1 (a) when the volume fraction (ϕ) is 0.45 almost 50 % of the droplets happen to be of 1.568 μm in diameter and 35 % are of 3.136 μm in diameter, and just 15 % droplets are of larger sizes. Increasing ϕ to 0.6 changes the drop sizes as well as size distribution as seen in Fig. 4.1(b). In this case it was observed that 60 % of droplets were having 3.33 μm diameter while 13 % of size 6.66 μm and 20 % of 9.99 μm in diameter. Further increasing ϕ to 0.69 changes the distribution again as seen in Fig. 4.1 (c), one could find that the dominant droplet diameters in this case were 6.66 μm, 9.99 μm and 13.32 μm having frequencies of 36 %, 28 % and 20 % respectively. The Sauter mean diameters calculated from the droplet size distribution are shown below:

Volume fraction (ϕ)	0.45	0.60	0.69
Sauter mean diameter, d_{32} (μm)	3.97	11.84	14.26

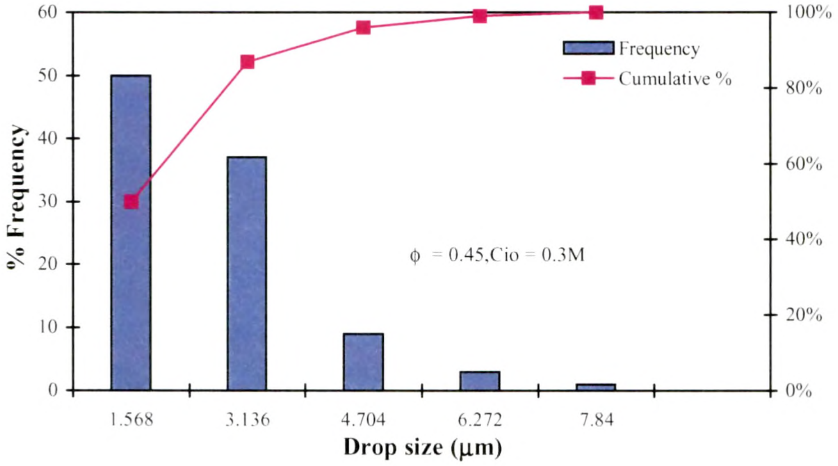

Fig 4.1(a): Internal drop size distribution at $\phi = 0.45$ ($C_{io} = 0.3M$, $W_{surf} = 3\%$)

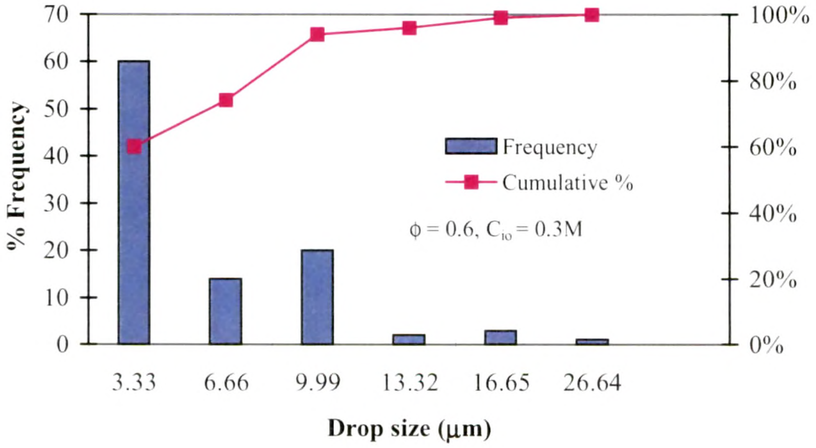

Fig 4.1(b): Internal drop size distribution at $\phi = 0.6$ ($C_{io} = 0.3M$, $W_{surf} = 3\%$)

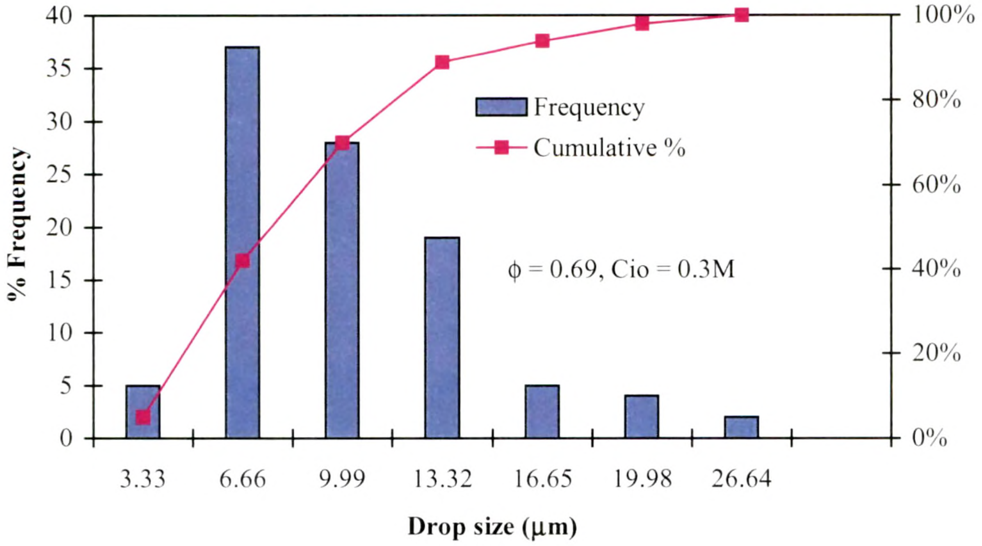

Fig 4.1(c): Internal drop size distribution at $\phi = 0.69$ ($C_{io} = 0.3M$, $W_{surf} = 3\%$)

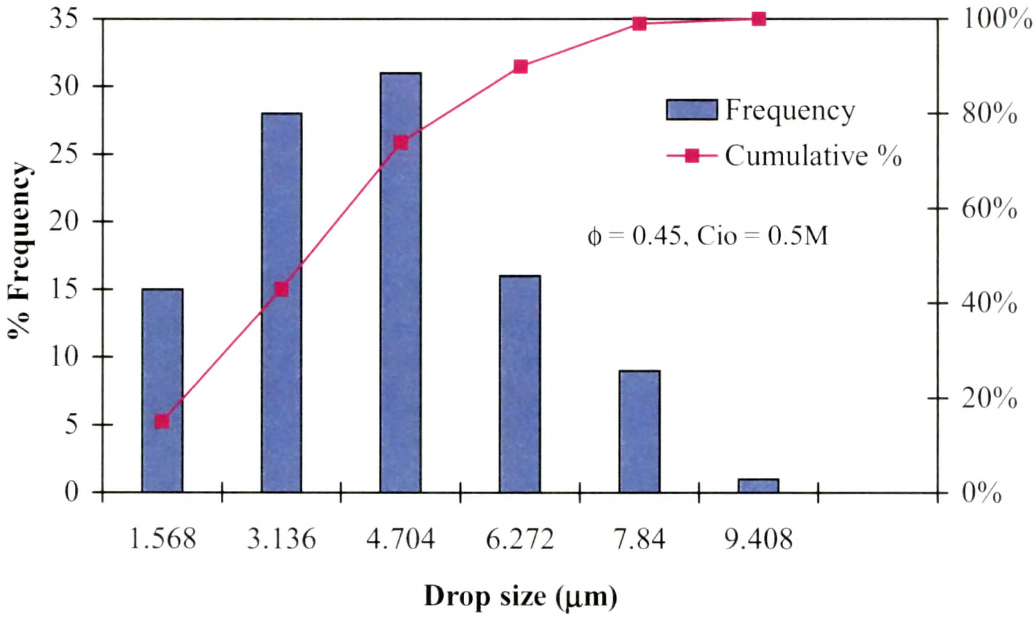

Fig 4.1(d): Internal drop size distribution at $\phi = 0.45$, and $C_{io} = 0.5$ M($W_{surf} = 3\%$)

Fig. 4.2 shows the photomicrographs of internal droplets at ϕ values of 0.45, 0.5 and 0.69 respectively. One can clearly distinguish the changing internal droplet size with increasing ϕ. Interestingly, the largest drop size observed in this work is also shown in Fig. 4.2 and was an ellipsoid shaped droplet having major axis of 33.3 μm and minor axis of 26.4 μm. Such nonspherical drops were observed only for values of $\phi = 0.69$. Literature (Morrison and Ross, 2002) suggests that, above a volume concentration of about 70%, the properties of an emulsion either becomes discontinuous (phase

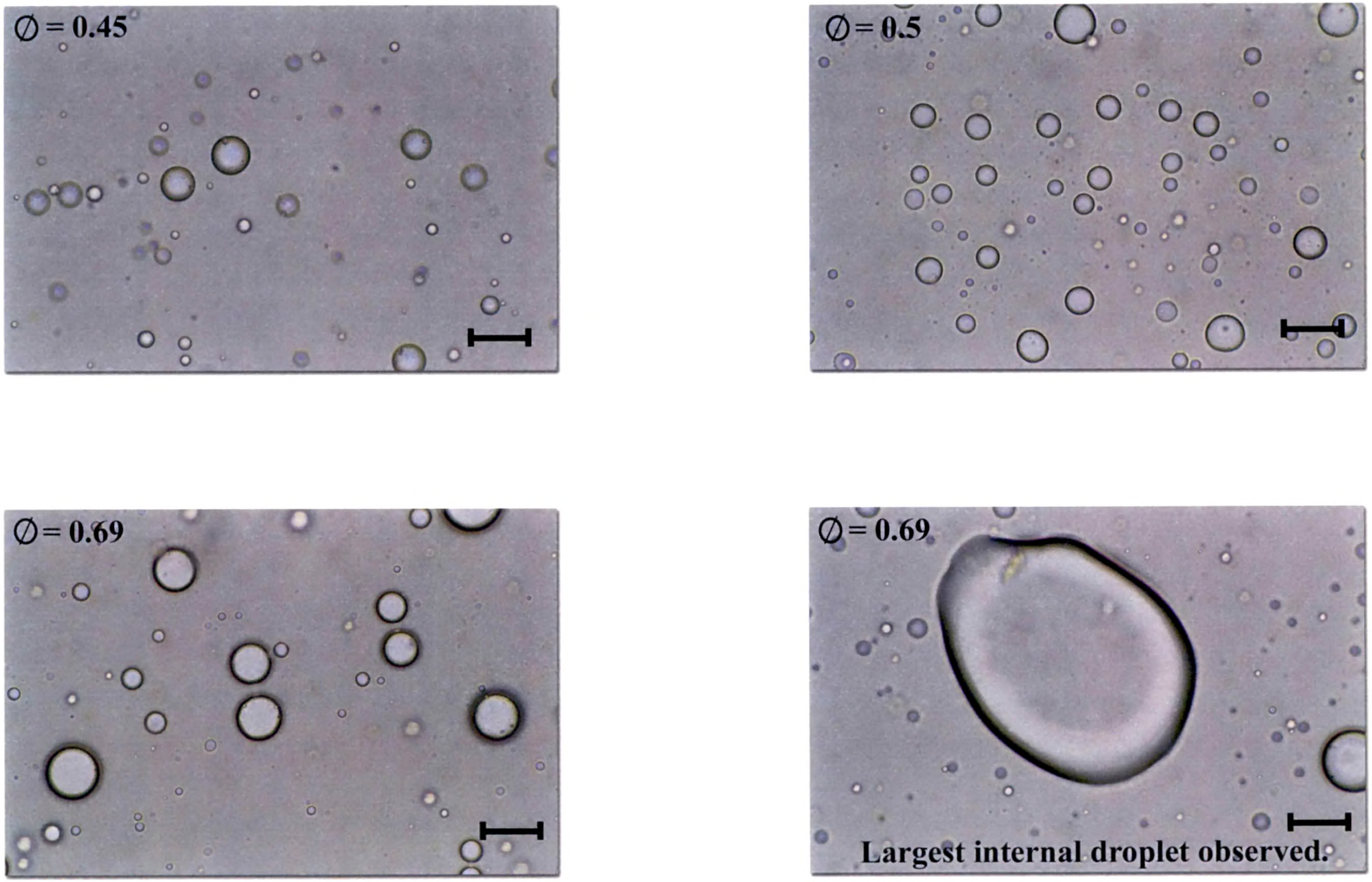

Fig. 4.2: Photomicrographs of internal phase droplets at different Ø (Span 80=3%, Cio=0.3M, Bar = 10μm)

inversion) or remain continuous with the production of deformed droplets in contact; perhaps what was observed was an onset of the second phenomena.

Change in internal drop size distribution with increasing NaOH concentration in the inner phase (C_{io}) is shown in Fig. 4.1(d). The emulsion studied had internal phase fraction $\phi = 0.45$ with $C_{io} = 0.5M$. These results could be contrasted with Fig. 4.1(a) that reports the drop size distribution data for an emulsion having $\phi = 0.45$ with $C_{io} = 0.3$ M. It could be clearly made out, from Fig. 4.1(d), that the internal droplet size of the emulsion showed a definite increase with increase in C_{io}. When $C_{io} = 0.3$ M almost 50 % of the droplets happened to be of 1.568 μm in diameter and 35 % were of 3.136 μm in diameter with the value of $d_{32} = 3.97$ μm while when C_{io} was increased to 0.5 M only 15% of droplets happened to be of 1.568 μm in diameter, 28 % droplets were of 3.136 μm, 32 % are of 4.7 μm and 16 % were of 6.27 μm diameter respectively, this distribution lead to value of $d_{32} = 5.907$ μm.

Droplet size distributions for $C_{io} = 0.15$ M were also evaluated. However, it was not possible to precisely measure the drop size distribution microscopically because a large number of very small size droplets existing in the microscopic field. Hence, the droplet size distribution of these emulsions was measured using Malvern 2000 particle size analyzer. The results are listed as Malvern output in Appendix A. The Sauter mean diameters calculated for droplet size distributions with changing internal phase concentrations at $\phi = 0.45$ are listed below:

Internal phase concentration, C_{io} (M)	0.15	0.3	0.5
Sauter mean diameter, μm	2.844	3.97	5.907

Reproducibility of results, particularly with unstable dispersed systems such as emulsions, is difficult to achieve. However, it is interesting to note that microscopic observation of inner phase of emulsion having $\phi = 0.45$, $C_{io} = 0.3$ M resulted in values of $d_{32} = 3.97$ μm, while emulsion having the same composition and prepared under identical conditions, but drop sizes determined using Malvern 2000, resulted in values of $d_{32} = 3.998$ μm. A close fit observed not only confirmed the reproducibility of the results but also assured that more or less the same size distributions were returned every time the emulsion was prepared using methodology discussed in Chapter 3.

4.2.2 *Specific gravity of emulsions*

The specific gravities of emulsions, as measured at 30 ± 1° C are reported in Table 4.1. These emulsions were prepared using kerosene as membrane phase (specific gravity 0.8084 at 30°C) Span 80 as surfactant and NaOH as the internal phase.

In the range of parametric variations studied in this work, the only factor that brings about a change in specific gravity is the internal phase fraction ϕ. Changes in surfactant concentration W_{surf} (expressed as wt % of oil phase) does not make any significant change in the specific gravity of the emulsion nor does internal phase NaOH concentration C_{io} induce any change in the specific gravity of the emulsion

Table 4.1:Effect of emulsion composition on specific gravity of emulsions

S.No	Variation	ϕ	C_{io} (M)	W_{surf} wt %	Specific gravity
1	ϕ	0.40	0.30	3 %	0.8985
2		0.45	0.30	3 %	0.9075
3		0.50	0.30	3 %	0.9113
4		0.55	0.30	3 %	0.9260
5		0.60	0.30	3 %	0.9339
6		0.69	0.30	3 %	0.9420
7	C_{io} variation	0.45	0.15	3 %	0.9044
8		0.45	0.50	3 %	0.9106
9	C_{io} variation	0.50	0.15	3 %	0.9112
10		0.50	0.50	3 %	0.9135
11	W_{surf} variation	0.45	0.30	1 %	0.9070
12		0.45	0.30	4.7 %	0.9075
13		0.50	0.30	1 %	0.9112
14		0.50	0.30	4.7 %	0.9168

4.2.3 *Rheological properties of emulsions*

Information about the rheological properties of the extracting W/O emulsions enables one to optimize the process of preparation of these emulsions. Practical emulsions are never monodisperse with reference to drop sizes and droplet size distribution influences the rheological properties. Emulsions with a low content of dispersed phase

($\phi < 0.1$) are Newtonian fluids. In very dilute emulsions, viscosity increases linearly as ϕ increases, with more concentrated emulsions ϕ exerts a greater influence and viscosity changes from Newtonian to non-Newtonian. The non-Newtonian character is initially pseudoplastic but in very concentrated systems may become plastic and exhibit viscoelasticity.

Viscosity was determined using Cone and Plate rheometer as described in Chapter 3. The emulsions showed a shear thinning non-Newtonian behaviour. Effect of surfactant concentration W_{surf}, internal phase NaOH concentration C_{io}, and internal volume fraction ϕ on the viscosity of W/O emulsions were investigated.

Results indicate that the surfactant concentration W_{surf} in the operating range of this work did not affect the viscosity of the W/O emulsion. It was observed that for emulsions having $\phi = 0.45$ and $C_{io} = 0.3$ M NaOH, prepared with Span 80 concentrations of 1%, 3%, and 4.7 % wt, registered viscosities of 13.32 mPa.s, 13.32 mPa.s and 13.50 mPa.s respectively at shear rates of 38.4 s^{-1} at 30°C.

4.2.3.1 Effect of ϕ on η

Table 4.2 shows the viscosities measured for emulsions having different internal volume fractions (ϕ) that contained only water in its internal phase (i.e $C_{io} = 0$). These data were obtained at different shear rates and are plotted in Fig. 4.3.

Table 4.2: Effect of ϕ on viscosity (η) at different shear rates. ($C_{io} = 0$)

		Shear rate s^{-1}				
		38.4	57.6	76.8	96.0	115.2
S.No.	ϕ	η mPa.s				
1	0	1.56	1.56	1.56	1.56	1.56
2	0.45	17.82	15.20	13.62	12.67	12.18
3	0.50	22.14	19.00	17.40	16.41	15.80
4	0.60	59.03	51.51	47.99	45.49	43.93
5	0.64	98.38	85.74	78.22	72.94	69.10
6	0.69	440	---	---	---	---

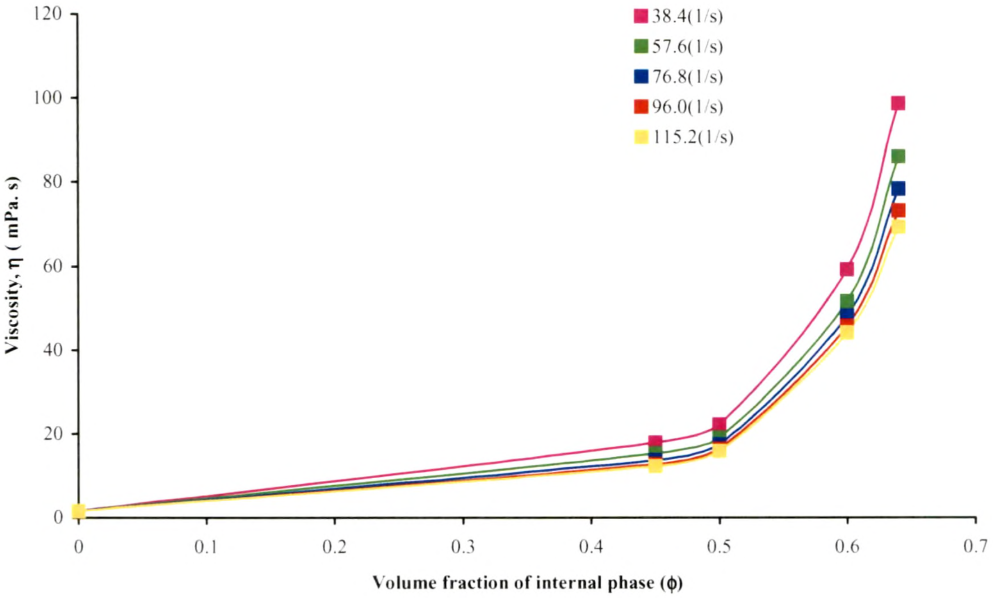

Fig. 4.3: Effect of ϕ on viscosity (η)at different shear rates (C_{io} = 0)

It is evident from Table 4.2 and Fig. 4.3 that η increases with increase in ϕ, this is a behavior that is general with emulsions (Becher 1983, Morrison and Ross 2002), In fact, all sensible properties increase with increase in ϕ. The significant point is the enormous increase in viscosity beyond ϕ = 0.64. Measurements could not be made at shear rates greater than 38.4 s^{-1} because limiting torque values of the instrument were reached.

Even though emulsions are seldom composed of droplets of uniform size, droplets begin to make close contact between 60 and 70 % internal volume concentration progressively and the random nature of dispersion gives way to more structured dispersions. It is important to note that the upper limit of ϕ i.e. ϕ_{max} is approximately 0.64 for random close packing of spheres and roughly 0.71 for the closest possible arrangement of spheres i.e. face centered cubic packing or hexagonal close packing (Hiemenz and Rajagopalan, 1997).

4.2.3.2 Effect of C_{io} on η

The objective of the above study was to get a base line in order to compare the rheological behaviour of extracting emulsions that have NaOH, a strong electrolyte in its internal phase. Experiments were conducted with emulsions containing 0.3 M NaOH in its internal phase and the effect of ϕ on η at different shear rates was studied. Table 4.3 shows this viscosity data measured for seven emulsions having different internal volume fractions (ϕ). This data is plotted in Fig. 4.4.

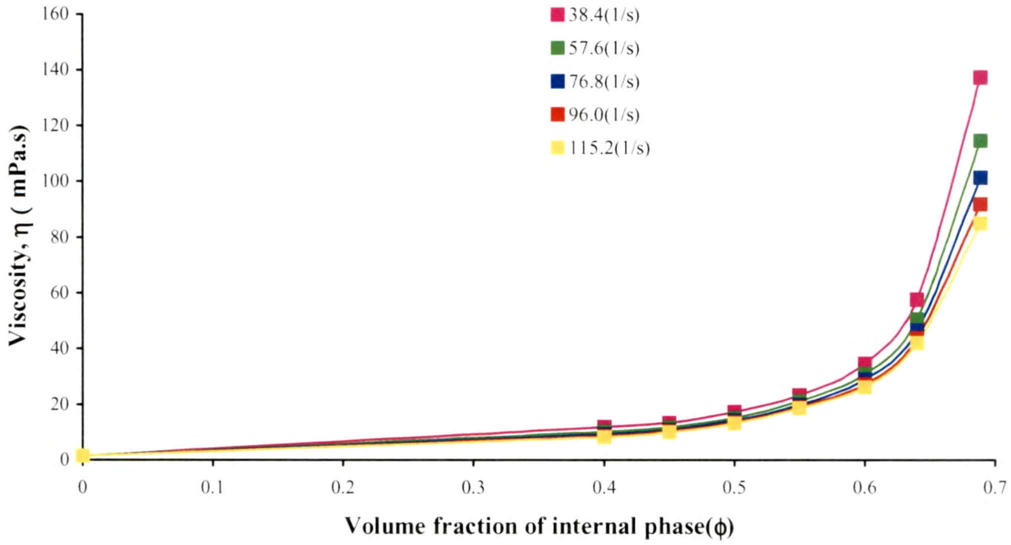

Fig. 4.4: Effect of ϕ on viscosity (η)at different shear rates (C_{io} = 0.3M)

Table 4.3:Effect of ϕ on η for emulsions containing NaOH in internal phase (C_{io} = 0.3 M).

		Shear rate s^{-1}				
		38.4	57.6	76.8	96.0	115.2
S.No.	ϕ	η mPa.s				
1	0	1.56	1.56	1.56	1.56	1.56
2	0.4	11.94	10.28	9.24	8.86	8.30
3	0.45	13.32	11.68	10.83	10.32	9.98
4	0.50	17.22	15.24	14.19	13.61	13.20
5	0.55	23.40	21.12	19.83	19.03	18.52
6	0.60	34.73	31.03	28.91	27.33	26.26
7	0.64	57.59	50.55	46.55	43.76	42.01
8	0.69	137.25	114.53	101.25	91.75	84.94

Table 4.3 and Fig. 4.4 show the effect of presence of NaOH in the emulsion on the values of η. It can be clearly made out that η decreases with the presence of NaOH in

the internal droplet phase of the emulsion, for all shear rates as well as with all values of the internal phase fraction.

In order to investigate this aspect, emulsions were prepared varying the internal phase NaOH concentration with different internal phase fractions and it was observed that presence of NaOH in the internal phase led to a decrease in η compared to the case where NaOH was not present. This behaviour is shown in Table 4.4 and Fig. 4.5

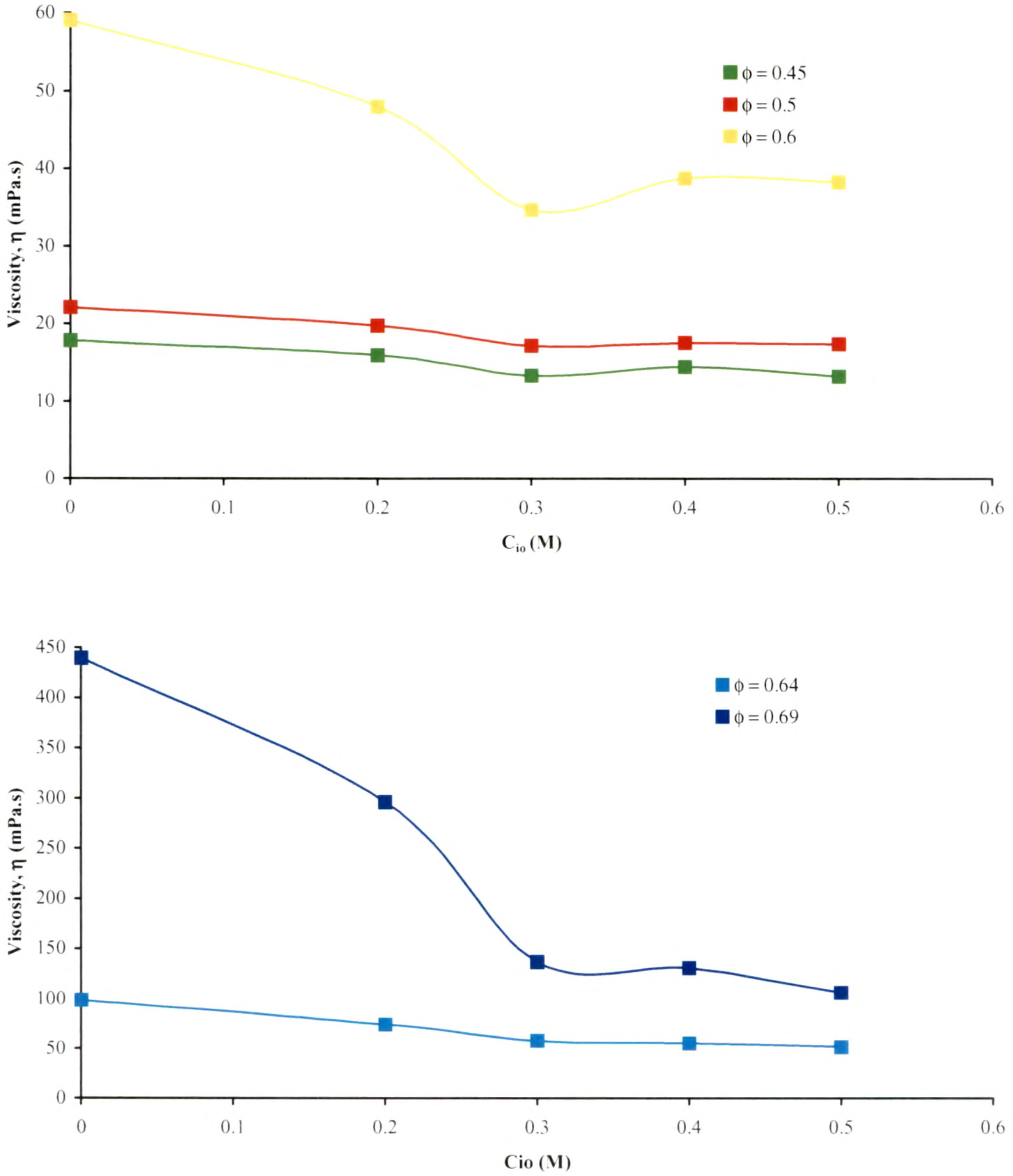

Fig. 4.5: Effect of Cio on η at different values of φ

Table 4.4: Effect of C_{io} on η at different values of ϕ

		ϕ				
		0.45	0.5	0.6	0.64	0.69
S.No.	C_{io}	η mPa.s at shear rates of 38.4 s^{-1}				
1	0	17.82	22.14	59.03	98.38	440
2	0.2	15.96	19.80	47.99	73.80	296.08
3	0.3	13.32	17.22	34.73	57.59	137.25
4	0.4	14.46	17.58	38.87	69.10	131.01
5	0.5	13.26	17.46	38.39	51.83	106.05

Influence of electrolytes present in the inner phase of W/O emulsions on rheological behaviour of such emulsions is not well chronicled. Sherman (1983) reported that hydration of the emulsifier layer adsorbed around the drops in an emulsion would influence the rheological properties. Addition of electrolytes alters the degree of hydration, the effective thickness of the hydrated adsorbed emulsifier layer decreasing as the electrolyte concentration increases. It is perhaps this reduction in effective thickness of the hydrated layer that contributes to the reduction in viscosity with an increase in NaOH concentration.

One remarkable feature that is observed in Fig. 4.5 is that when C_{io} is 0.3 M the η versus C_{io} plots pass through minima. This behaviour was exhibited by the emulsions having ϕ of 0.64 or lower, when $\phi = 0.69$ such behaviour was not observed. Without attempting to forward any reason for such behaviour in W/O emulsions; it is worthwhile to mention that Grüneisen in 1905 reported negative curvature at the dilute end of the viscosity-concentration curve for aqueous electrolyte solutions of 16 salts in water. The inflection of the curve was at about 0.3 mol/kg. Applebey (Horvath, 1985) also reported similar behaviour in 1910 and this behavior is known as the Grüneisen effect.

The Power Law model and the Bingham model could conveniently represent the rheological nature of the system. These models essentially differ in the way they treat the system. The Power Law model treats the system as a liquid like substance with some deviation of its properties from those of a Newtonian fluid, while the Bingham model treats the system as a solid-like substance with a yield point. The expressions for these two models are as below:

$$\text{Power Law model} \qquad \eta_{eff} = K\,\nu^{\,n-1}$$

Where ν is the shear rate (s^{-1}), K is the consistency index, n is the power law index

$$\text{Bingham model} \qquad \eta_{eff} = \eta_{pl} + P_y/\nu$$

Where η_{pl} is the plastic viscosity, P_y is yield strength

The Power Law model has a broader applicability because it is based on treatment of liquid like properties of disperse systems (Yurtov and Koroleva, 1996). Usually at high values of ϕ it makes the model inappropriate for description of η of concentrated W/O emulsions. However, such difficulties were not encountered in this work. Table 4.5 also lists the relevant values of model parameters and the quality of fit obtained using these two models. Since these models fitted the experimental data very well, the higher parameter models were not explored.

Table 4.5: Power law and Bingham parameters for the extracting emulsions

	Power law model			Bingham model		
ϕ	Consistency Index,(mPa.s)	Power law Index	% Fit	Plastic Viscosity (mPa.s)	Yield Stress (mN/m^2)	% Fit
0.4	40.3	0.66	99.1	6.43	2.16	99.6
0.45	34.4	0.74	99.0	8.3	1.93	99.9
0.50	41.2	0.76	99.0	11.2	2.32	99.9
0.55	50.7	0.79	99.3	16.0	2.87	99.7
0.60	91.3	0.73	99.8	23.1	4.7	98.7
0.64	163.4	0.71	99.3	34.2	9.25	99.4
0.689	674.2	0.56	99.9	58.5	31.5	98.6

4.2.4 *Interfacial Tension* (σ)

The interfacial tension between extracting emulsion and aqueous solution of phenols has a very important bearing on the globule sizes during extraction runs. The interfacial tensions were measured using the Du Nuoy apparatus. Initially, the interfacial tension between kerosene (the membrane material) and phenol containing water, kerosene with Span 80 and water containing phenol were measured. It was found that at 30°C the interfacial tension between kerosene and water containing phenol was 31.5 mN/m.

Changing the phenol concentration in the range of 200 mg/dm^3 to 800 mg/dm^3 did not alter this value. Similarly, changing over from phenol to o-cresol or p-cresol as solute in the aqueous phase also returned the same interfacial tension values. However, addition of 1 % (wt) Span 80 in the kerosene phase resulted in a substantial reduction in the interfacial tension that was recorded as 5 mN/m. Further addition of Span 80 up to 3 % (wt) of kerosene did not alter this value. This indicated that Span 80 concentration of 1 % itself was well above its critical micelle concentration.

The interfacial tension between phenolic water and W/O emulsions prepared with 3% Span 80 in the kerosene phase but having water in its internal phase recorded 5 mN/m when $\phi = 0.45$; 7.5 mN/m when $\phi = 0.6$ and 14 mN/m when $\phi = 0.69$. The increase in internal phase volume causes the interfacial film of surfactant molecules to expand more and more over a large number of water droplets resulting in a decrease in its density and compactness. It appears that this phenomenon is responsible for the increase in the interfacial tension values.

It was further noticed that even a small presence of NaOH in the internal phase (0.01 M) resulted in an increase in σ from 5 mN/m to 7.5 mN/m for emulsions having $\phi = 0.45$. Similar trend was observed for emulsions of other internal phase fractions. Data obtained for σ between emulsion and phenolic water under a variety of conditions are reported in Table 4.6 and Fig. 4.6 and Fig. 4.7. It appears that an increase in NaOH concentration almost results in an action that could be interpreted as deactivating the emulsifier and rendering it away from the surface.

Table 4.6: Effect of ϕ and C_{io} on interfacial tension (σ)

C_{io} =	0.01 M	0.15 M	0.3 M	0.4 M	0.5 M
ϕ	σ (mN/m)				
0.45	7.5	18.2	20.6	23.0	23.5
0.60	9.2	19.5	22.4	24.0	24.0
0.64	10.0	19.5	22.5	23.5	23.5
0.69	14.1	23.0	27.8	28.2	29.2

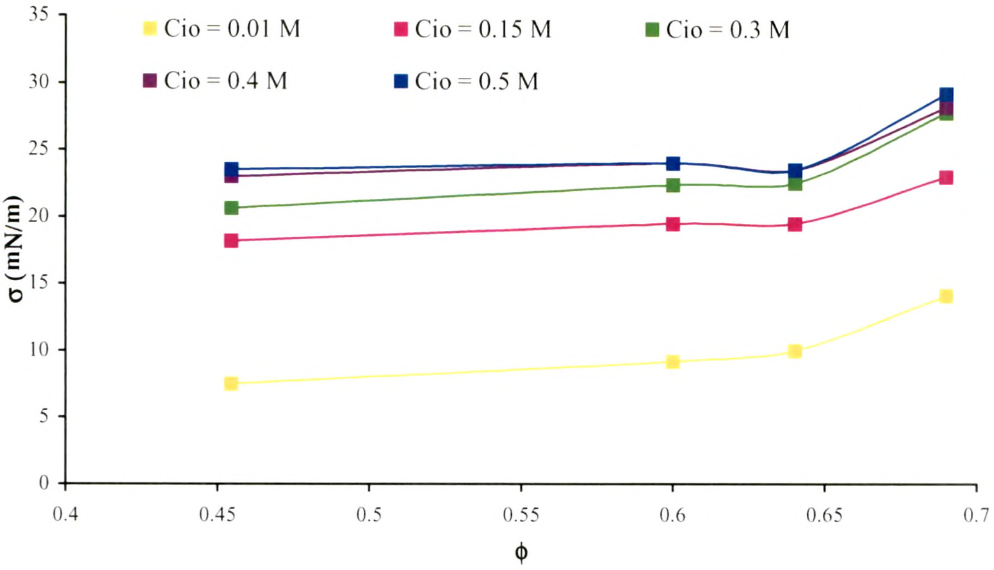

Fig. 4.6: Effect of ϕ on σ

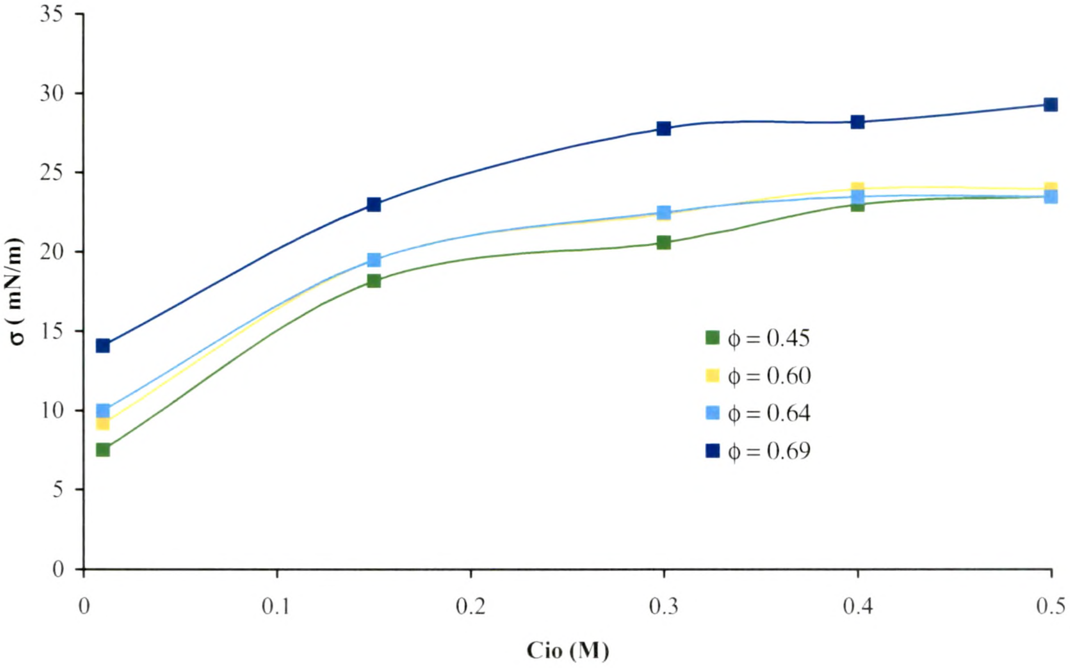

Fig. 4.7: Effect of C_{io} on σ

4.3 DISPERSION BEHAVIOUR OF EMULSIONS

The extracting W/O emulsions containing NaOH in its internal phase when dispersed in the feed solution by agitation breaks down and forms a multitude of tiny globules each of approximate size ranging from 0.5 to 3.0 mm. Thus, a very large number of emulsion globules can be formed easily to produce a large mass transfer area adjacent to the external continuous phase. Each emulsion globule contains numerous tiny encapsulated droplets of sizes ranging from 1μm to 30 μm in diameter. The internal mass transfer surface area, typically 10^6 m^2/m^3, is very much larger than the external mass transfer surface area of globules. Such large inner phase surface areas warrant rapidity of the overall extraction process. Even if the rates of stripping reaction are slow the huge surface areas more than compensate for it.

The effectiveness of the ELMs is never constrained by the inner surface areas. It is rather the external surface of dispersed globules that often dictates the rates of mass transfer. In order to ensure rapid mass transfer, it is necessary to disperse the emulsion appropriately in the continuous phase. The smaller the globule sizes, the larger the number of globules and larger the surface areas. Generally, the Sauter mean diameter d_{32} is used to characterize the globule size. The size of the emulsion globule depends on the viscosity of the emulsion, characteristics and concentration in the emulsion, intensity and mode of mixing (Ohtake *et al.* 1987).

In order to assess the dispersion characteristics of various ELMs in feed solutions, emulsions were prepared, with different internal phase fractions and varying internal phase NaOH concentrations and dispersed in the feed. These dispersions were photographed and the globule sizes were measured using imaging software Photoshop 7. Since interfacial tensions between the aqueous solution of the solutes taken up in this study (phenol, o-cresol, p-cresol and 2-chlorophenol) and the W/O emulsions were the same, it was decided to study the dispersion behaviour primarily in aqueous solutions containing approximately 500 mg/dm^3 of phenol.

A number of pilot runs were performed to judge the dispersion characteristics visually. The ELMs used in these runs had internal phase fraction $\phi = 0.45$, Span 80 concentration in the oil phase of 3 wt %, internal phase NaOH concentration of 0.3 M and the treat ratio (emulsion volume/feed volume) was maintained at 1:15. It was observed that at 135 rpm the emulsion got well dispersed in the continuous phase and in the stirred extractor assembly used in this work. It was visually observed that below

135 rpm the emulsion was just not adequately dispersed and even at 135 rpm there was some amount of emulsion residing as a film on the surface of the aqueous phase.

Increasing the stirring speed to 155 rpm resulted in a dispersion that is typical of ELMs. The globules appeared to be of uniform size and almost spherical in nature. Globule sizes appeared to remain constant over the period of run and they were smaller in size in comparison with the globule sizes observed at 135 rpm. On stopping the agitation the globules separated very quickly leaving the aqueous very clear.

Fig. 4.8 shows the dispersion history of the emulsion globules. Although it was visually observed that within a minute of addition of the emulsion to the continuous phase the dispersion became uniform, but globule size measurements indicated that after 1 minute of stirring, the globule sizes were larger as compared to the globule sizes measured after 3 minutes of stirring and thereafter. The Sauter mean diameter (d_{32}) obtained were 1.316 mm, 1.128 mm, 1.106 mm, 1.087 mm and 1.066 mm after 1 min, 3 min, 10 min, 15 min and 30 min respectively.

The histograms representing the globule size distributions after 1min, 3 min and 30 min of stirring are shown in Fig. 4.9. It is evident from these globule size distributions that the emulsion globule sizes decreases in the first half of the run. There was no significant change in the Sauter mean diameter after 3 minutes duration of the experimental run.

4.3.1 Effect of stirring speed

Dispersion behaviour of the emulsions was investigated at stirring speeds of 135 rpm, 155 rpm and 185 rpm respectively. Stirring speeds greater than 185 rpm resulted in severe swelling and emulsion leakage, hence they were not considered. Emulsion globule sizes progressively decreased with increase in stirring speeds as expected. However, at stirring speeds of 185 rpm it was observed that emulsion swelling was more. Further, at the end of the run when stirring was stopped, the phase separation was delayed due to formation of very small globules, which took time to settle. Fig. 4.10 shows the dispersion behaviour at stirring speeds of 135 rpm, 155 rpm and 185 rpm at time durations of 1 min, 3 min and 30 min respectively.

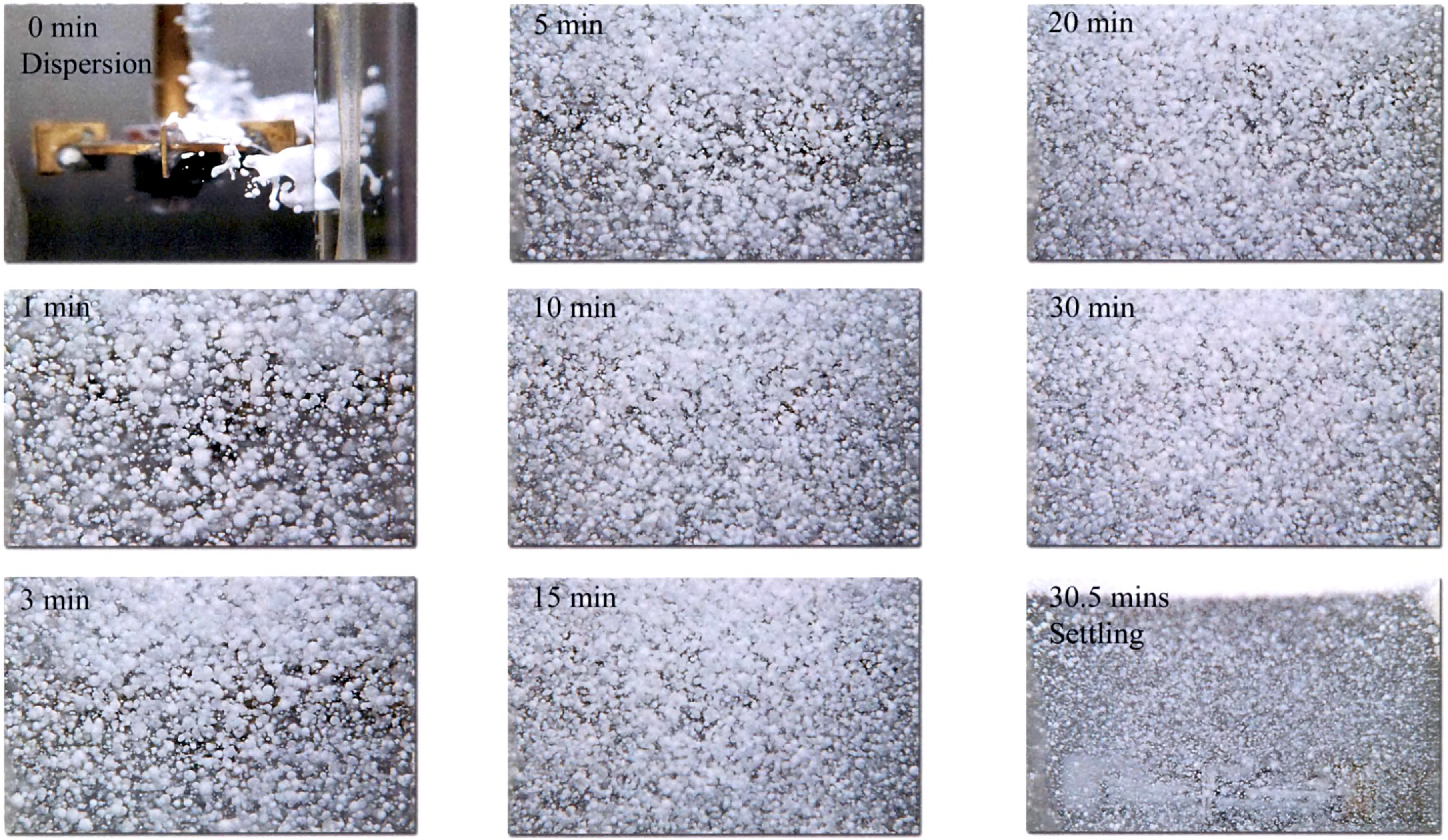

Fig. 4.8: Snapshots showing dispersion history of emulsion globules
(N= 155rpm, $\varnothing = 0.45$, Span 80=3%, Cio=0.3M, TR=1:15)

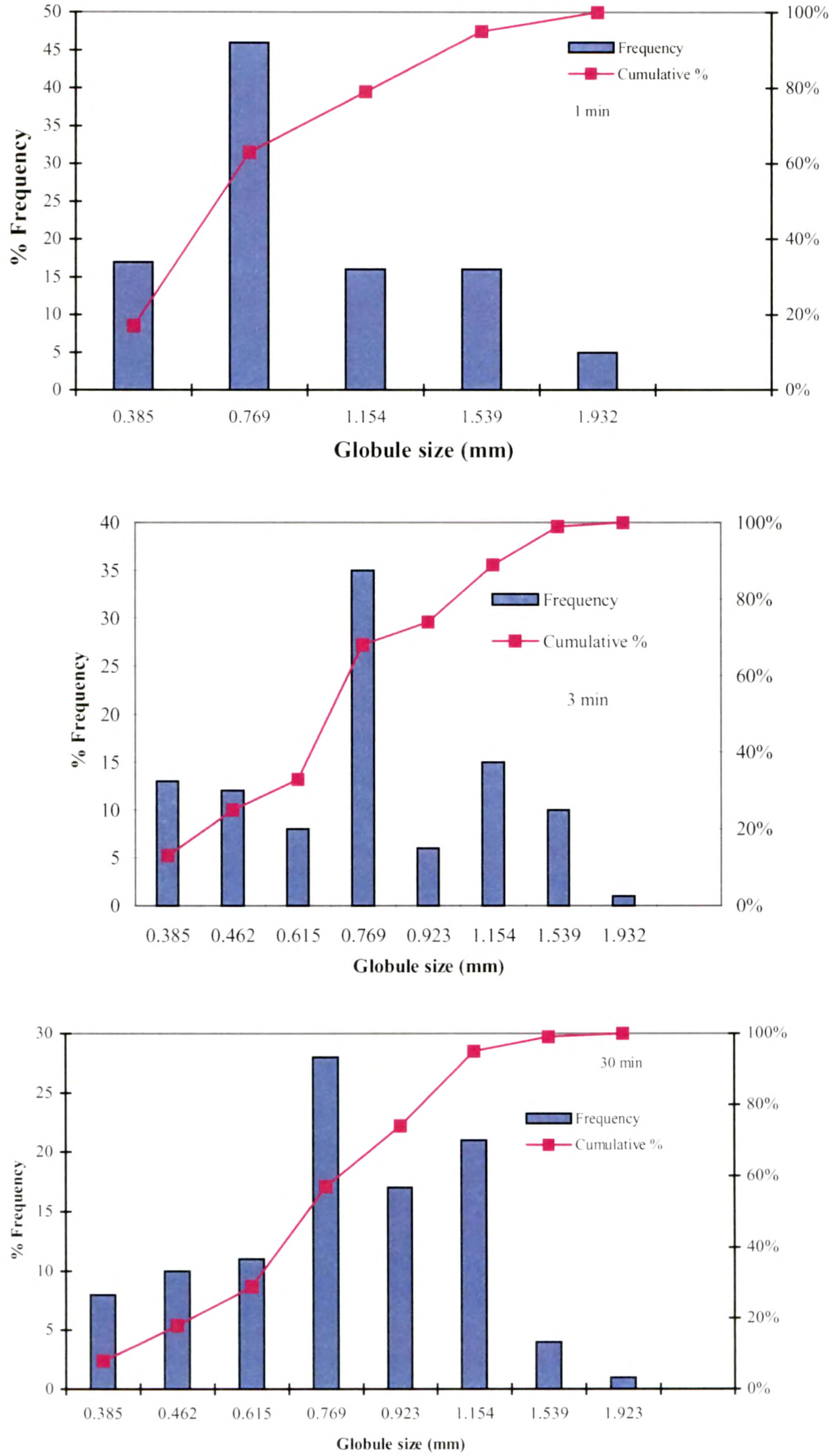

Fig 4.9: Globule size distribution a: 1min, b: 3min, c: 30min

(N = 155 rpm, ϕ = 0.45, Span80 = 3%, C_{io} = 0.3M, TR = 1:15)

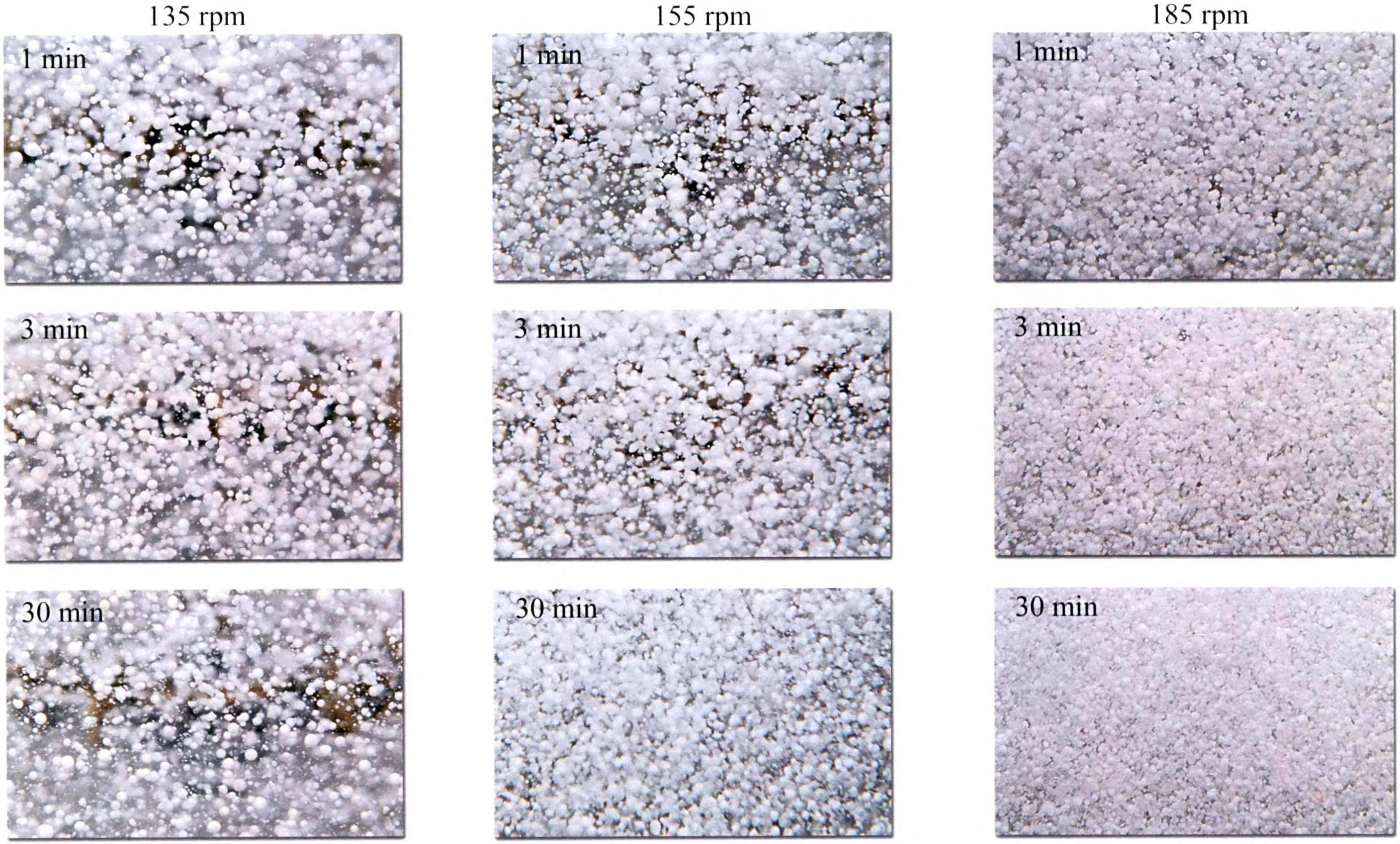

Fig. 4.10: Effect of stirring speed on emulsion globule dispersion.
(Ø=0.45, Span 80=3%, Cio=0.3M, TR=1:15)

The globule size distributions at 135 rpm, 155 rpm and 185 rpm are presented in form of histograms in Fig. 4.11.

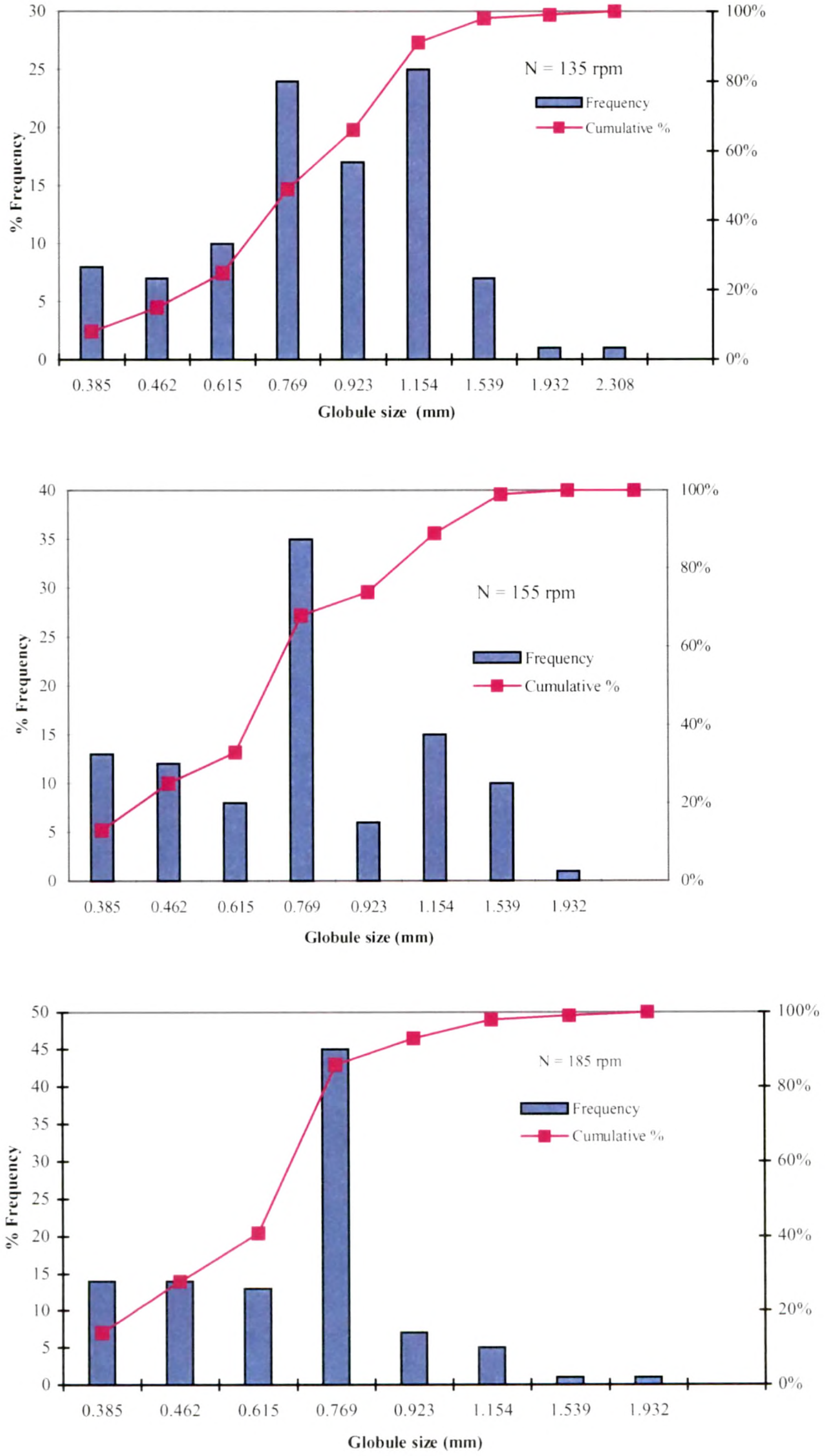

Fig. 4.11: Effect of stirring speed on emulsion globule size distribution ($\phi = 0.45$, Span80 = 3%, $C_{io} = 0.3M$, TR = 1:15)

These globule size distributions were measured after 3 minutes of stirring for all cases. It was felt that measurements made after 3 minutes duration was appropriate for two reasons: - firstly the emulsion globule size distribution almost reaches a steady state by this time, secondly in extraction by ELMs almost half the extraction is already over by three minutes time of stirring. In a way, 3 minutes represented the average conditions for extraction.

The Sauter mean diameters (d_{32}) obtained from these distributions were 1.152 mm, 1.128 mm, and 0.8743 mm at 135 rpm, 155 rpm and 185 rpm respectively. It was curious to find that 0.769 mm size globules were the most prominent in all the three size distributions. At stirring speeds of 135 rpm, 155 rpm and 185 rpm the fraction of droplets having diameter of 0.769 mm were 24 %, 35 % and 45 % respectively. In fact the change in distribution results largely from the relative amount of 0.769 mm globules in the whole distribution.

Although there was no significant change in the d_{32} values at 135 rpm and 155 rpm, fundamentally the dispersion characteristics were different. This difference stems from the globule size distributions at these three stirring speeds. If one considers 0.769 mm globule size as the basis of comparison then we find that when the stirring speed is 135 rpm 49 % of globules are $\leq$ 0.769 mm, at 155 rpm 68 % globules are $\leq$ 0.769 mm and at 185 rpm 86 % globules are $\leq$ 0.769 mm indicating that with an increase in stirring speeds the distribution tends towards the smaller sized globules Further it is observed that at 135 rpm there exists two dominant sizes 0.769 mm and 1.154 mm, in fact 1.154 mm globules are more in number. This trend is not observed in the other two distributions.

4.3.2 Effect of internal phase volume fraction (ϕ)

Effect of ϕ on globule size distributions was studied for three values $\phi = 0.45$, $\phi = 0.5$ and $\phi = 0.69$. Globule sizes increase with internal phase volume fraction ϕ. Fig. 4.12 portrays photographically the dispersion behaviour of emulsions having ϕ of 0.45, 0.5 and 0.69 at stirring speed of 155 rpm. Stirring speed of 155 rpm was selected because it not only gave a stable globule size but also because the swelling and leakage were low in comparison with speed of 185 rpm. Fig. 4.13 presents the globule size distributions in form of histograms at 3 minutes duration of the run.

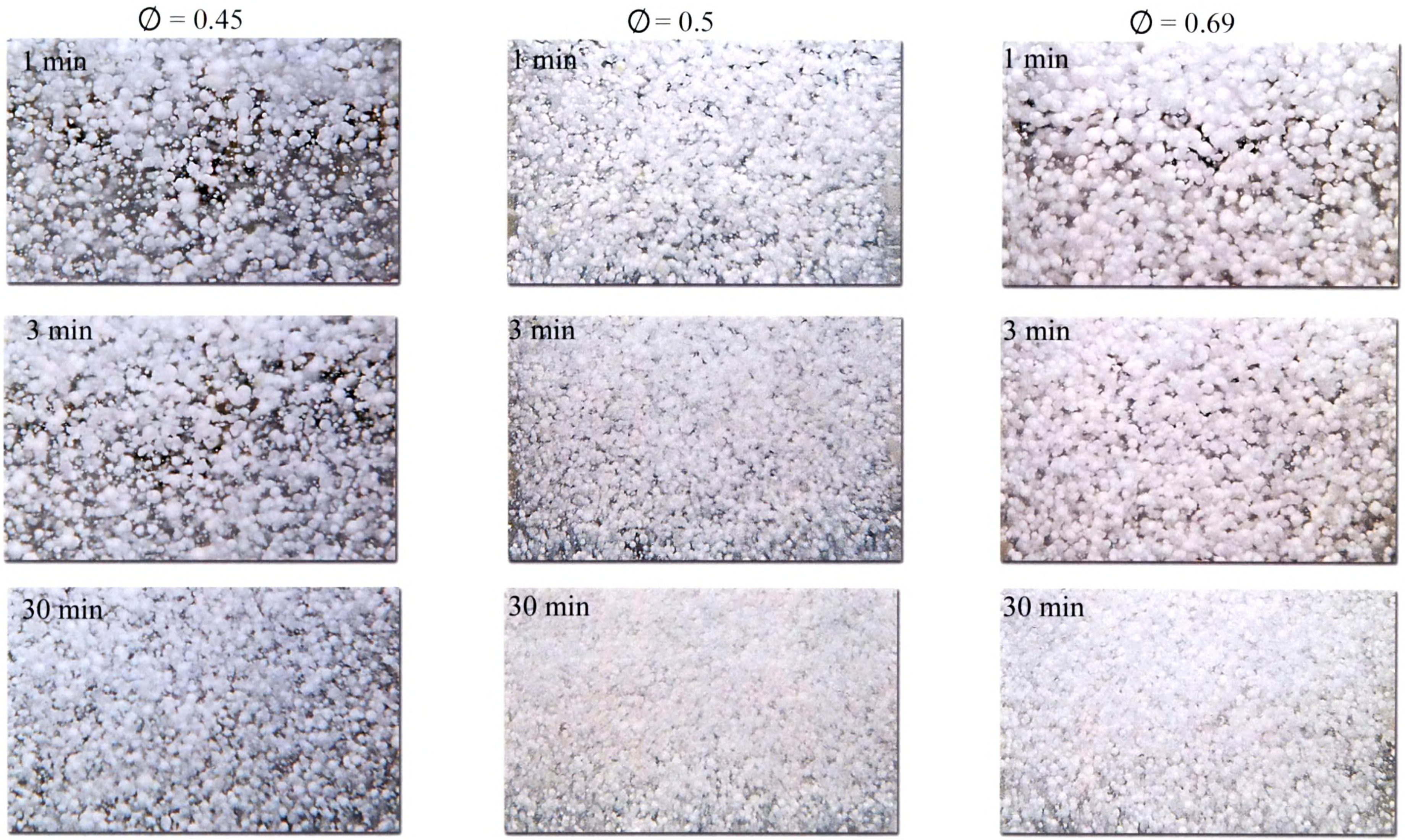

Fig 4.12 : Effect of Volume Fraction of Internal Phase (Ø) on Emulsion Globule dispersion.
(N = 155 rpm)

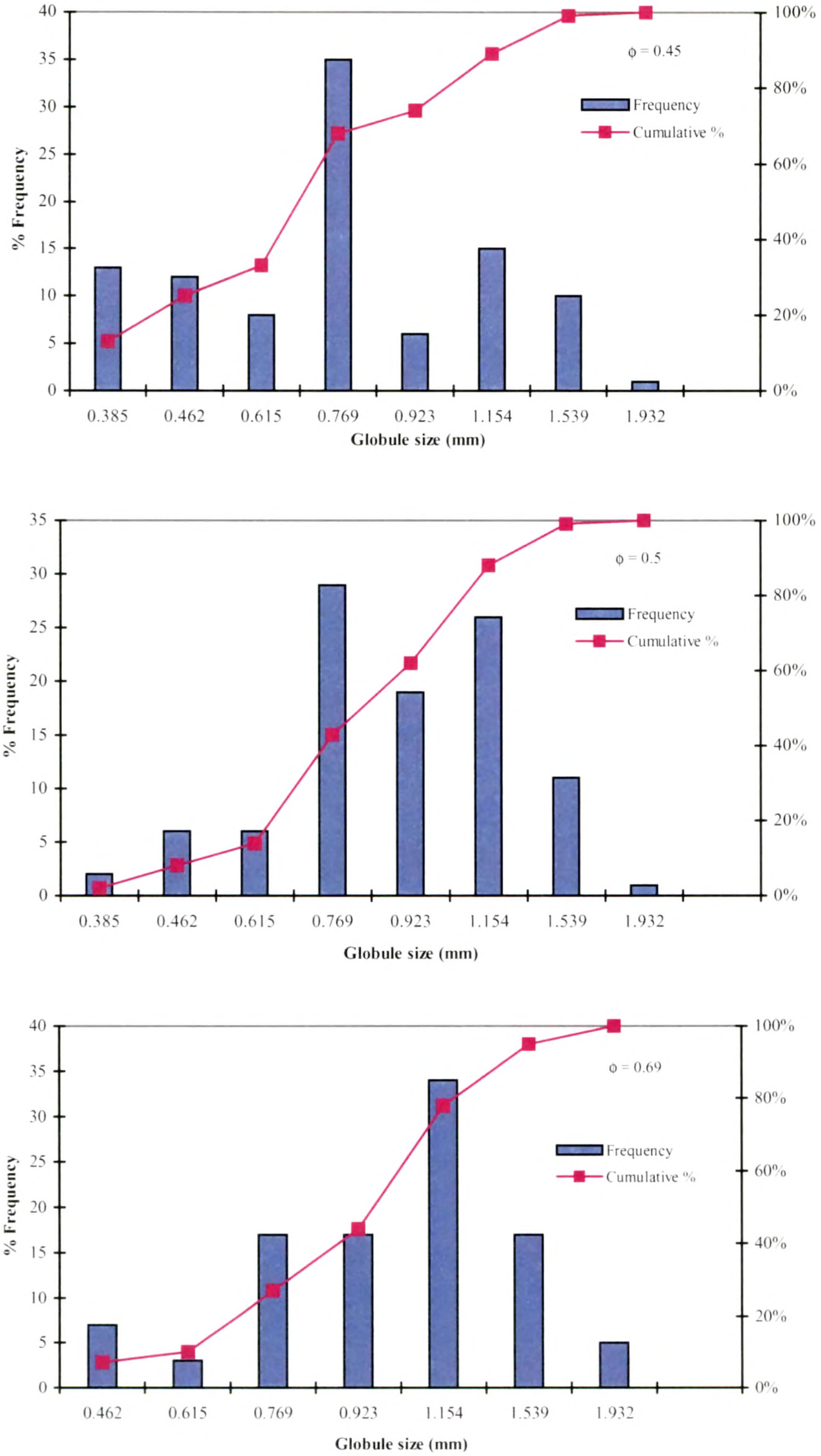

Fig. 4.13: Effect of φ on emulsion globule size distribution

(N = 155 rpm, Span80 = 3%, C_{io} = 0.3M, TR = 1:15)

Comparing the histograms for $\phi = 0.45$ and $\phi = 0.5$ a sharp decrease was observed in the fraction of globules below 0.769 mm diameter in the case of $\phi = 0.5$. When $\phi = 0.45$ globules below 0.769 mm were 33 % of the distribution, while for $\phi = 0.5$ it was just 14 % of the total. There is a corresponding large increase in globule sizes of 0.923 mm and above for $\phi = 0.5$. In some respects the distribution of globules having $\phi = 0.5$ at 155 rpm is similar to the distribution with $\phi = 0.45$ at 135 rpm, in both these distributions there are two globule sizes in comparable amounts and they are 0.769 mm and 1.154 mm.

Emulsions having $\phi = 0.69$ show globule size distribution completely different from that observed in previous cases. In this case, the 0.769 mm size globules is no longer the dominant size. As seen from Fig. 4.13 the globule size of 1.154 mm is the dominant size. The Sauter mean diameter for this distribution turns out to be 1.312 mm. Comparing the three histograms shown in the above-mentioned Fig. one finds a definite shift towards larger globule size as ϕ increases while keeping all other conditions identical. The physical properties that bring about changes in drop size distribution and the d_{32} values are listed in the table below. It appears d_{32} varies linearly with σ, however influence of viscosity is more complex.

ϕ	η mPa.s	σ mN/m	$d_{32} \times 10^3$ m
0.45	13.32	20.6	1.128
0.50	17.22	22.4	1.156
0.69	137.25	27.8	1.312

4.3.3 Effect of internal phase reagent concentration on dispersion characteristics

Changing the concentration of NaOH in the internal phase of emulsion brings about a change in the viscosity of the emulsion and the interfacial tension between the emulsion and the continuous phase. Hence, it is expected that the globule size distribution of emulsions is likely to be influenced by the change in the NaOH concentration (C_{io}) of the emulsion phase.

Dispersion experiments were performed with three emulsions having C_{io} values 0.15 M, 0.3 M and 0.5 M. Fig. 4.14 shows snapshots of the dispersion taken at time

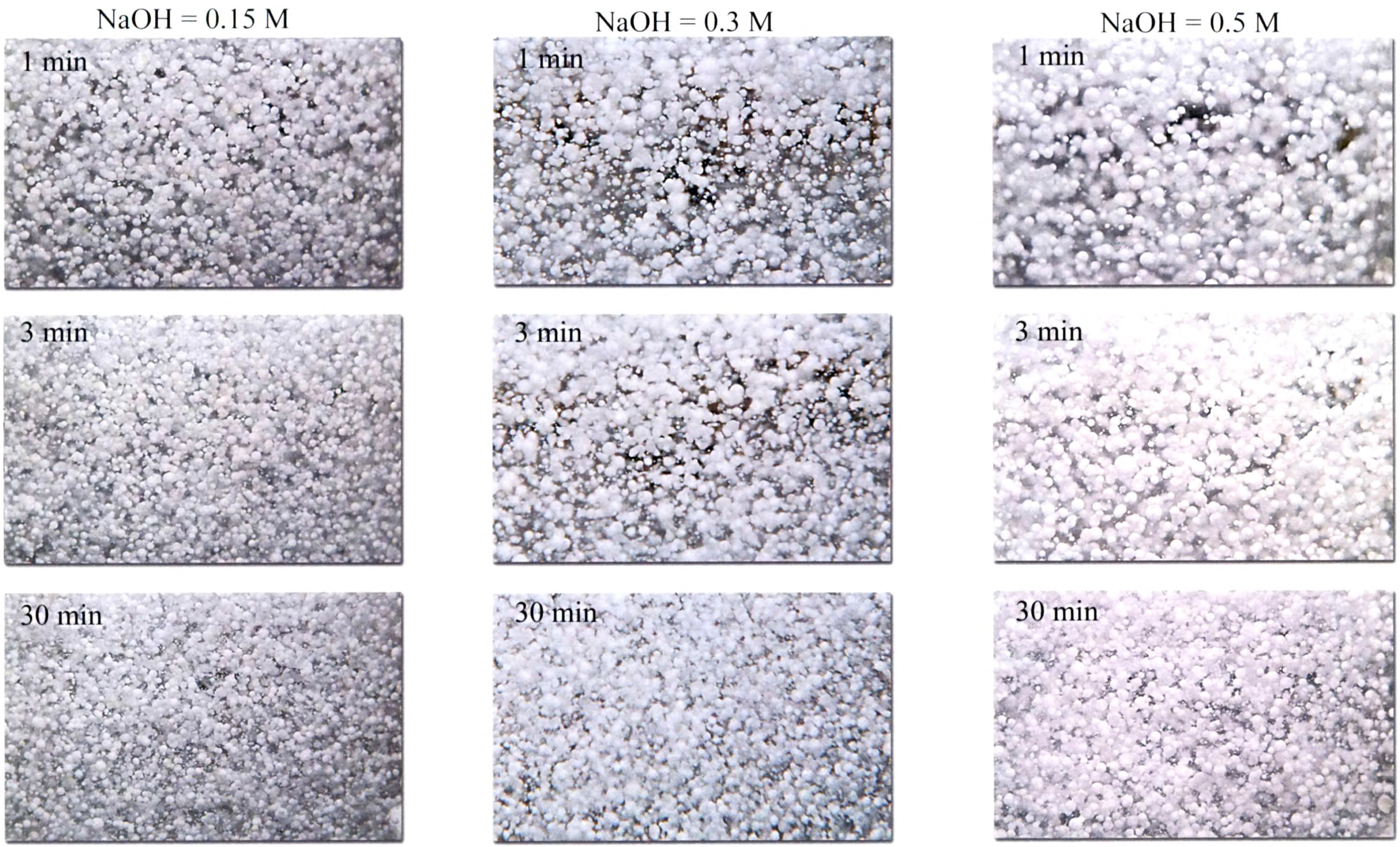

Fig. 4.14: Effect of initial NaOH concerntration (Cio) in the internal phase on emulsion globule dispersion. (N=155rpm, $\varnothing$=0.45, Span 80=3%, TR=1:15)

intervals of 1 min, 3 min and 30 min for emulsions having $\phi = 0.45$, stirrer speed of 155 rpm and treat ratio of 1:15. The globule size distribution is given in the form of histograms in Fig. 4.15.

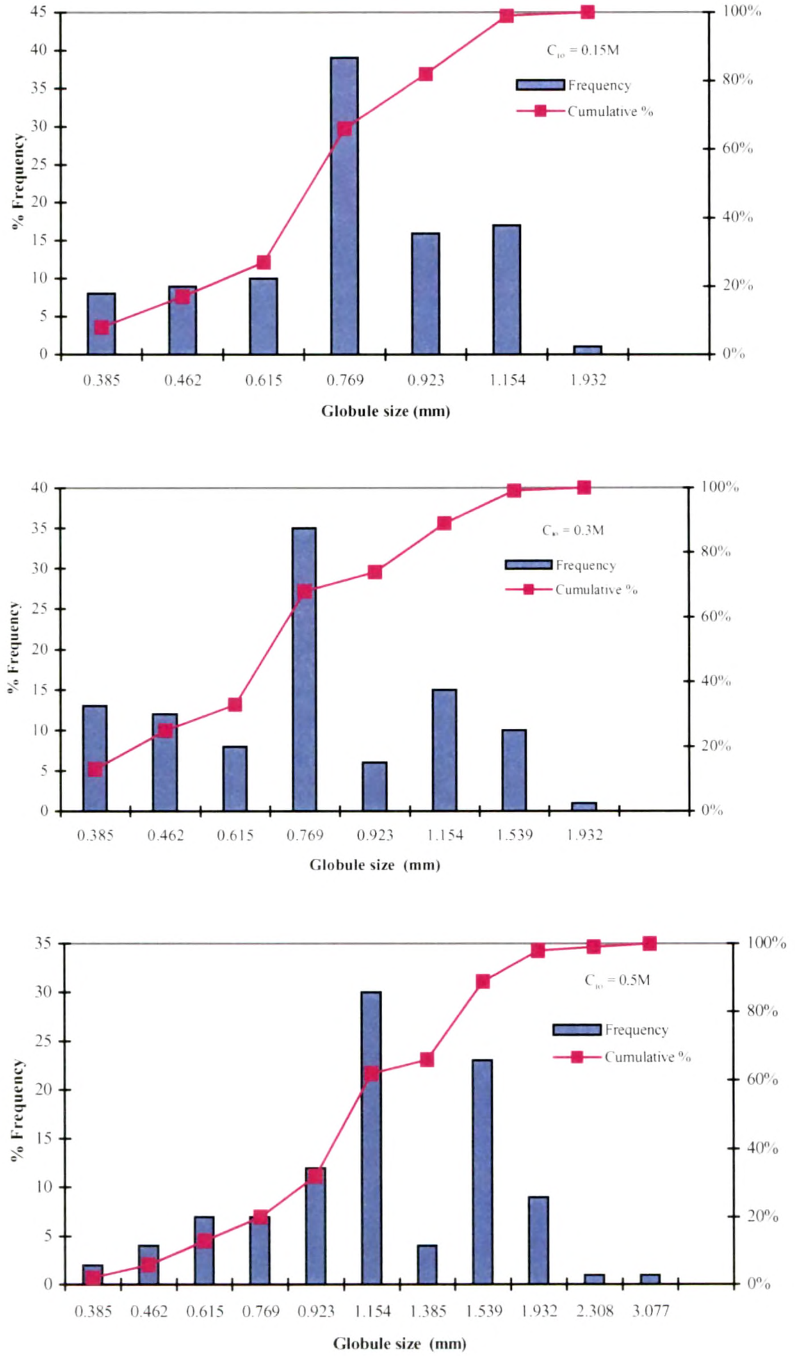

Fig. 4.15: Effect of C_{io} on emulsion globule size distribution

($N = 155$ rpm, $\phi = 0.45$, Span80 = 3%, TR = 1:15)

It is seen that at C_{io} = 0.15 M the dominant globule size in the distribution is 0.769 mm, 39 % of the total globules are of this size. Comparing histograms shown in Fig. 4.15 we find that at C_{io}= 0.15 M, about 66 % of globules are ≤ 0.769 mm while in case of C_{io} = 0.3 M, 68 % globules are ≤ 0.769 mm in size but increasing C_{io} to 0.5 M results in just 20 % of globules ≤ 0.769 mm.

Thus, one can observe that while globule size distributions with C_{io} 0.15 M and 0.3 M have some similarity, the globule size distribution for C_{io} = 0.5 M is very different. The distribution with C_{io} =0.15 M returns d_{32} = 0.988 mm as against d_{32} = 1.128 mm for C_{io} = 0.3 M. This difference in d_{32} values arises from the disappearance of 1.539 mm globules from the distribution measured for C_{io} = 0.15 M.

The dispersion of emulsion with C_{io} = 0.5 M shows two dominant globule sizes i.e. 1.154 mm (30 %) and 1.539 mm (23 %) and it also has 9 % globules of 1.923 mm size. No other emulsion had such large number of globules of 1.923 mm. This distribution returns a d_{32} of 1.493 mm. Among all the emulsion dispersions studied in this work, the emulsion with C_{io}= 0.5 M is the most polydisperse and has largest value of d_{32}.

4.3.4 Effect of Treat ratio

Increasing the Treat ratio, i.e. the amount of the W/O emulsion added to the feed phase is expected to influence the globule size distributions. In the range of experiments performed with variation in TR no significant change in globule sizes were visually observed for Treat ratios ranging from 1:15 to 1:7.5. However, at treat ratio of 1: 6 there was an increase in the globule size.

Dispersion experiments were conducted at Treat ratio of 1:6 using W/O emulsions having ϕ = 0.45 and C_{io} = 0.3 M and the stirring speed maintained at 155 rpm. The results were compared with results obtained at Treat ratio of 1:15.

Fig. 4.16 portrays photographically the dispersion at times of 1 min, 3 min and 30 min of the run duration.

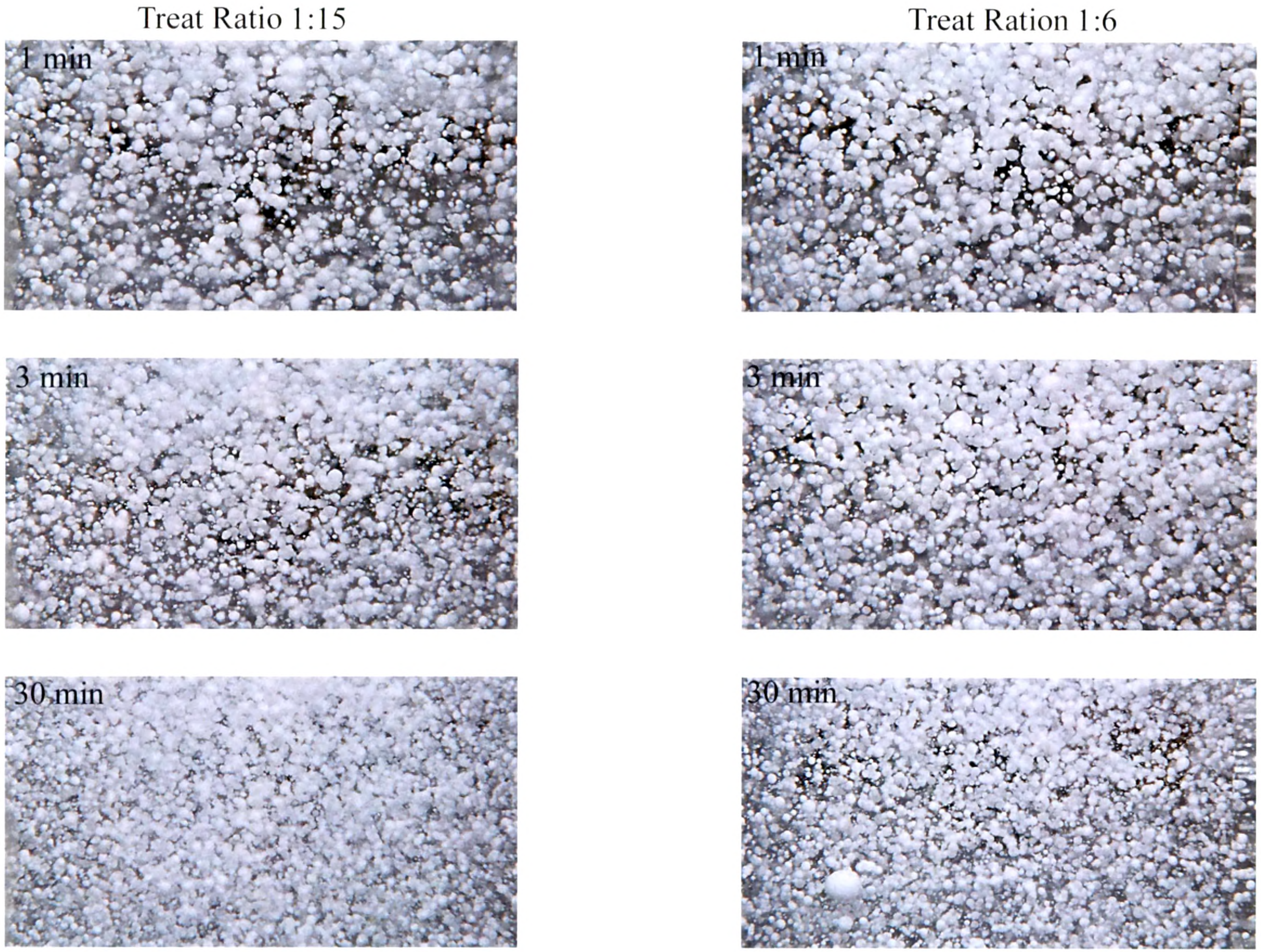

Fig. 4.16: Effect of treat ratio (TR) on emulsion globule dispersion.
(N=155rpm, Ø=0.45, Span 80=3%, Cio=0.3M)

Fig. 4.17 shows the globule size distributions at Treat ratio of 1:6 and Treat ratio of 1:15 in form of histograms. It is seen that the globule size distribution widens at TR =1:6 and comparing the two distributions one finds that the dominant globule size shifts from 0.769 mm to 1.154 when treat ratios are increased from 1:15 to 1:6. Further, only 39 % of the total globules are ≤ 0.769 mm when TR = 1:6 as compared to 68 % of the total globules ≤ 0.769 mm when TR = 1:15. This indicates a definite shift of the distribution towards larger globule sizes when Treat ratios are increased.

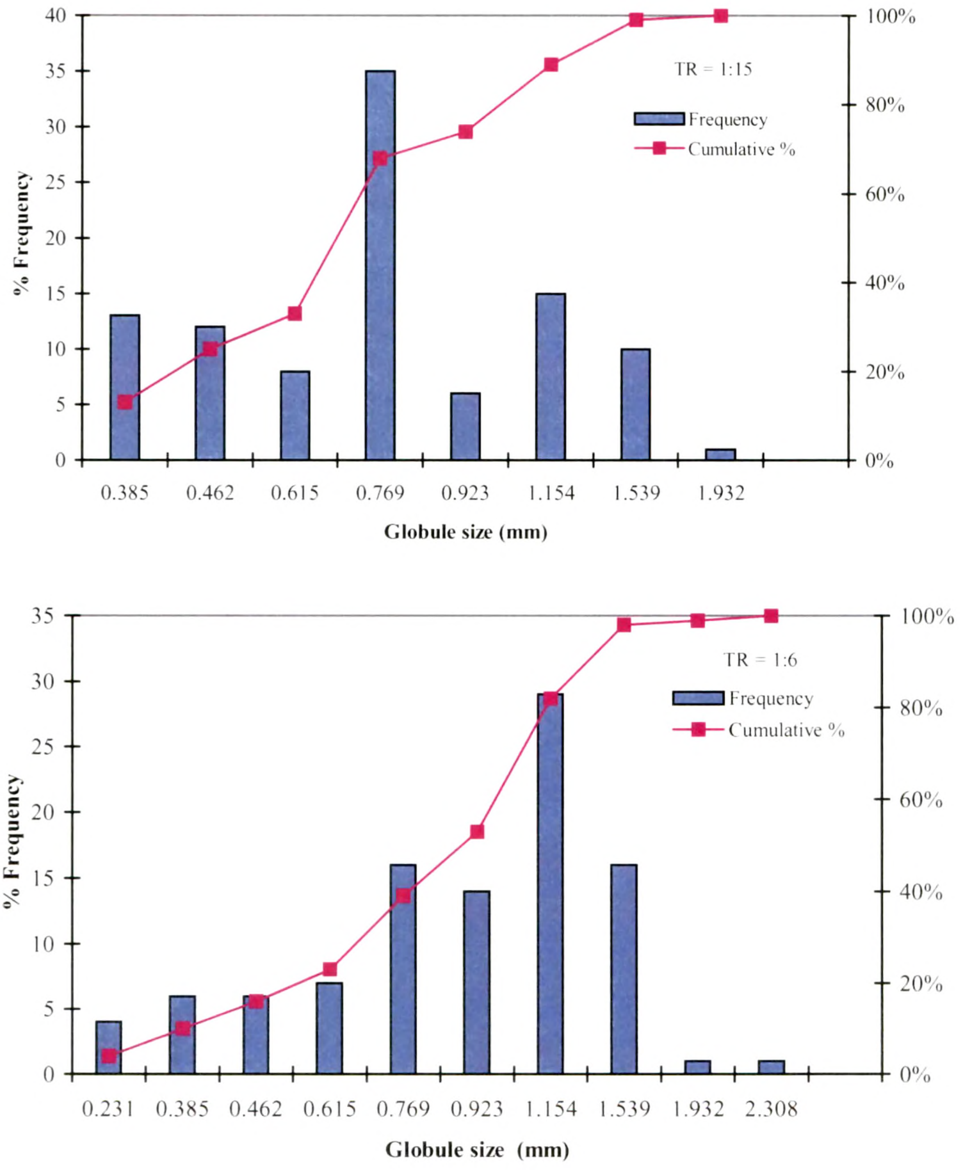

Fig. 4.17: Effect of TR on emulsion globule size distribution

(N = 155 rpm, $\phi = 0.45$, Span80 = 3%, Cio = 0.3M)

4.3.5 Prediction of globule sizes

Table 2.1 lists the globule size correlations developed to predict the mean globule size (d_{32}) for stirred dispersions of emulsions in the continuous aqueous phase. The correlation by Ohtake *et al.* (1987) is widely used to estimate globule sizes in the absence of data of d_{32}.

$$\mathbf{d_{32}/\,d_I = 0.12\ We^{-0.5}} \qquad (4.1)$$

where d_I is the impeller diameter.

Rautenbach and Machhammer (1988) also proposed a correlation to predict mean globule sizes particularly for ELM systems. The advantage of this correlation (Equation
4.2 below) is that it accounts for the variation in Treat ratio of the emulsion.

$$\mathbf{d_{32}/\,d_I = 0.11\ (\nu_{em}/\,\nu_e\,)^{0.32}\ We^{-0.7}\ [(V_{em}\,)\,/(V_{em} + V_e\,)\,]^{0.1}} \qquad (4.2)$$

Where ν_{em} and ν_e are the kinematic viscosities of the emulsion and the external phase respectively. V_{em} and V_e are the volume of the emulsion and the continuous external aqueous phase respectively.

Both these correlations were used to predict the mean emulsion globule size (d_{32}) for the various emulsions studied in this work and the results are compared with the experimental values of d_{32} obtained from the globule size distributions. These results are reported in Table 4.7. The lack of agreement between the d_{32} values calculated using the two correlations with the experimentally obtained values of d_{32} is not surprising because dispersions from which they were developed had diverse characteristics. The predicted d_{32} values of the two correlations also do not agree.

The correlation of Ohtake underestimates the d_{32} values but it predicts the trend of data reasonably well. Although numerous reasons could be attributed for the lack of fit between experimental and predicted values of d_{32} but it appears that the main point of difference stems from the range of interfacial tension between emulsion and continuous phase studied by Ohtake and the range of σ this investigation.

Table 4.7: Prediction of emulsion globule sizes

ϕ	N (rpm)	TR	C_{io} M	d_{32} (mm) Expt.	We	d_{32} (mm) Ohtake	Error %	d_{32} (mm) Rautenbach	Error %
0.45	135	1:15	0.3	1.1520	34.44	1.063	7.725	0.9047	21.46
0.45	155	1:15	0.3	1.1283	45.37	0.9264	17.89	0.7456	33.91
0.45	185	1:15	0.3	0.8735	64.64	0.7761	11.15	0.5822	33.35
0.50	155	1:15	0.3	1.1559	41.73	0.9659	16.44	0.8572	25.84
0.69	155	1:15	0.3	1.3120	33.62	1.076	17.98	1.9173	-46.1
0.45	155	1:15	0.15	0.9879	51.36	0.8707	11.86	0.6819	30.97
0.45	155	1:15	0.5	1.4932	39.77	0.9894	33.74	0.8174	44.45
0.45	155	1:6	0.3	1.2950	45.37	---	---	0.8214	36.57

The Ohtake correlation was developed for emulsion that registered σ values ranging from 2 to 10 mN/m, while in this investigation it ranges from 18.2 mN/m to 27.8 mN/m. Necessarily larger values of interfacial tension would lead to larger globule sizes. The single parameter dependence of the Ohtake correlation makes it convenient to modify this correlation appropriately in order to fit experimental data. The modified Ohtake correlation in the range of experimentally obtained data is given below:

$$\mathbf{d_{32}/\,d_I = 0.135\ We^{-0.5}} \qquad (4.3)$$

This correlation fits the data points with an absolute error of 7.36 %. In this correlation, the index of Weber number is retained at –0.5 as suggested by Ohtake *et al.* Attempt was also made to obtain a correlation of the Ohtake type by regression analysis, which results in the under-mentioned correlation.

$$\mathbf{d_{32}/\,d_I = 0.218\ We^{-0.61}} \qquad (4.4)$$

A comparison of experimental globule diameters with predicted globule diameters using these two modified correlations are shown below.

We	34.44	45.37	64.64	41.73	33.62	51.36	39.77	Abs. Error in %
d_{32} (mm) Expt.	1.152	1.128	0.873	1.156	1.312	0.988	1.493	
$d_{32} = 0.135\ We^{-0.5}\,(d_I)$	1.196	1.042	0.873	1.087	1.211	0.979	1.113	7.36
$d_{32} = 0.218\ We^{-0.61}(d_I)$	1.309	1.106	0.891	1.164	1.328	1.025	1.198	6.15

Although the absolute error ([$\sum$ {Abs((expt d_{32} – pred d_{32})/expt d_{32})} /n] x 100) of Equation (4.4) is relatively lower but it seems more appropriate to use Equation (4.3) because it retains the index of Weber number as –0.5 that was obtained by Ohtake by regression of a large data bank. It may, however, be pointed that Shinnar (1961) suggested a power of –0.6 to the Weber number in his derivation of maximum stable drop diameter based on the assumption that there is hardly any difference between the densities and viscosities of the two phases. That assumption is, however, not valid in this case since the viscosities of the two phases are widely different.

It is difficult to comment on the lack of fit using the Rautenbach and Machhammer correlation since very little information is available on the range of physical properties and operational parameters used to develop this correlation.

4.4 DISTRIBUTION COEFFICIENTS AND EFFECTIVE DIFFUSIVITIES

Distribution coefficient of the phenolic solutes between water and the membrane phase and the effective diffusivities of the solutes within the emulsion globule are two important parameters that have considerable influence on the extraction of solutes using ELMs. These parameters need to be estimated or experimentally obtained. Once these parameters are known a physical understanding of the ELM separation process is facilitated using mathematical models.

4.4.1 Distribution coefficients of phenols between kerosene and water

The distribution coefficient α' for phenol, o-cresol, p-cresol and 2-chlorophenol were experimentally determined by equilibrating equal volumes of aqueous solute phase with kerosene phase at 30°C. Data were obtained for initial aqueous concentrations ranging from 200 mg/dm^3 to 800 mg/dm^3 except for the case of 2-chlorophenol where the data were collected for initial concentrations ranging from 100 mg/dm^3 to 500 mg/dm^3. Not all data points could be accommodated in the linear range. The distribution coefficient plots are reported for the four solutes in Fig. 4.18.

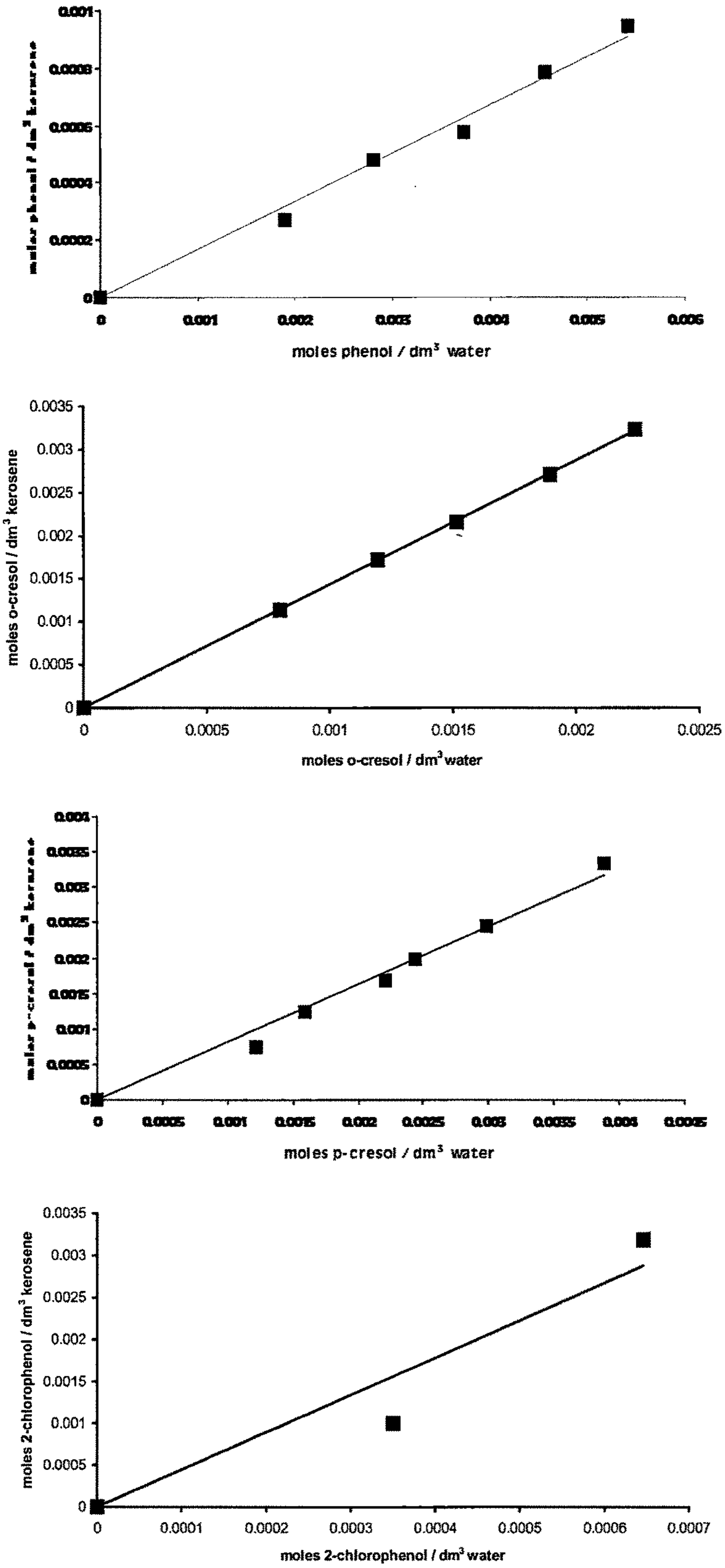

Fig. 4.18: Distribution coefficients of phenols

Table 4.8 below reports the distribution coefficients and the correlation coefficient of fitted equation to the experimentally obtained data points for the four solutes.

Table 4.8 Distribution coefficients of Phenols between kerosene and water

Solute	K	R^2
Phenol	0.1679	0.9899
o-cresol	1.4345	0.9999
p-cresol	0.8189	0.9854
2-chlorophenol	4.4659	0.9230

4.4.2 Prediction of effective diffusivities of various solutes in the W/O emulsion

In order to predict the effective diffusivities (D_{eff}) of the individual solutes such as phenol, o-cresol etc within the emulsion globules, it is necessary to first estimate the diffusion coefficients of these solutes in both water and kerosene phase. The Wilke-Chang equation was used to evaluate the diffusion coefficients of the various solutes in both water and kerosene.

The effective diffusivity is a parameter that is difficult to measure. Till date only Fudu *et al.* (1985) attempted to experimentally determine D_{eff} under non-reactive conditions using a diffusion cell containing a bundle of diffusion tubes each 2mm in diameter filled with emulsion.

Most investigators estimated the effective diffusion coefficients using the Jefferson-Witzell – Sibbett equation (Jefferson *et al.* 1958, Crank 1975) following the lead of Ho *et al.* (1982) who were the first investigators to conveniently use this equation that had been originally proposed for conductive heat transfer in dispersed systems for estimation of D_{eff} in ELMs.

The Jefferson – Witzell – Sibbett equation was used to estimate the effective diffusivity of phenols in the emulsion mixture based on concentration driving force defined in terms of membrane phase concentration. The only emulsion parameter that influences the effective diffusivities is the internal volume fraction ϕ. The calculated values of the effective diffusivities for the various solutes taken up in this investigation are presented in Table 4.9. Relevant details of the equation and the calculation procedure are discussed later in Chapter 6.

Table 4.9: Effective diffusivities of Phenols in ELMs.

Solute	phenol	o-cresol	p-cresol	o-chlorophenol
D_i (m^2/s) =	1.041×10^{-9}	9.26×10^{-10}	9.26×10^{-10}	9.318×10^{-10}
D_m (m^2/s)=	1.176×10^{-9}	1.046×10^{-9}	1.046×10^{-9}	1.053×10^{-9}
ϕ	$D_{eff} \times 10^{10}$ (m^2/s)	$D_{eff} \times 10^{10}$ (m^2/s)	$D_{eff} \times 10^{10}$ (m^2/s)	$D_{eff} \times 10^{10}$ (m^2/s)
0.40	7.2614	9.8218	9.9138	8.4143
0.45	7.2772	9.7485	9.8469	8.2089
0.50	7.3291	9.6880	9.7923	8.0348
0.55	7.4324	9.6154	9.7276	7.8174
0.60	7.5469	9.5562	9.6758	7.6307
0.69	7.8486	9.4383	9.5755	7.2216

4.5 EXTRACTION OF PHENOL

Extraction of phenol using ELMs was investigated by a number of investigators. Li and coworkers (1972, 1974, 1982) are notable among them. The objective of this study of extraction of phenol using ELMs was two fold: To test the suitability of the W/O extracting emulsions prepared in this work and to gather exhaustive data with well characterized emulsions and in that process to attempt to address some of the lacuna existing in the understanding of extraction of phenols using ELMs. It was also felt that an integrated study of the four phenolic solutes chosen in this work would provide a deeper understanding of the mechanism of Type I transport and the influence of the various emulsion parameters and process parameters on the extraction behaviour.

The study was organized as a sequence of experimental runs to ascertain the effect of different variables on extraction. First the dispersion behaviour of the emulsion was investigated in order to fix up the stirring speed for future experiments. Next the influence of changes in emulsion characteristics on extraction behaviour was studied by changing the internal phase fraction of the W/O emulsion, the surfactant concentration in the membrane, and the internal phase reagent concentration. After exploring the influence of the emulsion characteristics on the extraction, the influence of changes in process parameters such as the Treat ratio (volume of emulsion to feed), feed concentration and temperature of extraction was investigated. Finally, the parameter that influenced the extraction behaviour most significantly was identified and critically analyzed.

4.5.1 Effect of stirring speed

Stirring speed has a direct influence on the extraction behaviour. Globule size distribution is affected by stirring rates, higher stirring rates lead to formation of smaller globule sizes thereby increasing the external interfacial area and hence the rates of mass transfer. Stirring rates also influence membrane stability; higher stirring rates lead to greater membrane swelling and membrane breakage. Stirring speed has to be selected so that an optimal performance level is achieved. Once stirring speed is selected the effect of other variables on extraction is determined.

Initial experimental runs were conducted to study the effect of stirring speed on extraction of phenol from feed solution containing almost 500 mg/dm^3 of phenol (500 ppm, C_{eo}= 5.319E-03 moles/dm^3), the extracting W/O had an internal phase volume (ϕ) of 0.45, the concentration of NaOH in the internal phase was 0.3 M. Treat ratio of 1:15 was maintained during the extraction by dispersing 40ml of the emulsion in 600 ml of the feed solution. Under these set of conditions, the molar ratio (M) of NaOH in the internal emulsion phase to the phenol in the feed phase turns out to be 1.7.

As discussed in the previous section (4.3) minimum stirring speed of 135rpm was necessary to keep the emulsion in a state of dispersion, while above 185 rpm emulsion swelling and breakage becomes substantial. Hence extraction of phenol was carried out at 3 stirring speeds 135, 155 and 185 rpm respectively. The results of these extraction runs are shown in Fig. 4.19.

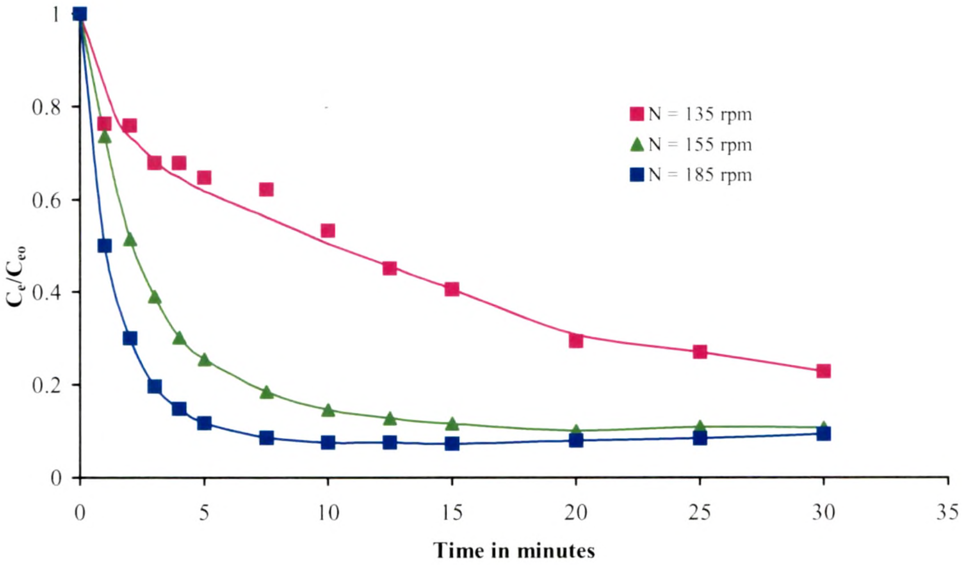

Fig. 4.19: Effect of stirring speed on extraction of phenol

(ϕ = 0.45, Span 80 = 3%, C_{io} = 0.3M, TR = 1:15)

It is apparent from Fig. 4.19 that extraction at 135 rpm is inferior in comparison with the extraction at 155 rpm and 185 rpm. This behaviour is largely attributed to incomplete dispersion of the emulsion in the external phase, keeping in view that at 135 rpm most of the emulsion globules were positioned at the upper part of the vessel and there was a thick film of emulsion floating above the aqueous solution.

Increasing the speed to 155 rpm, the extraction profile shows a pattern that is typical of ELM extraction, a sharp decay was observed in the solute concentrations of the feed in the first five minutes followed by a slower decay for the next 10 minutes and thereafter a steady plateau till the end of the experimental run. Further increasing stirring speeds to 185 rpm shows a more rapid decay in the first 5 minutes followed by plateau in concentration till the end of the run.

It is interesting to note that, after 15 minutes time duration, the extraction curve obtained for 155 rpm comes very close to that for 185 rpm. The terminal concentration for both the runs remains almost the same. However, the initial extraction rates for 185 rpm run was more than that obtained for 155 rpm run. This feature could be conveniently explained by the fact that at 185 rpm the emulsion breaks down into smaller sized globules providing more interfacial area thereby enhancing the rates of mass transfer.

This is evident by comparing Fig. 4.11 (b) and (c), it is found that although for both cases the most frequent globule size is 0.769 mm but at 185 rpm the frequency of this size is 45 % while at 155 rpm it happens to be 35 %. Moreover, at 185 rpm 86 % of the globules are up to 0.769 mm diameter while, at 155 rpm 68 % of the globules is in this size range. The corresponding Sauter mean diameters obtained for the two distributions are 1.1283 mm and 0.8735 mm respectively at 155 rpm and 185 rpm.

Although in this set of runs phenol extraction was found to be quicker when stirring speeds were 185 rpm but setting stirring speeds at 155 rpm for future experiments seemed to be more appropriate for the following reasons.

i. Emulsion stability was suspect at conditions of shear existing at 185 rpm. Even small fluctuations of power causing an increase in the rpm during the run could cause emulsion globule rupture and down loading the contents of the internal emulsion phase in the continuous phase thereby disturbing the entire extraction profile. Past experience (Solanki and Sengupta, 2003) with phenol extraction using toluene based ELMs indicated that substantial membrane breakage could be encountered above 180 rpm.

ii. There was considerably large swelling of the emulsion at 185 rpm due to water transport. Swelling is recognized to be a prelude to membrane rupture.

iii. Globule sizes visually observed at 155 rpm were of fairly uniform size through out the experimental run, and the globules retained their spherical identity. At 185 rpm the globule sizes are very small and it is difficult to distinguish individual globules due to obscuration. Further it was observed that settling times taken for dispersions of 185 rpm were very large in comparison to that for 155 rpm.

iv. Differences in extraction profiles of 155 rpm and 185 rpm were not observed in case of the other solutes. Since this study was defined to be an integrated study of four phenols it was necessary to retain emulsion, dispersion, process parameters identical in all four cases in order to evolve a basic understanding of the factors affecting extraction and their interplay.

Taking the above points into consideration stirring speeds were maintained at 155 rpm for all subsequent experimental runs.

4.5.2 Effect of internal phase volume fraction (ϕ)

Change in ϕ leads to a change in all emulsion properties as discussed in sections 4.1 to 4.3. In the existing literature variation in values of ϕ have not been well investigated as can be seen from Table 2.2. Increasing ϕ increases the density, viscosity and interfacial tension of the emulsion. It also increases the loading capacity of the emulsion as it increases the molar ratio (M) of NaOH to phenol.

Experimental runs were carried out for extraction of phenol from aqueous feed streams containing about 500 mg/dl of phenol using ELMs that contained 0.3 M NaOH in its internal phase. The treat ratio of emulsion to feed was 1:15 and stirring speeds of 155 rpm was maintained in all the runs. Internal phase volume fraction (ϕ) was varied from 0.4 to 0.6 in four steps. The results of these extractions are shown in Fig. 4.20.

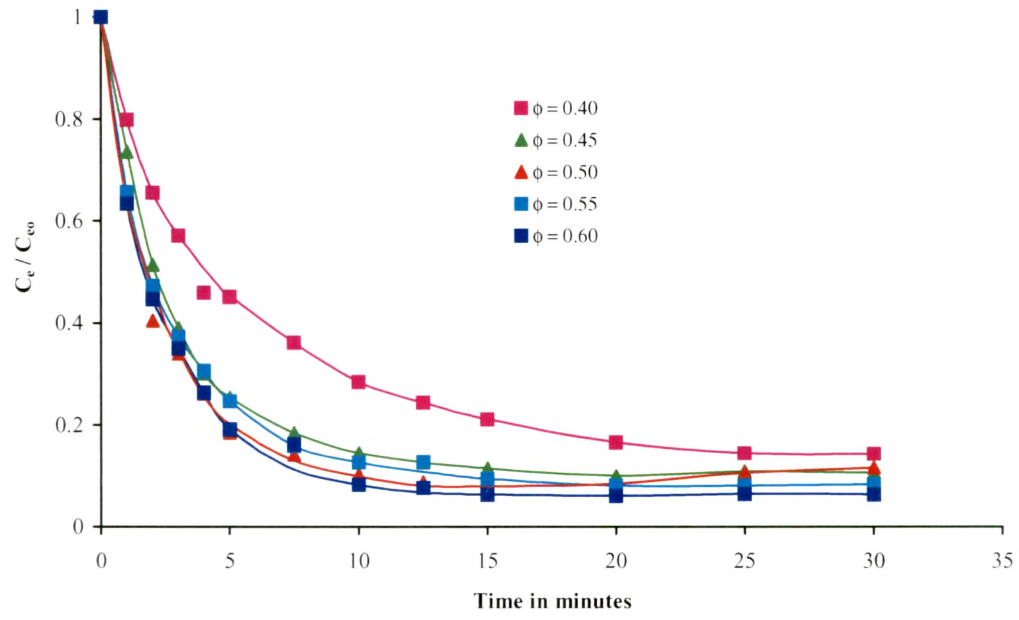

Fig. 4.20: Effect of ϕ on extraction of phenol

(N = 155 rpm, Span80 = 3%, C_{io} = 0.3M, TR = 1:15)

The phenol extraction curve for the case of $\phi = 0.4$ lies distinctly above all other curves indicating a slower rate of extraction of phenol. It is interesting to note that, in this particular case, the interfacial tension between the emulsion and the feed is lower than that obtained for all other cases; indicating that smaller globule sizes would be obtained in comparison with other emulsions having $\phi>0.4$ under identical stirring conditions leading to greater external surface area, moreover internal surface areas would also be greater than cases of $\phi>0.4$ since internal drop sizes also increase with ϕ. Emulsion viscosity is also lower for the case $\phi = 0.4$ in comparison with $\phi > 0.4$, further according to the Jefferson equation the effective diffusivity values of phenol in the emulsion does not change significantly with change in ϕ.

While all the above-mentioned factors do favour rapid extraction of phenol using ELMs having $\phi = 0.4$ in comparison with cases where $\phi > 0.4$, there are two factors which go against it. Firstly when $\phi = 0.4$ the molar ratio of NaOH to phenol is less in comparison with cases when $\phi > 0.4$ indicating lower capacity of the ELM for extraction which is evident from the Fig. 4.20 since the curve for ϕ reaches a plateau much higher C_e/C_{eo} values.

Secondly the emulsion morphology does play a very important role in defining extraction rates; larger values of ϕ would mean internal droplets crowding together in the emulsion globule and at any radial plane within the globules more droplets would be encountered in comparison with case where ϕ value is low. Therefore, it results in longer diffusional path length to be traversed when the ϕ value is low in comparison with the case when ϕ value is high. Increased path lengths within the globule certainly slow down the rates of extraction thereby resulting in profiles as seen in the Fig. 4.20. This aspect may also be thought of as transport through thick membranes.

Focusing attention on $\phi \geq 0.45$ and greater it was found that extraction curves crowd near each other in the first five minutes of the run there after they diverge out, each reaching its plateau in its own way depending on the capacity of the emulsion to extract the solute. Thus it was observed that for the emulsion with $\phi = 0.6$, where the molar ratio $M = 2.25$, the curve not only slide from the bottom but also showed greatest amount of solute removal in comparison with the other runs with $\phi < 0.6$.

It is observed that the curves of $\phi = 0.5$, $\phi = 0.55$, $\phi = 0.6$ superimpose on each other for three minutes, while the curve for $\phi = 0.45$ passes slightly above these curves and is through out distinguishable, surprisingly greater amount of extraction is seen for $\phi = 0.5$ in comparison to that for $\phi = 0.55$ up to 15 minutes sampling time. Such behaviour cannot be attributed to any single factor may have to do with the complex interplay of various emulsion and dispersion characteristics. It is felt that membrane morphology changes beyond certain value of ϕ, and it has a lot to do with the extraction behaviour.

However, during the course of extraction experiments, it was realized that although in literature investigators (Table 2.2) preferred to use emulsions with $\phi = 0.5$, but more stable membranes were obtained in this work with $\phi = 0.45$. In order to gather deeper understanding of the influence of ϕ on extraction it was decided to study the effect of other major variables at two different values of ϕ i.e. at $\phi = 0.45$ and $\phi = 0.5$. It may be noted that $\phi = 0.5$ corresponds with an emulsion containing equal volumes of oil and water phases, while $\phi = 0.45$ corresponds to an emulsion containing equal mass of water and kerosene.

4.5.3 Effect of surfactant concentration

Emulsions prepared with optimal amount of surfactant are necessary for successful implementation of ELM process. Too little surfactant renders the membrane weak and unstable while excess of surfactant adds to diffusional resistance and creates difficulty in demulsification step. Further, excess of surfactants often lead to excessive water transport thereby swelling up the emulsion that could precipitate globule rupture.

In this study, the surfactant (Span 80) concentration is expressed in % wt based on the membrane phase. Effect of Span 80 concentration was investigated at $\phi = 0.45$ and $\phi = 0.5$ keeping other parameters constant such that the stirring speed was set at 155 rpm, feed concentration was 500 mg/dl, NaOH concentration was 0.3 M in the internal phase.

The results of experimental runs are shown in Fig. 4.21(a) with $\phi = 0.45$ and Fig. 4.21 (b) with $\phi = 0.5$. It comes as no surprise to find that emulsions prepared with W_{surf} = 1 % the extraction curve pass well above the extraction curves for emulsions prepared with $W_{surf} \geq 3$ %, while the extraction curves with emulsion containing W_{surf} = 3% and W_{surf} = 4.7 % superimpose on each other. This behaviour is attributed to emulsion stability. A number of investigators (Goto *et al.* 1987, Ma and Shi 1987, Hirato *et al.* 1990) observed that a critical surfactant concentration exists, at which the number of surfactant molecules oriented at the membrane interface is sufficient to make the membrane stable. Above this critical surfactant concentration, a further increase in surfactant appears unnecessary for membrane stability.

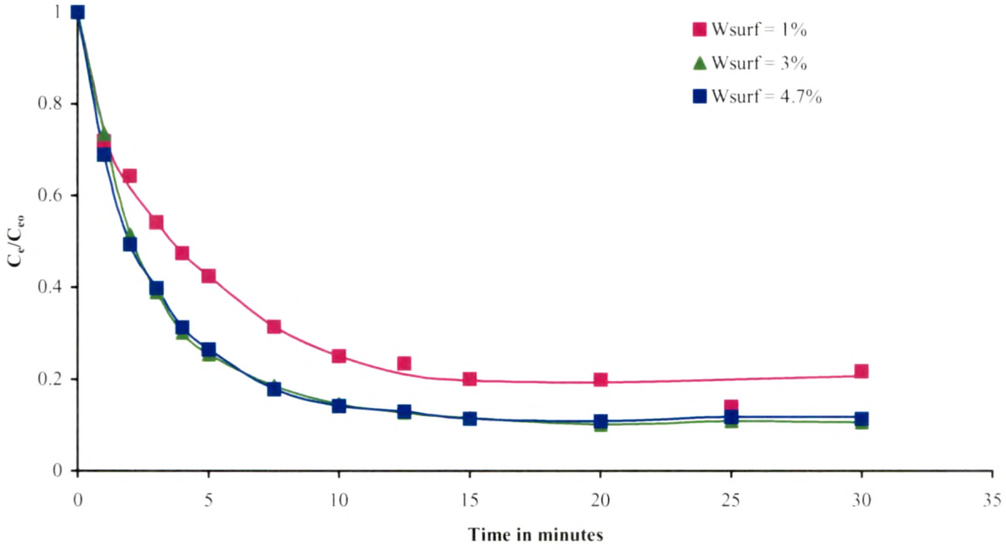

Fig. 4.21(a): Effect of surfactant concentration on extraction of phenol (N = 155 rpm, $\phi = 0.45$, $C_{io} = 0.3M$, TR = 1:15)

When the surfactant concentration in the membrane is inadequate the inner phase is not properly encapsulated within the membrane matrix and this leads to initial leakage of the internal phase after the emulsion is added to the feed. Ho and Li (1984) reported such behaviour and there is evidence of such behaviour in this work. It was observed that with emulsions containing 1 % surfactant concentration the final volume of emulsion collected at the end of the run registered a 3 ml decrease in volume; this 3 ml emulsion loss accounts for 1.35 ml of aqueous phase leakage, which accounts for 4.05 x 10^{-4} M of NaOH leaked to the external phase. The NaOH leaked out during initial dispersion would form an equivalent amount of phenolate that is insoluble in the membrane thereby reducing the effective removal by about 12.69 %; when one compares the extraction curves with W_{surf} = 1 % with that of W_{surf} = 3% in Fig. 4.21(a) it is almost the same amount by which these two curves differ. Thus, even a small leakage of internal phase though seemingly not significant could profoundly affect the emulsion performance.

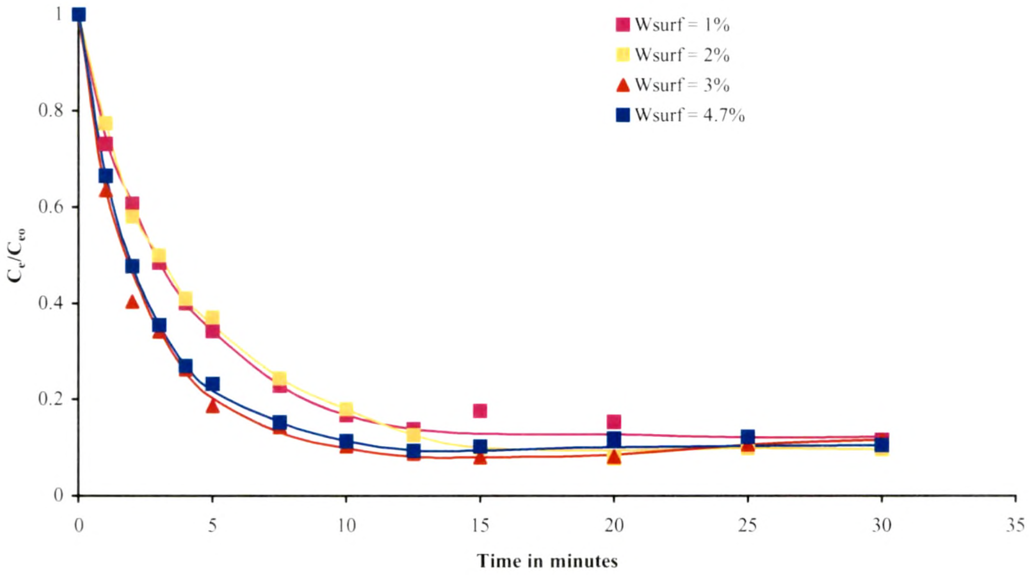

Fig. 4.21 (b): Effect of surfactant concentration on extraction of phenol (N = 155 rpm, $\phi = 0.5$, $C_{io} = 0.3M$, TR = 1:15)

Almost similar behaviour can be noticed in Fig. 4.21(b) where $\phi = 0.5$. In this set four surfactant variations were studied. In the initial 10 minutes the curves for 1 % surfactant variation superimposes on the curve for W_{surf} = 2 %, while the curves for 3 % and 4.7 % surfactant concentration again superimpose on each other. The curve for 2 % surfactant concentration provides additional insight on the effect of surfactant concentration on ELM extractions.

The 2 % curve flattens out at a different value in comparison with 1 % curve indicating that although both emulsions are not stable but emulsion with 2 % surfactant is relatively more stable and does not break out after the initial breakage during dispersion; the final volume of the emulsion was just 1ml less than the initial amount introduced. When surfactant amount is increased to 3% and 4.7 % in the initial stages there is no membrane leakage/breakage while at a later stage after 15 minutes or so there appears to be some signs of membrane globule rupture that corresponds with an increase in C_e / C_{eo} values. This trend arises due to swelling of the emulsion and its breakage due to shear in which the surfactant concentration plays a synergistic role by facilitating water transport inside the emulsion.

Comparing the extraction curves of emulsions with different values of ϕ but same surfactant concentration one finds that the difference is significant when W_{surf} = 1 %, it totally diminishes when W_{surf} = 4.7 %. One plausible explanation that could be extended for this behavior is that the diffusion resistance increases significantly with increase in W_{surf} so as to overcome any advantage gained by increase in ϕ . However, it was found that neither the emulsion viscosity, nor the interfacial tension between the emulsion and the feed phase changed in the range of surfactant variations studied in this work. Another possibility is that the enhanced surfactant concentration alters the drop size distribution of the suspended droplets in the emulsion in almost the same fashion making both emulsions behave identically.

4.5.4 Effect of internal phase reagent concentration (C_{io})

Increasing the internal phase reagent (NaOH) concentration leads to an increase in the capacity of the emulsion to extract more solute. Experiments on phenol extraction with ELMs were carried out using emulsions having ϕ = 0.45 and ϕ = 0.5 and five different internal phase concentrations. In all of these experimental runs the treat ratio was 1: 15, stirring speed 155 rpm, and feed concentration was 500 mg/dm^3.

Results of these experimental studies are plotted in Figs. 4.22(a) and 4.22(b) for the cases of ϕ = 0.45 and ϕ = 0.5 respectively. Some relevant details are also listed below that gives a basis for comparison between the experimental runs.

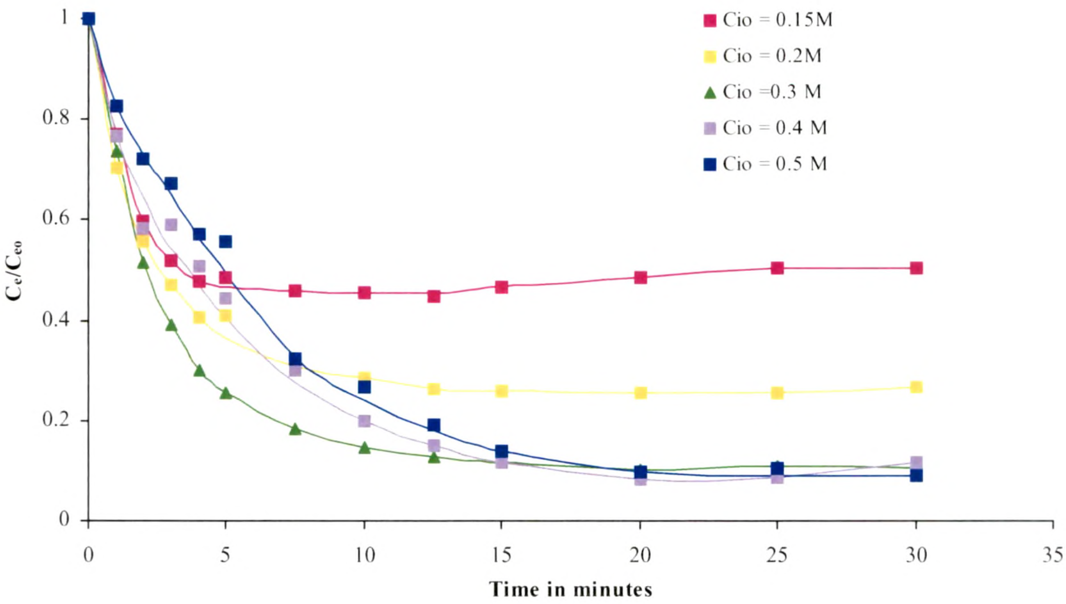

Fig. 4.22(a): Effect of C_{io} on extraction of phenol

(N = 155 rpm, $\phi = 0.45$, Span 80 = 3%, TR = 1:15)

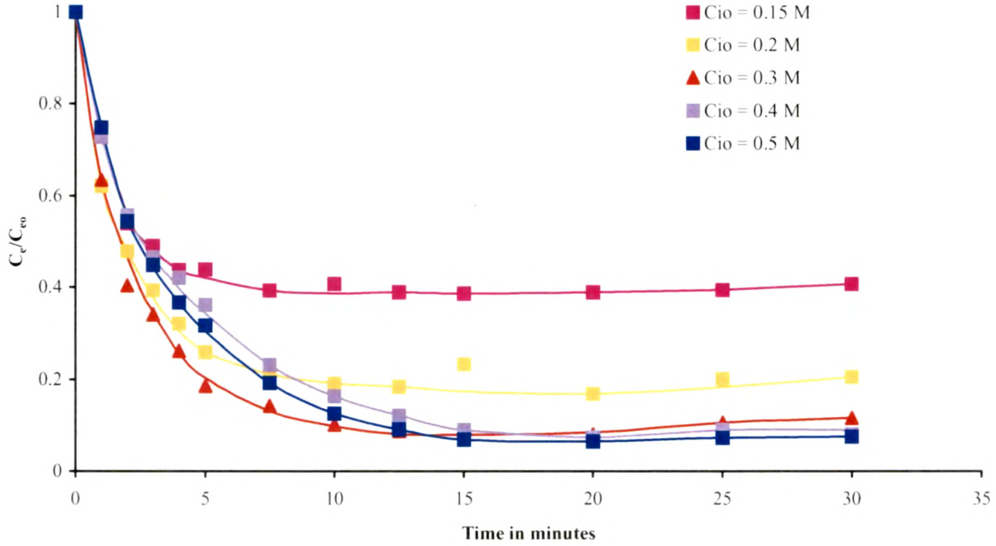

Fig. 4.22 (b): Effect of C_{io} on extraction of phenol

(N = 155 rpm, $\phi = 0.5$, Span 80 = 3%, TR = 1:15)

C_{io} (M)		0.15	0.2	0.3	0.4	0.5
$\phi = 0.45$	Molar ratios of NaOH to phenol (M)	0.83	1.19	1.69	2.29	2.80
$\phi = 0.5$		0.94	1.23	1.87	2.48	3.03

Comparing the extraction plots at $\phi = 0.45$, as shown in Fig. 4.22(a) it is observed that increasing the concentration of NaOH in the internal phase of the emulsion increases the molar ratio of NaOH / phenol in the system and correspondingly leads to greater extraction of phenol. It is particularly interesting to compare the run having $C_{io} = 0.15$ M with $C_{io} = 0.2$ M. It is also observed that there is a sharp increase in extraction with small increase in concentration of NaOH in the internal phase of the emulsion. However, from the data tabulated above there is sharp increase in molar ratios of NaOH to phenol in these two cases. There is a transition of NaOH from limiting reactant to excess reactant when C_{io} is increased from 0.15 M to 0.2 M.

Almost similar behaviour is seen when C_{io} is increased from 0.2 M to 0.3 M and the increase in the molar ratio leads to an increase in extraction capacity of the emulsion and a greater removal of phenol is obtained at all sampling times. Comparing the extraction curves obtained for C_{io} values of 0.3, 0.4 and 0.5 the extraction curves obtained for C_{io} values of 0.4 M also 0.5 M pass above the curve obtained for $C_{io} =$ 0.3 M for the first 15 minutes of the run indicating lower extraction rates up to sampling times of 15 minutes. Thereafter these two curves plateau at C_e/C_{eo} values of 0.09 almost near the final $C_e/C_{eo} = 0.1$ obtained for the curve having $C_{io} = 0.3$ M. This behaviour seems anomalous since increase in C_{io} certainly increases the emulsions capacity for extraction of phenol but this is not manifested in the results obtained for cases of C_{io} values of 0.4 and 0.5.

The anomalous behaviour observed could be explained by considering the emulsion characteristics that were discussed in previous sections. Referring to the histograms shown in Fig. 4.3 and Fig. 4.14, one can easily make out that internal drop sizes and the emulsion globule size both increase with an increase in internal phase NaOH concentration of the extracting W/O emulsion. Thus, at NaOH concentration $C_{io} = 0.5$ M, where $d_{32} = 1.4932$ mm forms 22,946 globules from 40 ml of dispersed phase generating total external surface area of dispersed droplets = 0.1607 m^2 while in case of $C_{io} = 0.3$ M, where $d_{32} = 1.128$ mm forms 53,185 globules from 40ml of dispersed phase generating total external surface area of 0.2126 m^2.

The decrease in external surface area with increase in NaOH concentration and simultaneous decrease in the inner surface area with increasing concentrations both have an inhibiting effect on the rates of mass transfer which is reflected in the extraction plots. Secondly the decrease in emulsion viscosity that was observed at 0.3 M observed in Fig. 4.5 which is expected to have favoured the diffusion of phenol in the emulsion

It is interesting to note that excess capacities to extract phenol in the ELMs with high NaOH concentration in the internal phase is often wasted in single stage extractions. Assuming that all the phenol extracted gets converted into phenolate ions in the internal phase with undissociated phenol not existing in the membrane phase, NaOH utilization was 65.8 %, 66.5 %, 53.2 %, 40.2 % and 32.1 % for C_{io} of 0.15 M, 0.2 M, 0.3 M, 0.4 M and 0.5 M respectively. Chan and Li (1974) while discussing on this aspect commented that more than 50 % NaOH utilization was usually never encountered.

The effect of C_{io} on the extraction of phenol at $\phi = 0.5$ shows a behaviour that is absolutely similar to the effect observed for $\phi = 0.45$ and is seen in Fig. 4.22 (b). Comparing Figs. 4.22(a) and 4.22(b) one can make out that extraction of phenol is approximately 10 % more in almost all cases when $\phi = 0.5$ while all other trends remain the same. This feature was expected and understandable in the light of the earlier discussion in Section 4.5.3.

4.5.5 Effect of Treat ratio (TR)

Treat ratio is a process parameter and defined as the ratio of volume of emulsion to feed. Increasing the treat ratio means increasing the emulsion content in the system. It is a term synonymous with solvent to feed ratio used in liquid-liquid extraction. Many investigators (Chan and Li 1974, Chang and Li 1983, Kim *et al.* 1983) studied phenol extraction with treat ratio as high as 1:2. However, for commercial applications such large values of treat ratio are unwarranted. A more reasonable value for treat ratio would be around 1: 10 and lower. Ho *et al.* (1982), Boyadzhiev *et al.*(1984), Fudu *et al.* (1985) experimented in this range.

In this investigation the effect of treat ratios were studied in the range of 1:20 to 1:6 using W/O emulsions with $C_{io} = 0.3$ M and $W_{surf} = 3$ %(wt). The emulsions were always dispersed at 155 rpm and the feed concentration was almost 500 mg / dm^3 for all the runs. Two sets of emulsions were studied one with $\phi = 0.45$ and the other having $\phi = 0.5$, and results of these experiments are plotted in Figs. 4.23 (a) and 4.23 (b) respectively.

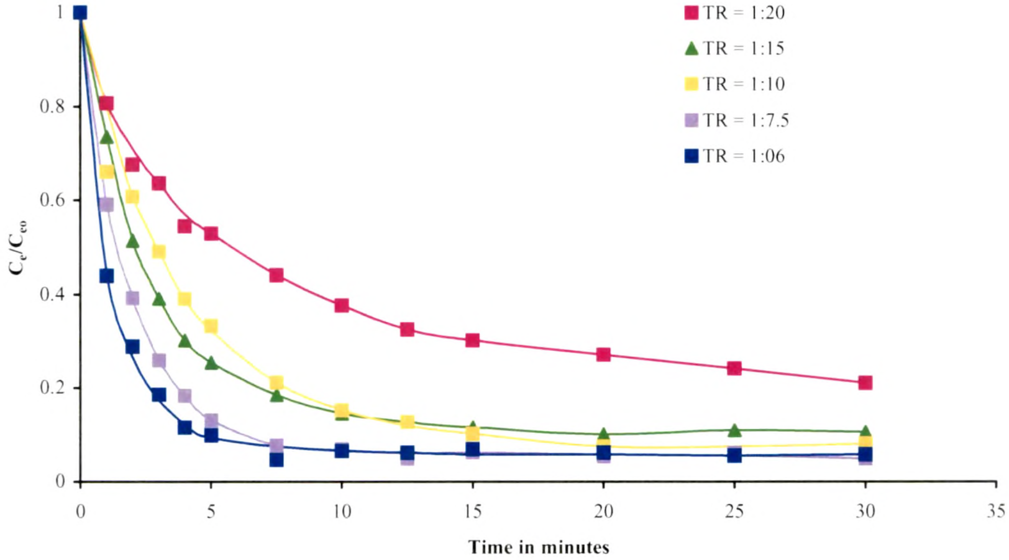

Fig. 4.23 (a): Effect of TR on extraction of phenol

(N = 155 rpm, $\phi = 0.45$, Span 80 = 3%, C_{io} = 0.3M)

Increasing treat ratio certainly increases the capacity for extraction. However, other physicochemical factors also have a role to play. When the total volume of the feed is kept constant, low treat ratio would mean that less amount of emulsion is introduced in the system. If one assumes that the Sauter mean diameter d_{32} remains constant irrespective of the amount of emulsion in the system, one would conclude that the number of globules formed would be less when less emulsion is introduced and this would lead to a decrease in the external surface area available. Hence, low treat ratios not only reduce the extraction capacity of the emulsion it would also reduce the rate of extraction. This trend is visible in both Figs. 4.23 (a) and Fig. 4.23 (b).

One must however take into consideration the fact that when treat ratios are continuously increased at some stage the globule size distributions also change. In this study with emulsion having $\phi = 0.45$, the d_{32} value was found to be 1.128mm when treat ratio was 1:15 and it was 1.295 mm for treat ratio of 1: 6. Increase in globule sizes is also visually observed and is expected to happen in view of the crowding of globules in the dense dispersion of emulsion in the continuous aqueous phase that promotes coalescence of globules

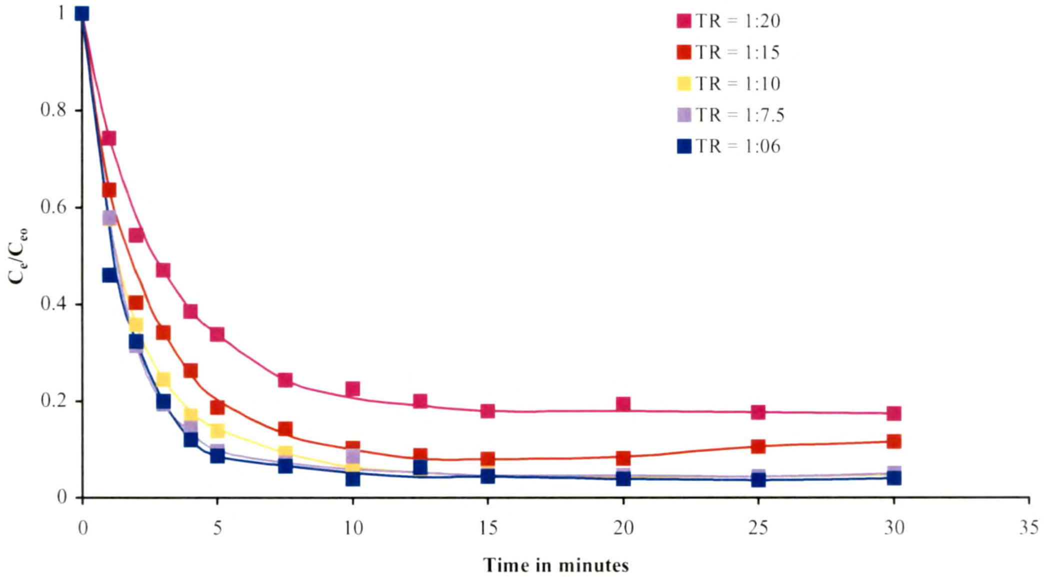

Fig. 4.23 (b): Effect of TR on extraction of phenol

(N = 155 rpm, ϕ = 0.5, Span 80 = 3%, TR = 1:15)

Fig. 4.23 (a) poses a number of queries that are difficult to resolve. The initial rates of extraction at treat ratio of 1:10, are less than the initial rates at treat ratio of 1: 15. Incidentally in this range, the dispersion of emulsion in continuous phase is not dense enough that a major change in globule size distribution would manifest and change d_{32} values. This type of freak behaviour was not observed in any other run in this system. It could perhaps be due to improper dispersion of the emulsion during initial stages.

Further, it is observed the extraction curve for treat ratio 1:7.5 merge with the curve for treat ratio of 1:6 after 10 minutes of the run. The initial rates with treat ratio 1:6 are more than that for 1:7.5 not just due to an increase in extraction capacity but also due to increase in the surface area for mass transfer, in view of more amount of emulsion present in the system.

Interestingly, the experimental runs for treat ratio variation with $\phi = 0.5$ does not show the anomalies observed in the earlier runs. In these runs, the extraction curve for treat ratio 1:7.5 and that for treat ratio 1:6 superimpose on each other indicating that above a treat ratio of 1:7.5 not much advantage can be gained by putting more emulsion in the system. However, comparing both these Figs., even with a small increase in ϕ a considerable increase in extraction rates is achieved particularly at low treat ratios. A summary of these 10 runs with treat ratio variation is presented below:

		Treat ratio				
		1:20	1:15	1:10	1:7.5	1:6
$\phi = 0.45$	Molar ratio	1.25	1.69	2.60	3.50	4.24
	% Phenol removal	80	90	94	95.2	94.3
	% NaOH utilization	62.5	53.2	36.2	27.2	22.2
$\phi = 0.50$	Molar ratio	1.4	1.87	2.78	3.78	4.72
	% Phenol removal	82.5	92	95.6	95.6	96.3
	% NaOH utilization	59	49.2	34.3	25.3	20.4

In the literature there were instances where almost 99 % of phenol was removed within 10 minutes but in all such cases the treat ratio was kept very high and high removal was recorded but with very low NaOH utilization. It is time to design ELM systems that would give high removal coupled with greater utilization of NaOH.

4.5.6 Effect of initial phenol concentration (C_{eo})

Effect of initial phenol concentration is complimentary to the effect of internal phase concentration and also to the effect of treat ratio. Emulsions having same extraction capacities were tried out with feed solutions with different initial feed compositions; this led to a change in the molar ratios NaOH to phenol and expected to reflect on the extraction profiles.

In this investigation, initial feed concentrations were varied in the range of 200 mg/dm^3 (200ppm) to 800 mg/dm^3 (800ppm). ELMs with $\phi = 0.45$ also $\phi = 0.5$ were used for extraction, in both sets emulsions were prepared having surfactant concentration of 3 % (wt) and internal phase concentration of 0.3 M. Treat ratio and stirring speed were maintained at 1: 15 and 155 rpm respectively hence it is expected that the globule size distribution in each set of runs would remain more or less constant.

Results of these experiments are shown in Fig. 4.24 (a) for $\phi = 0.45$ and Fig. 4.24 (b) for $\phi = 0.5$. It can be seen in Fig. 4.24 (a) that in the first two minutes all the curves tend to superimpose on each other thereafter they diverge out and plateau according to the capacity of the emulsion to extract and trap phenol. When feed phenol concentration was 803.5 mg/dm^3 the extraction curve flattened out at a higher value of C_e/C_{eo}; this was expected, keeping in view the fact that molar ratio of NaOH to phenol in this case was 0.94, the lowest among all runs.

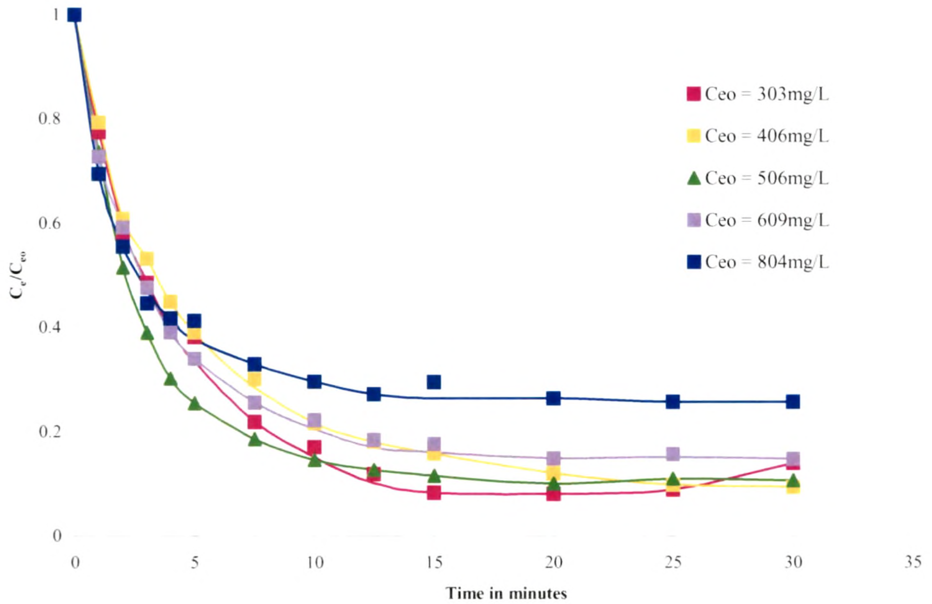

Fig. 4.24 (a): Effect of initial phenol concentration on extraction (N = 155 rpm, $\phi = 0.45$, Span 80 = 3%, $C_{io} = 0.3$M, TR = 1:15)

The initial rate of extraction when phenol concentration was 505.7 mg/dm3 appeared to be the highest indicating an optimal combination of parameters in this run. During the first minute, the experimental run with phenol concentration of 803.5 mg/dm^3 registered the maximum change in C_e/C_{eo} which could be attributed to the increased solubility of phenol in kerosene at higher concentrations of phenol in aqueous phase, the distribution coefficient being 0.2036 at 803.5 mg/dm^3 in comparison with 0.1719 at 505.7 mg/dm^3.

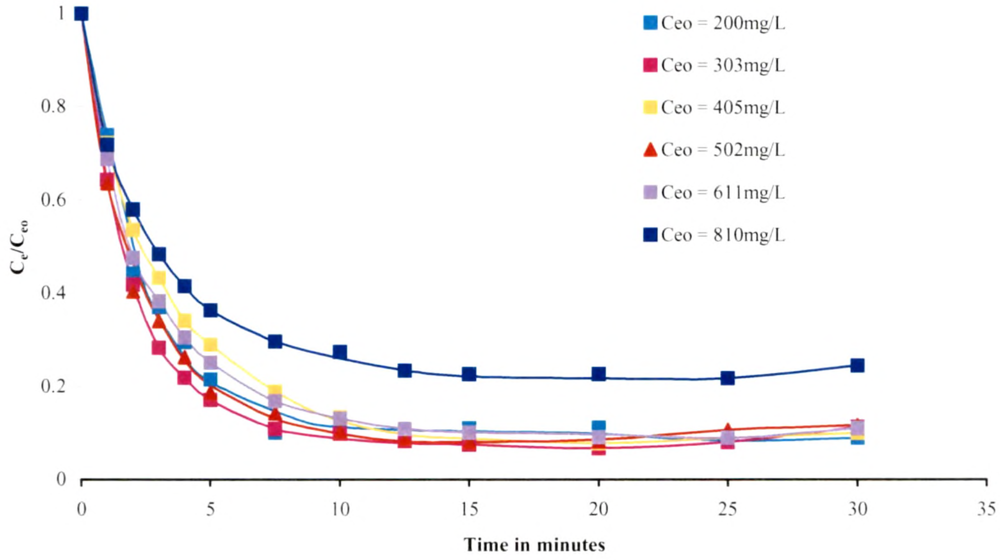

Fig. 4.24 (b): Effect of initial phenol concentration on extraction

(N = 155 rpm, ϕ = 0.5, Span 80 = 3%, C_{io} = 0.3M, TR = 1:15)

Another aspect that needs to be seen is that when initial concentrations are increased the same amount of emulsion extracts greater amounts of phenol during the run, if capacity is not a constraint. This aspect is evident from the table given below that highlights some of these features.

C_{eo} mg/dm^3	303	406	505.7	609	803.5
Actual removal mg/dm^3	278.7	368.2	454.8	519	596.4
$(1-C_e/C_{eo})$ x 100	91.97	90.68	89.94	85.21	74.23
Molar ratios	2.82	2.10	1.69	1.40	1.06
% NaOH Utilization	32.54	43.1	53.23	60.73	69.81

One should note that when the initial phenol concentration is higher the internal droplets in the peripheral region of the globule are more rapidly saturated with phenol and further extraction is possible when the phenol permeates further inside the globules. At low initial concentrations of phenol since the droplets in the periphery trap most of phenol hence a fast rate of removal is recorded. Percent NaOH utilization is another parameter that gives a qualitative idea of the extent of solute penetration in globules; more the % NaOH utilization, the deeper the penetration of phenol within the globules. Since more diffusional resistance will certainly encounter deeper penetration of phenol within the globules, it would always be associated with slower rates of removal. This is evident from the extraction plot for C_{eo} = 803.5 mg/dm^3.

In Fig. 4.24 (b), where $\phi = 0.5$, similar overall trend is noticed as that for extraction curves for $\phi = 0.45$. However, in this case the internal droplets have greater capacity to trap phenol due to increase in ϕ, hence extent of extraction is more at all initial phenol concentrations. The most interesting feature of this figure is that the extraction curves for C_{eo} = 611 mg/dm^3 and C_{eo} = 502.47 mg/dm^3 almost move together through out the course of run. Further except for the extraction curve for C_{eo} = 809.6 mg/dm^3 all the other curves crowd together. Surprisingly the initial rates for the run with C_{eo} = 200.2 mg/dm^3 are less than that observed for the run with C_{eo} = 502.47 mg/dm^3 this feature may be attributed to the relatively low distribution coefficient of kerosene to water that is 0.144 when C_{eo} = 200.2 mg/dm^3 in comparison to 0.172 for C_{eo} = 502.47 mg/dm^3.

When C_{eo} = 406 mg/dm^3 the value of the distribution coefficient (kerosene to water) is 0.154, which is lower than the distribution coefficients at other concentrations this results in initially lower rates of extraction that is observed in both Fig. 4.24 (a) and Fig. 4.24 (b).

4.5.7 Extraction of phenol at constant molar ratio (M)

A critical analysis of the various experimental results discussed above made one thing apparent. Whenever large amounts of phenol were extracted, the NaOH utilization was quite low and the molar ratio NaOH / phenol was reasonably high. The molar ratio, in a way, is a measure of the capacity of the emulsion to extract any solute. Whenever the internal phase concentration C_{io} is changed or the treat ratios are changed or even when initial feed concentrations are changed, it always results in change of the molar ratio of NaOH / phenol. Therefore it was felt that true assessment of the effects of treat ratio as well as the effect of initial phenol concentration on extraction behaviour could only be obtained by maintaining a constant molar ratio of NaOH / phenol in all these runs.

4.5.7.1 Effect of treat ratio at constant molar ratio

Extraction runs were performed by maintaining the molar ratio of NaOH / phenol while changing the treat ratio of emulsion to feed. As in the earlier case, two different sets of experiments were carried out one with emulsions having $\phi = 0.45$ and the other having $\phi = 0.5$. Molar ratio of 1.7 was chosen as the value that would be maintained for treat ratio variations using emulsions with $\phi = 0.45$. The value of 1.7 corresponded to the molar ratio of NaOH /phenol when initial phenol concentration was 500 mg/dm^3, treat ratio is 1: 15 and $C_{io} = 0.3$ M with feed volume being 0.6 dm^3. With emulsions having $\phi = 0.5$ the molar ratio of NaOH / phenol was maintained at 1.88 using similar considerations as mentioned above.

When treat ratios were varied in order to maintain $M = 1.7$ or $M = 1.88$ as the case may be, the internal phase concentration of NaOH, C_{io}, were appropriately modified such that in each case the value of M was close to its desired value. It was recognized that changes in C_{io} would some what affect the overall extraction kinetics due to changes in internal droplet distribution also the emulsion globule sizes; however, compared to the advantage of gaining information on the extraction kinetics at constant emulsion capacity these affects appear to be marginal.

In all runs of variation of treat ratios at constant molar ratio, the initial phenol concentration was about 500 mg/dm^3, Span 80 concentration was 3 %(wt) of kerosene phase and stirring rates was maintained at 155 rpm. The results of extraction with emulsions having $\phi = 0.45$ are shown in Fig. 4.25 (a) and for emulsions with $\phi = 0.5$ are shown in Fig. 4.25 (b). These Figs., present revealing information and may be contrasted with Fig. 4.23 (a) and 4.23 (b) respectively.

Fig. 4.25 (a) shows that all extraction curves obtained for varying treat ratios eventually converge at a time interval of 25 minutes; convergence is expected because the capacities of all the emulsions are the same. Of particular interest is the curve for treat ratio of 1:20 if we contrast this curve in Figs. 4.23 (a) with that in Fig. 4.25 (a) one can make out the significant change that has resulted by maintaining $M = 1.7$ in the second case; in the previous case M was 1.25.

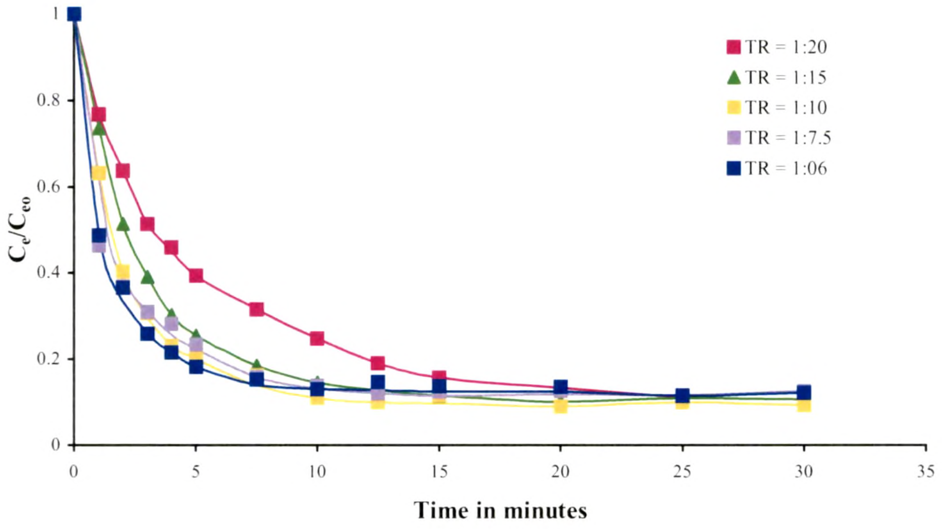

Fig. 4.25(a): Effect of TR on extraction at $M = 1.7$

(N = 155 rpm, $\phi = 0.45$, Span 80 = 3%)

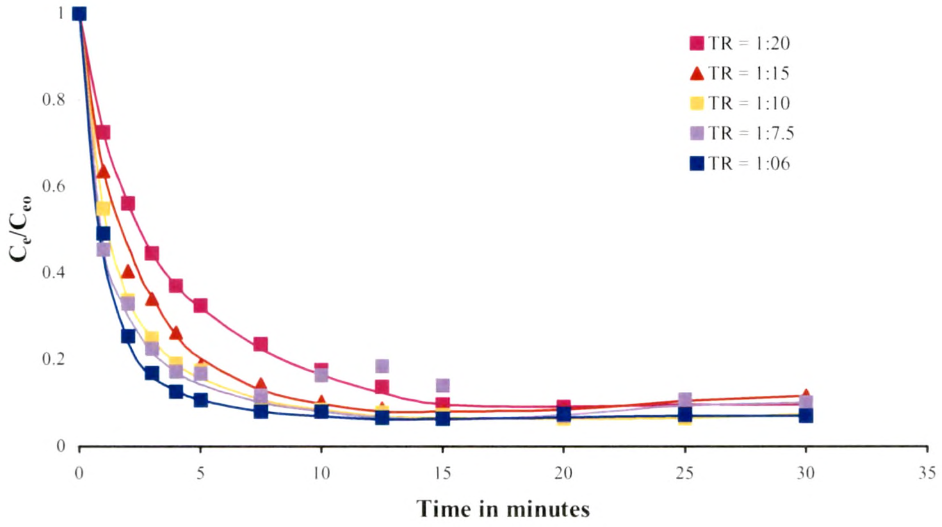

Fig. 4.25 (b): Effect of TR on extraction at $M = 1.88$

(N = 155 rpm, $\phi = 0.5$, Span 80 = 3%)

However, in spite of considerable improvement in extraction rates, still the behaviour of this particular run was not in tune with the other curves of Fig. 4.25 (a) Two plausible reasons are the following:- 1) Emulsion amount added is less hence number of drop formed is less. 2) Since TR = 1:20 in order to maintain $M = 1.7$, C_{io} has to be greater than 0.3 M; when C_{io} increases there is a corresponding increase in inner droplet sizes. Further increase in C_{io} also increases the globule sizes; the net result is larger globules with large internal drops hence comparatively low external surface areas also low internal surface areas. On the whole this particular treat ratio run is area disadvantaged. What is remarkable is that it makes it up to converge with other runs at 25 minutes it is felt that phenol penetration within the globule must have been deepest in this case.

The other runs shown in Fig. 4.25 (a) show the usual behaviour up to about 5 minutes duration thereafter there is slightly jerky behaviour particularly observed in the run for TR = 1:6 this run involves comparatively the largest amount of emulsion with lowest values of C_{io} resulting in small globule sizes also small internal droplet sizes. In terms of surface area this run is expected to have the maximum surface area and the difference between the extraction curves of TR = 1:20 and TR = 1:6 in the Fig. 4.25(a) stems out mostly from their differences in surface areas.

Due to the very large surface area available, the run for TR = 1:6 gives largest initial rates of extraction with the globules getting saturated rapidly with phenol. However, due to over crowding of the globules, coalescence as well as leakage/breakage also seem to be setting in though these features are not very prominent. This behaviour seems to be slightly more pronounced in the extraction with TR = 1: 7.5. It is seen that runs with treat ratio of 1:10 and 1:15 show the overall best behaviour. The table below presents the summary of experiments with varying treat ratios at $M = 1.7$ using emulsions with $\phi = 0.45$. It is seen that the NaOH utilization in all runs was identical.

Treat ratio	Molar ratio	% Recovery of phenol	% NaOH utilization
1:20	1.685	89.33	53.01
1:15	1.69	89.94	53.23
1:10	1.70	91.08	53.51
1:7.5	1.70	88.39	52.07
1:6	1.70	88.49	52.03

Fig. 4.25 (b) presents the extraction behaviour using ELMs having $\phi = 0.5$ with $M = 1.88$. As expected, the behaviour of these runs are almost identical to those shown in Fig. 4.25 (a). One point of difference is that the curves do not converge into one

another they come very close but retain their identities. Each extraction run charts its own path as per extraction rates that appear to be proportional to the surface area available. Expectedly the recoveries are marginally more than those obtained with ELMs having $\phi = 0.45$ but that is understandable in view of the slight increase in molar ratios.

4.5.7.2 Effect of initial phenol concentration at constant molar ratio

Experiments were performed to assess the effect of initial phenol concentrations at molar ratio $M = 1.7$ using ELMs having $\phi = 0.45$ and at $M = 1.87$ using ELMs with $\phi = 0.5$. ELMs were prepared in their usual manner with $W_{surf} = 3$ %, the Treat ratio and stirring speeds were maintained at 1:15 and 155 rpm respectively. In order to maintain constant molar ratios with varying initial phenol concentration values, the internal phenol concentrations were appropriately varied. Results of these experiments are shown in Fig. 4.26 (a) and Fig. 4.26 (b) respectively. They may be contrasted with Figs. 4.24 (a) and Fig. 4.24 (b) discussed earlier

Case 1: $\phi = 0.45$

Fig. 4.26 (a) shows a behaviour that is contradictory to the one observed in Fig. 4.24 (a). This is particularly true for the run where $C_{io} \approx 800$ mg/ dm^3, in the former figure this curve moves down exponentially reaches plateau after 20 minutes and shows maximum removal of phenol (91 %); while in the latter Fig., this curve passes above all other curves and registers minimum removal of phenol (74%). This difference stems out of the fact that in the first case molar ratio was1.7 while in the second case it was just 0.94.

Another peculiarity that is observed while comparing Fig. 4.26 (a) and Fig. 4.24 (a) is that the initial rates of extraction for the 800 mg/dm^3 run is quite less and in fact least, when $M = 1.7$ in comparison with the run when $M = 0.94$ where initial rates were highest. This feature is explained in cognizance of the fact that to balance $M = 1.7$ when $C_{eo} \approx 800$ mg/dm^3 it is necessary to correspondingly increase C_{io} values up to 0.48 M. Increasing C_{io} leads to an increase in globule size also inner droplet sizes of the emulsions leading to a reduction in overall surface area of mass transfer thereby decreasing the mass transfer rates.

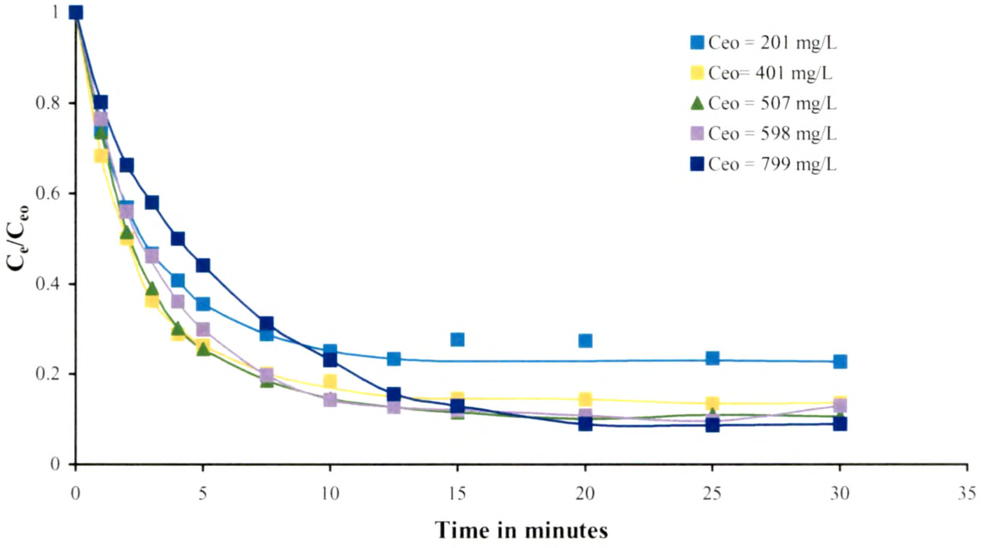

Fig. 4.26(a): Effect of initial phenol concentration on extraction at M = 1.7 (N = 155 rpm, ϕ = 0.45, Span 80 = 3%)

On the same lines the increase in initial rates of the run with $C_{eo} \approx$ 400 mg/dm^3 at M = 1.7 in comparison with the earlier run having M = 2.1 may be explained. In order to balance M = 1.7, the NaOH concentration in the emulsion phase was appropriately reduced to 0.24 M. This lowering of C_{io} leads to a decrease in globule sizes as well as internal droplet sizes resulting in increase in mass transfer area and hence an increase in the initial rates of extraction.

It is further observed from Fig. 4.26 (a) that when $C_{eo} \approx$ 200 mg/dm^3, recovery of phenol is least at M = 1.7, although the initial rates are comparable with other runs. It must be noted that C_{io} values were least in this run. Initially high extraction rates were because of the large mass transfer surface areas obtained due to reasons discussed earlier. It appears that after the initial phase of extraction wherein almost half the phenol was extracted, the phenol concentration in the external feed phase became quite low. Similarly, the internal droplets in the peripheral region of globules also got exhausted of NaOH due to phenol uptake. This results in substantial decrease in phenol solubilized in the membrane phase and also deeper movement into the globule to get reacted and entrapped. This run turns out to be an example of a low driving force diffusion limited transport.

Overall, from Fig. 4.26(a), one finds that extraction run with C_{eo} = 500 mg/dm^3 gives the best performance in terms of extraction rates. The overall % removal of phenol was nearly same in all runs and summary of these runs are listed below:

C_{eo} mg/dm^3	M	% recovery of phenol	Phenol remaining unextracted mg/dm^3	% NaOH utilization
200.6	1.70	77.27	45.60	45.35
401.3	1.70	86.51	54.13	50.78
505.7	1.69	89.94	50.88	53.23
597.9	1.71	90.37	57.58	52.71
798.6	1.71	91.25	69.87	53.31

Case 2: $\phi = 0.5$

Fig. 4.26(b) shows the extraction behaviour of ELMs having ϕ = 0.5 at a molar ratio of M = 1.87. Although the extraction kinetics appears to be identical to Case 1 shown in Fig. 4.26(a), there are subtle differences. Most prominent difference is that all the curves show identical initial rates diverging only after 3 minutes, by that time about 50% extraction is already over. Further, one finds that for $C_{eo} \approx$ 800 mg/dm^3 the initial rates are not so distinctive as in the case of ELMs with ϕ= 0.45. Moreover, shifting of curves for $C_{eo} \approx$ 400 mg/dm^3 that was observed in previous case is not noticed here.

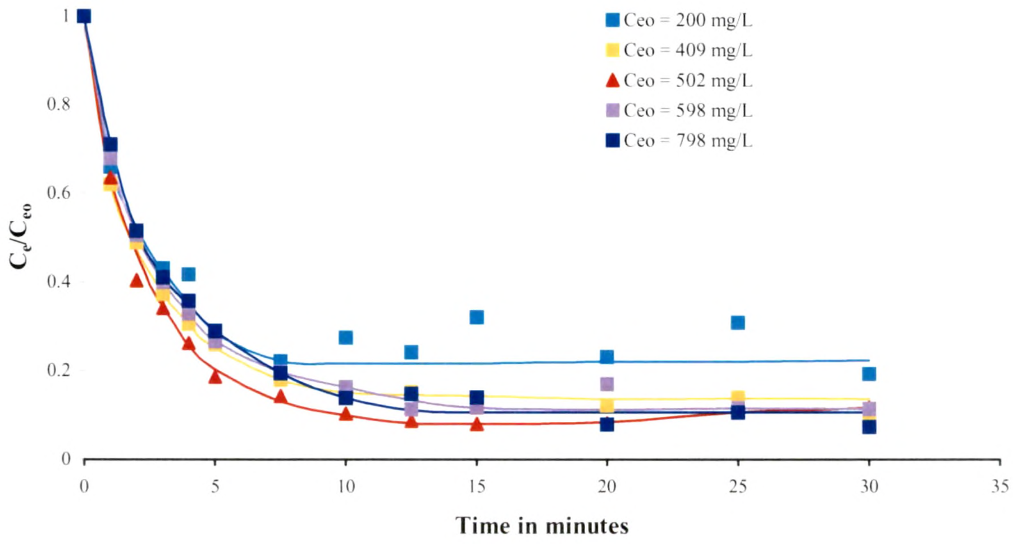

Fig. 4.26 (b): Effect of initial phenol concentration on extraction at M = 1.88 (N = 155 rpm, ϕ = 0.5, Span 80 = 3%)

The increase in ϕ leads to an increase in inner drop sizes as well as in emulsion globule sizes, this increase results in a surface area that is perhaps not significantly affected by changes of $C_{io.}$ In other words, the dominant influence on surface area is that of ϕ. The extent of extraction in all runs was marginally more than what were obtained in Case 1. This is attributed to the slight increase in molar ratios. NaOH utilization was in the range of 47 % to 49%, i.e. slightly on the lower side. As in Case 1, when $C_{eo} = 500$ mg/dm^3, best results were obtained both in terms of extraction rates as well as extent of extraction. This suggests that an optimal condition perhaps exists at this composition in terms of emulsion characteristics and also process parameters.

4.5.8 Effect of Temperature

ELMs are usually designed for operations at ambient conditions. This is particularly true for Type I transport mechanism which is oriented mostly towards water pollution control. However, ambient temperatures itself varies widely with geographical regions, seasons and also during the course of the day.

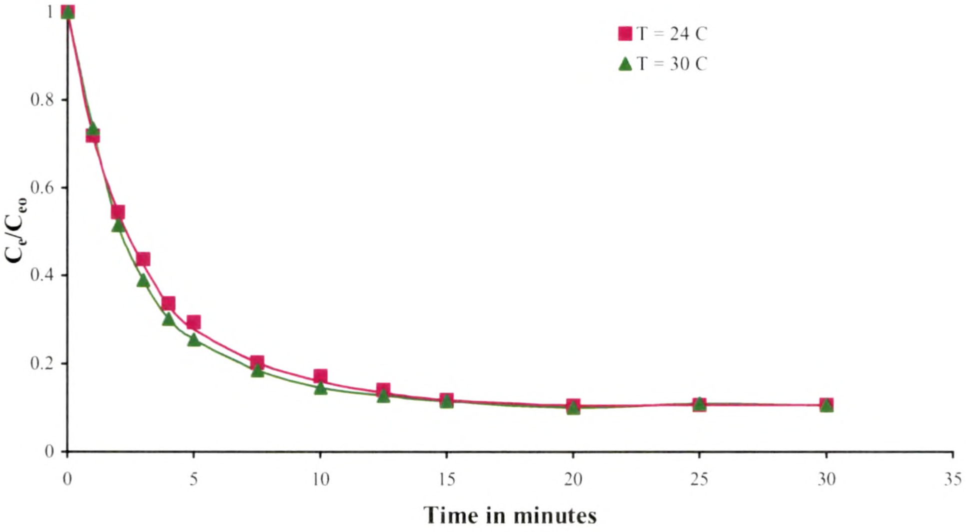

Fig. 4.27: Effect of temperature on extraction of phenol

(N = 155 rpm, $\phi = 0.45$, Span 80 = 3%, Cio = 0.3M, TR = 15)

In order to assess the effect of temperature variation that may take place during the course of the day on extraction of phenol, experiments were carried out at 24°C using ELMs having $\phi = 0.45$ containing $C_{io} = 0.3$ M NaOH and $W_{surf} = 3\%$. The stirring speed was 155 rpm and initial feed concentration C_{eo} = 500 mg/dm^3. The result of this extraction run is presented in Fig. 4.27 in comparison with an identical run carried out at 30°C having same emulsion composition. It can be seen that the effect of temperature in the range of 24 – 30°C is insignificant.

4.5.9 Effect of membrane material

In addition to kerosene, experiments were also carried out using hydro-cracker white diesel fraction as the membrane material. The ELMs having ϕ = 0.45, C_{io} = 0.3 M and W_{surf} = 3 % wt prepared from this diesel fraction had specific gravity of 0.9062, viscosity at shear rates of 38.4 s^{-1} was 18.46 mPa.s and partition coefficient of diesel/water at C_{eo} of 500 mg/dm^3 was 0.1486 at 30°C. These values may be contrasted with 0.9075, 13.32 mPa.s and 0.1719 for specific gravity, viscosity and partition coefficient respectively obtained for kerosene membranes under identical conditions.

It was observed that when dispersed in the feed, the diesel based ELMs rendered larger globules at 155 rpm. Result of this extraction run is presented in Fig. 4.28. It is observed that the diesel ELMs extract phenol more gradually in comparison with kerosene ELMs under otherwise identical conditions. There is considerable difference in the rates of extraction that is attributed to relatively low partition coefficient and high viscosity of the diesel based ELMs. It also appears that morphological differences could exist in these emulsions that may be responsible for the lower rates observed using diesel ELMs. However, this aspect was not investigated further.

In Fig. 4.28, data of an extraction run using toluene based ELMs (Solanki and Sengupta, 2003) under otherwise identical conditions are also plotted, the partition coefficient of phenol is very favorable to toluene and is 1.21 at 33°C, the high solubility results in very rapid extraction of phenol in the initial period of the run. However, toluene ELMs lack stability and are very susceptible to globule rupture. This aspect comes out clear in this run.

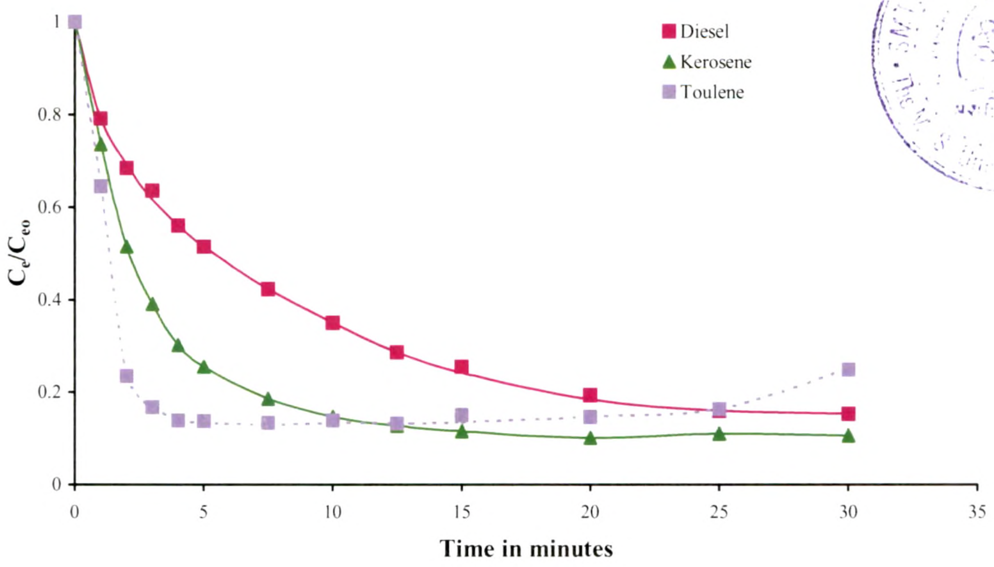

Fig. 4.28: Effect of membrane material on extraction of phenol

(N = 155 rpm, $\phi = 0.45$, Span 80 = 3%, Cio = 0.3M, TR = 15)

4.5.10 Effect of the delayed solute addition

There are instances in literature, where the emulsion was initially dispersed in water and after some time when the emulsion globules reached steady state distribution the solute was quickly poured in to achieve the desired initial solute concentrations (Kataoka *et al.* 1989, Banerjea *et al.* 2000).

Out of curiosity, an experimental run was performed where the emulsion having ϕ = 0.5, C_{io} = 0.3 M, TR = 1:15 was initially dispersed in water at 155 rpm for a time duration of 3 minutes. Thereafter the concentrated solute was poured in to ensure an initial feed concentration C_{eo} = 500 mg/dm^3. Results of this run denoted as Method B, are plotted in Fig. 4.29 and compared with the data obtained when the emulsion was dispersed directly in the aqueous phenol solution having the same initial phenol concentration of 500 mg/dm^3 denoted as Method A. The other emulsion and process conditions were similar.

It is seen that when the solute is added late, the extraction is more gradual and the initial rates are certainly lower than the case of Method B in comparison to Method A. If there had been no breakage, then both the curves would have converged at 30 minutes of the run. However, due to breakage in Method A, convergence is at 25 minutes. Method B does not show any breakage.

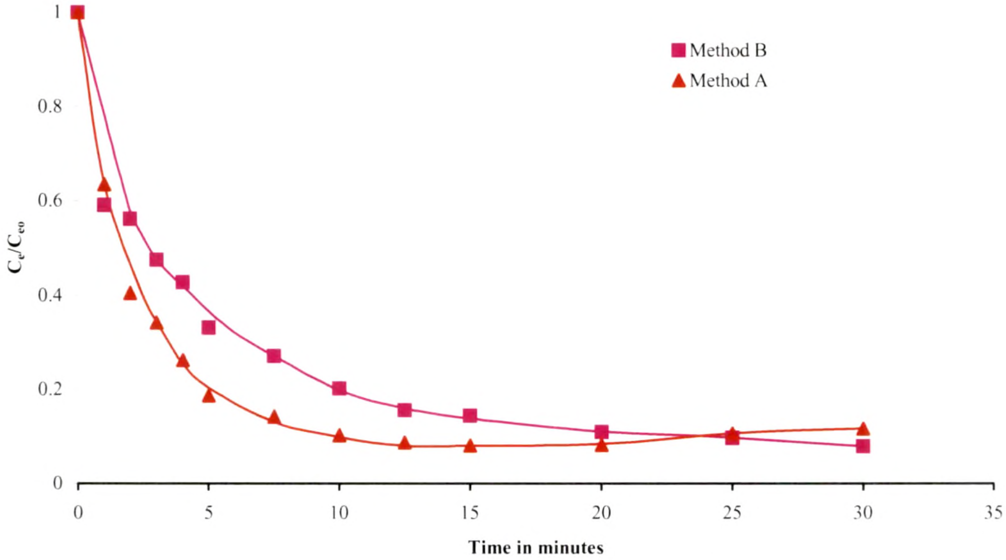

Fig. 4.29: Effect of delayed solute addition on extraction of phenol
(N = 155 rpm, ϕ = 0. 5, Span 80 = 3%, Cio = 0.3M, TR = 15)

It is difficult to explain the differences between Method A and Method B. It is curious to note that the actual difference in these curves begins at 2 minutes, which continues till 10 minutes. After 10 minutes there is almost no driving force for Method A, hence the gap between the curves decreases and the curve for Method B catches up with the curve for Method A. It is discussed in Section 4.3 that the emulsion globules undergo size rearrangements in the initial stages of the run. Perhaps, in the process of fission of emulsion globules, tiny globules having large surface areas are generated that lead to the observed differences in extraction behaviour. Another possibility could be that of micro-mixing effects playing some role.

4.6 EXTRACTION OF o-CRESOL

Extraction of o-cresol using ELMs has not been well studied; Teramoto *et al.* (1983) and Terry *et al.* (1983) focused some attention in this area. However, even these investigators did not attempt to make detailed investigations on the extraction of o-cresol using ELMs. In this study o-cresol extraction into ELMs are studied using well characterized W/O emulsions on the lines parallel to the extraction of phenol. In all nine parametric variations were studied over a span of about 70 experimental runs. Significant results obtained are presented in the following sections.

4.6.1 Effect of stirring speed

Influence of stirring speed on dispersion behaviour is reported in Section 4.3 and its effect on extraction of phenol is reported in Section 4.5.1. The effect of stirring speed on extraction was not expected to be different for o-cresol in comparison to that for phenol, since stirring speed primarily influences the dispersion behaviour and in both systems the dispersion behaviour was identical, because the ELM composition was similar. Moreover, the process conditions were also identical.

However, the effect of stirring speeds was studied under two different sets of conditions. Set I was identical to that discussed for phenol extractions while Set II involved ELMs that were stabilized with more amount of surfactant and also stirred at more speeds. The overall idea was to assess the stability of the ELM system.

Set I

The W/O emulsions were prepared using kerosene as the membrane phase and NaOH solution as the internal phase. The internal phase fraction ϕ was 0.45, Span 80 concentration $W_{surf} = 3\ \%$ (based on oil phase), internal phase NaOH concentration $C_{io} = 0.3$ M, the Treat ratio, TR = 1:15; o-cresol content in the continuous phase C_{eo} was about 500 mg/dm^3.

The emulsion was dispersed in the continuous phase at stirring speeds of 135 rpm, 155 rpm and 185 rpm. Results of the experimental runs are presented in Fig. 4.30 (a). The overall trend was similar to that observed for the case of phenol extraction shown in Fig. 4.19. Fig. 4.30 (a) shows that the extraction curve at 135 rpm lies well above the other two curves, the reason for such behaviour was attributed to the imperfect dispersion of the W/O emulsion in the continuous phase at 135 rpm.

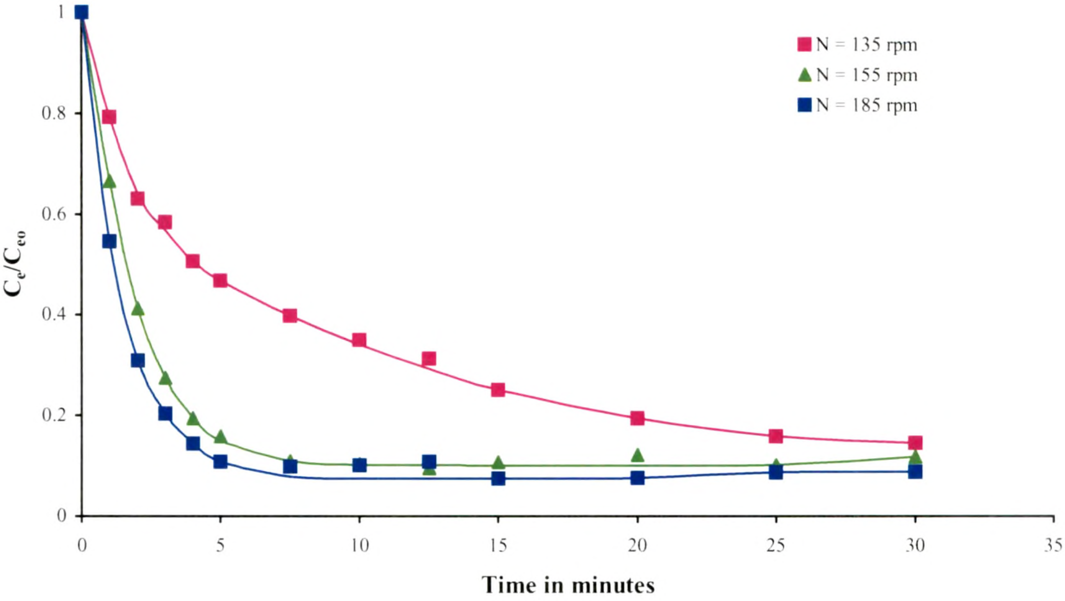

Fig. 4.30 (a): Effect of stirring speed on extraction of o-cresol

($\phi = 0.45$, Span80 = 3%, $C_{io} = 0.3M$, TR = 1:15)

Increasing stirring speed to 155 rpm showed a sharp increase in the solute extracted in the first 5 minutes of the run. Thereafter, the solute concentration in the continuous phase reaches plateau. Further increasing the stirring speed to 185 rpm showed a trend identical to N = 155 rpm, the only point of difference noted was the extraction was more at all sampling times at stirring speed N = 185 rpm. In the initial 2 to 3 minutes of the run about 10% more is extracted at 185 rpm, which by the end of 5 minutes settles to about 5 % more extraction of solutes. The net result is that both the extraction curves almost move parallel one below the other clearly distinguishable at all times.

The reason for relatively more extraction at 185 rpm was attributed to the increased surface area obtained at 185 rpm due to smaller globule sizes. At 155 rpm the globule Sauter mean diameter d_{32} is 1.1283 mm while at 185 rpm the d_{32} is 0.8735 mm. Based on these values of d_{32} the total globule surface area available in the system are 0.2126 m^2 (354 m^2/m^3 of continuous phase) at 155 rpm while at 185 rpm the total surface area available is 0.2747 m^2 (458 m^2/m^3 of continuous phase). This increase in the surface area caused more rapid extraction of o-cresol at 185 rpm.

When comparing the runs of 155 rpm with 185 rpm for the case of phenol vis-à-vis o-cresol, an interesting difference was observed. For the case of phenol in Fig. 4.9, the difference of extraction between 155 rpm and 185 rpm was of the order of 20% in the initial 3 minutes of the run while it was just 10 % in the case of o-cresol. In view of this difference, the relative natures of curves change significantly for both the cases. In the case of Fig. 4.30 both the curves representing 155 rpm and 185 rpm plateau at 5 minutes but in case of phenol the 185 rpm curve reaches plateau at 5 minutes while the 155 rpm curve reaches plateau quite late at 20 min.

Such behaviour is attributed to two causes: 1) The molar ratio M of NaOH to phenol was ≈ 1.7 while in case of cresol $M \approx 2$ (this difference stems from the molecular weight of o-cresol that is 108 kg/kmol while that for phenol is 94 kg/kmol, hence even when all other parameters remain constant for both cases the molar ratios will always be larger for cresols in comparison to phenols). 2) The distribution coefficient for o-cresol between kerosene and water is almost ten times the distribution coefficient for phenol between kerosene and water.

Set II

Severe globule breakage was observed at stirring speed above 185 rpm in the case of both phenol and o-cresol extraction using ELMs. An attempt was made to stabilize the emulsion with larger amount of surfactant. A series of runs were conducted with emulsions prepared using 4.7 % (wt) of Span 80 that were dispersed in the continuous phase at stirring speeds ranging from 135 rpm to 200 rpm.

The emulsion had an internal phase fraction $\phi = 0.45$, Span 80 concentration $W_{surf} = 4.7$ % (wt based on oil phase), internal phase NaOH concentration $C_{io} = 0.3$ M, Treat ratio TR =1:15 and o-cresol content in the continuous phase C_{eo} about 500 mg/dm^3. Results of these runs are shown in Fig. 4.30 (b).

Globule rupture is evident in Fig. 4.30 (b) for the 200rpm experimental run. The significant and steady increase in C_e/C_{eo} is testimony to this inference. Increasing surfactant concentration could not contain globule breakage. Comparing Figs. 4.30 (a) and 4.30 (b), it is observed the trend is almost similar at the other stirring speeds of 185 rpm, 155 rpm and 135 rpm.

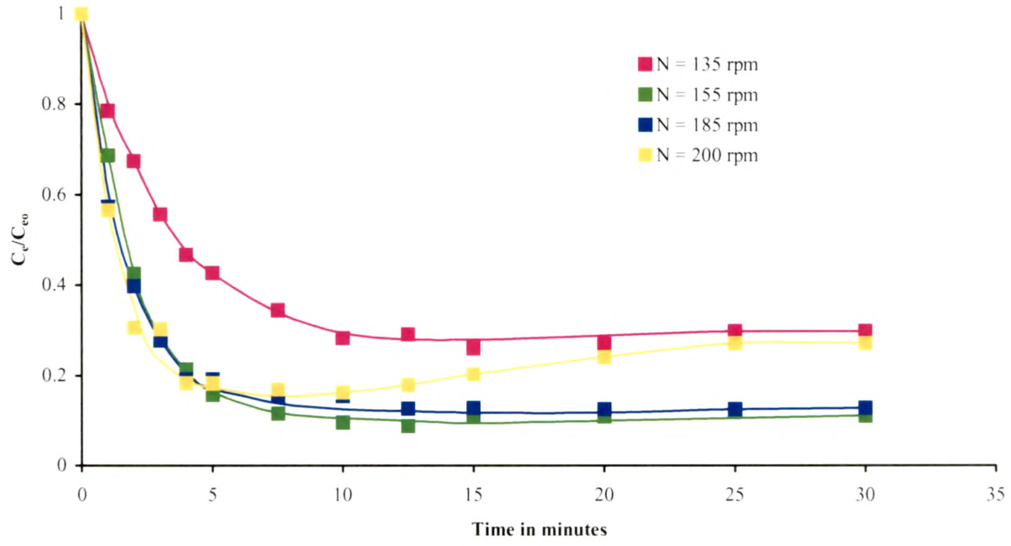

Fig. 4.30 (b): Effect of stirring speed on extraction of o-cresol ($\phi = 0.45$, Span 80 = 4.7%, $C_{io} = 0.3M$, TR = 1:15)

Increase in surfactant concentration increases the diffusional resistance for the movement of solutes inside the ELM globules. This feature is evident in view of the small decrease in the amount extracted at all sampling intervals as seen in Fig. 4.30 (b) in comparison with Fig. 4.30 (a). The curve for 185 rpm almost merges with the curve for 155 rpm in the initial 5minutes of the run. Even at other sampling intervals the points cluster together and for all practical purposes there is no difference between them.

Interesting behaviour is observed for the 135 rpm run with $W_{surf} = 4.7$ %m This curve lies well above the other curves in Fig. 4.30 (b) and reaches plateau after 7.5 minutes registering cresol extraction about 70% (i.e. final $C_e/C_{eo} = 0.3$). Such behaviour is not observed in Fig. 4.30 (a) when $W_{surf} = 3\%$, nor in Fig. 4.19 for phenol extraction at 135 rpm. In both these cases a plateau in concentration was not observed.

It is felt that this behaviour is prompted by imperfect dispersion of the W/O emulsion at 135 rpm coupled with inhibition of redispersion of the emulsion due to increase of W_{surf}. In all 135-rpm runs a thick film of emulsion resides on the upper surface of the water, but due to redispersion, this film is rejuvenated from time to time. This aspect appears to be inhibited in this particular run.

Evidence for this belief stems from the fact that the swelling of emulsion was the least in this particular run just 3 ml in comparison with the other two 135-rpm runs that had about 4 ml swell in volume. Moreover, this particular run used emulsion containing 4.7 % Span 80 instead of the usual 3 %. It is important to take cognizance of this aspect in view of the known behaviour of Span 80 to favour water transport.

4.6.2 Effect of internal phase volume fraction (ϕ)

ELM extractions are considerably influenced by the internal phase volume fraction ϕ of the W/O emulsions. Increasing ϕ increases the density, viscosity and interfacial tension of the emulsion. It also increases the loading capacity of the emulsion as it increases the molar ratio (*M*) of NaOH to concerned solute.

The effect of ϕ was studied in a set of seven runs, using W/O emulsions prepared with kerosene as the membrane phase and NaOH solution as the internal phase. Span 80 was the surfactant its concentration W_{surf} = 3 % wt (based on oil phase), internal phase NaOH concentration C_{io} = 0.3 M and Treat ratio TR= 1:15 was maintained in all these experimental runs. o-cresol content in the continuous phase (C_{eo}) was about 500 mg/dm^3 in all these runs. The emulsion was dispersed at 155 rpm in the continuous phase the results of the extraction of o-cresol with time, with variation in ϕ as a parameter are presented in Fig. 4.31.

Increasing ϕ from 0.4 to 0.69 did not make any significant change in the amount of o-cresol extracted. It is seen from Fig. 4.31 that in the first 5 minutes all the curves crowd together and by that time almost all the solute that could be extracted is already done, therefore the curves plateau after five minutes. The only exception is the run where ϕ = 0.69. This curve shows a rather relatively lower initial rate and moves above all other curves initially but reaches plateau at a lower residual cresol concentration at 10 minutes.

Slower rates are expected keeping in view the d_{32} = 1.312 mm for ϕ = 0.69 is larger than d_{32} obtained for the cases $\phi < 0.69$ having other factors identical. Since NaOH amount in the emulsion is also more when ϕ is more therefore somewhat more extraction was observed in this run in comparison to the case when ϕ = 0.45 or ϕ =

0.5. Almost similar behaviour is seen when $\phi = 0.625$ and $\phi = 0.60$. When $\phi = 0.4$ as expected the extent of removal was the least although the initial rates are the largest because this curve shows the most rapid decline in the first two minutes.

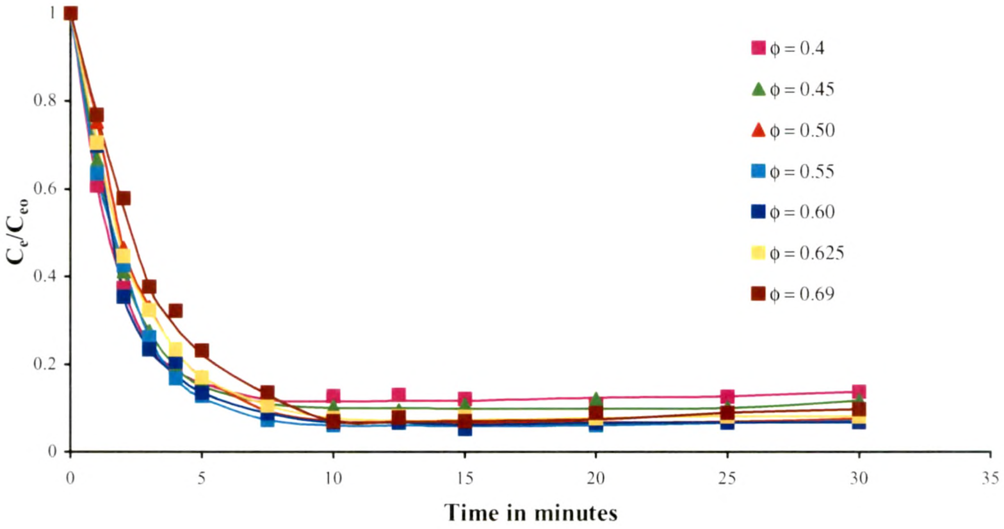

Fig. 4.31: Effect of ϕ on extraction of o-cresol

(N = 155 rpm, Span80 = 3%, C_{io} = 0.3M, TR = 1:15)

Further, when molar ratio was maintained at a constant value ≈ 2 by changing C_{io} values, for different values of ϕ the extraction curves almost merge together after 5 minutes showing same o-cresol recoveries and NaOH utilization as seen in Fig. 4.32.

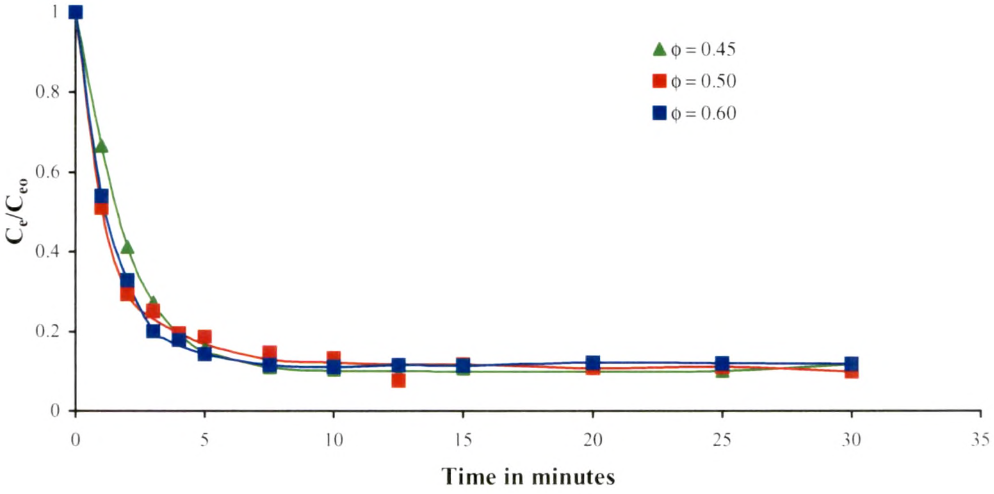

Fig. 4.32: Effect of ϕ on extraction of o-cresol at $M = 2$

(N = 155 rpm, Span80 = 3%, C_{io} = 0.3M, TR = 1:15)

4.6.3 Effect of surfactant concentration

Experiments were performed to study the effect of surfactant concentrations on the extraction of o-cresol at different internal phase volume fraction ϕ and the findings are chronicled below.

Case 1 $\phi = 0.45$

The emulsions used were prepared with kerosene as membrane phase and NaOH solution as the inner phase. The surfactant (Span 80) concentration was varied in the range of 1 % to 7.5 % (wt) of the kerosene phase, NaOH concentration for all runs was 0.3 M, the Treat ratio was maintained 1:15 and the emulsions were dispersed at 155 rpm in continuous phase containing $C_{eo} \approx 500$ mg/dm^3. The results of the various extraction runs are presented in Fig. 4.33 (a).

Increasing the Span 80 concentration from 1 % to 4.7 % does not influence the extraction. The extraction curves almost merge with each other and all runs plateau at $C_e/C_{eo} = 0.1$ between 7.5 minutes and 10 minutes. A single curve can be conveniently drawn to represent all the points for W_{surf} values of 1%, 2%, 3% and 4.7 %. However, when W_{surf} is 7.5 %, some emulsion breakage appears to be occurring after 5 minutes resulting in an increase of C_e/C_{eo} values that reach 0.2 at 30 minutes.

One reason for the emulsion rupture is perhaps the large swelling that takes place with increase in Span 80 concentrations. When $W_{surf} = 7.5$ % a 30 % swelling in emulsion volume was recorded while with $W_{surf} = 4.7$ % swelling was 12.5 %and with $W_{surf} = 3$ % emulsion swelling was 10 %.

What is intriguing is widely different behavior observed in o-cresol extraction and phenol extraction for variation in surfactant concentrations. The lumping of all data points in Fig. 4.33 (a) is not seen in Fig. 4.21 (a). This difference, in a way, seems to be perpetuated by the vastly different distribution coefficients for both cases.

In the presence of NaOH in the internal phase, W/O emulsions tend to be unstable. Increasing the surfactant concentrations increases the stability. When surfactant concentrations are low emulsion stability is less. In order to increase the stability either the NaOH concentration has to be less or the surfactant concentration has to be more. With reference to o-cresol extraction with ELMs containing 1 % surfactant concentration, it is very likely that due to the large distribution coefficient of o-cresol in kerosene over water, the membrane phase of the emulsion globules in a short time of contact with the continuous phase extracts the solute in the membrane phase. This in turn, also enhances the stripping rate resulting in quick depletion of NaOH in the internal phase of the W/O emulsion. Depletion of NaOH concentration leads to a corresponding increase in stability even at low surfactant concentrations. This eventually results in the lumping of the curves as seen in Fig. 4.33 (a).

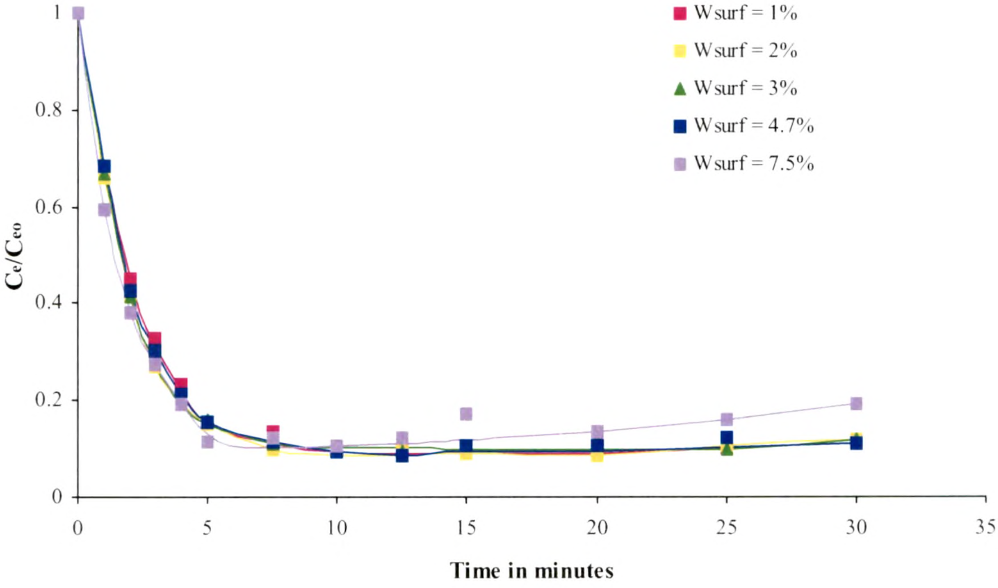

Fig. 4.33 (a): Effect of surfactant concentration on extraction of o-cresol (N = 155 rpm, $\phi = 0.45$, $C_{io} = 0.3$M, TR = 1:15)

Case II $\phi = 0.5$

Fig. 4.33 (b) depicts the extraction kinetics when the internal phase fraction $\phi = 0.5$. Surfactant concentration was again varied, from 1% to 7.5 % (wt), keeping all other process parameters identical. There is somewhat more resolution between the various curves that represent the extraction behavior at different surfactant concentrations but nothing concrete could be inferred. There is some evidence of drop breakage occurring at $W_{surf} = 7.5$ %. It is indeed surprising that even with a seven-fold increase in surfactant concentration, there is no trace of diffusional resistance to o-cresol transport into ELMs.

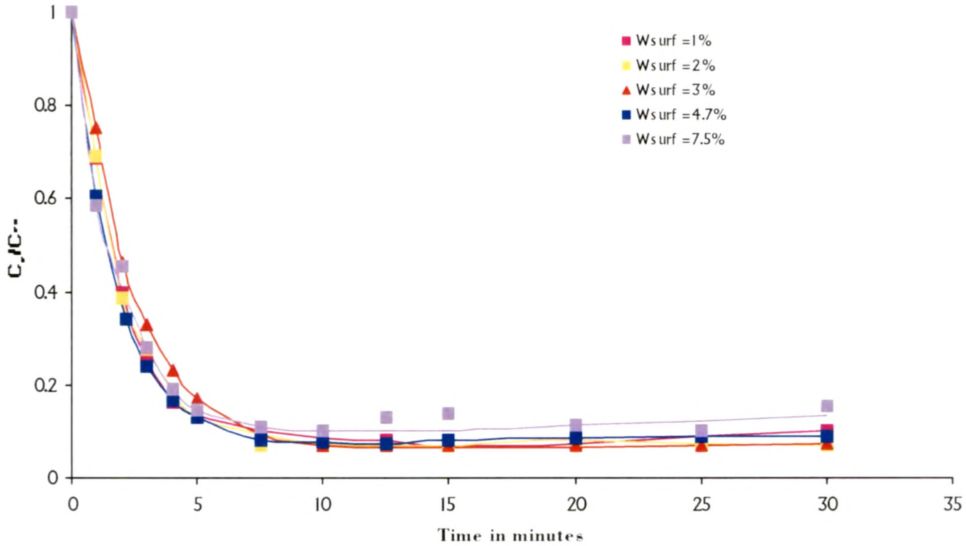

Fig. 4.33 (b) Effect of surfactant concentration on extraction of o-cresol

(N = 155 rpm, ϕ = 0.5, C_{io} = 0.3M, TR = 1:15)

Case III ϕ = 0.55

Fig. 4.33 (c) shows the extraction curves for o-cresol, using emulsions having ϕ = 0.55, with Span 80 concentrations ranging from 1% to 7.5% all other parameters were identical to previous cases.

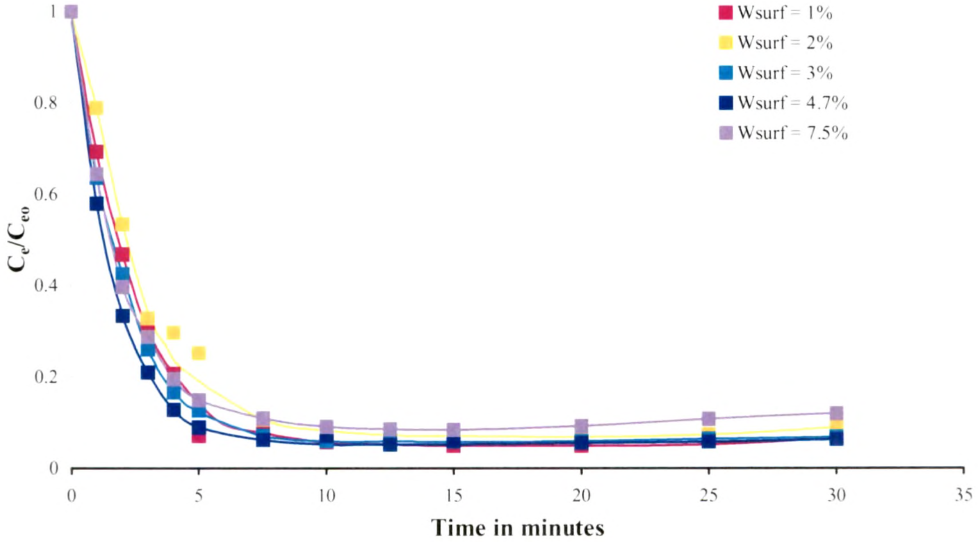

Fig. 4.33 (c) Effect of surfactant concentration on extraction of o-cresol

(N = 155 rpm, ϕ = 0.55, C_{io} = 0.3M, TR = 1:15)

In this figure it is observed that the curve, for surfactant concentration 7.5 % (wt), moves above the other extraction curves after 5 minutes duration indicating presence of diffusional resistance being set in with high surfactant concentration. It is interesting to find, while comparing the Figs. 4.33 (a),(b) and (c), that as ϕ increases the extent of extraction in all cases increases. This behavior is attributed to the increase molar ratio *M*, which is 1.95 for $\phi = 0.45$, 2.16 for $\phi = 0.5$ and 2.4 for $\phi = 0.55$.

4.6.4 Effect of internal phase reagent concentration (C_{io})

Effect of C_{io} on o-cresol extraction was studied using ELMs containing $W_{surf} = 3$ % (wt) that were dispersed in continuous phase having $C_{eo} \approx 500$ mg/dm^3 at 155 rpm. The effect of C_{io} was studied at $\phi = 0.45$ and $\phi = 0.5$.

Case I $\phi = 0.45$

Fig. 4.34 (a) shows the results of the extraction kinetics that was obtained for six variations of C_{io} ranging from 0.15 M to 0.6 M. Although up to 3 minutes all the curves cluster together, after 3 minutes each curve traces out its own pathway depending on the capacity of the ELM to extract the solute.

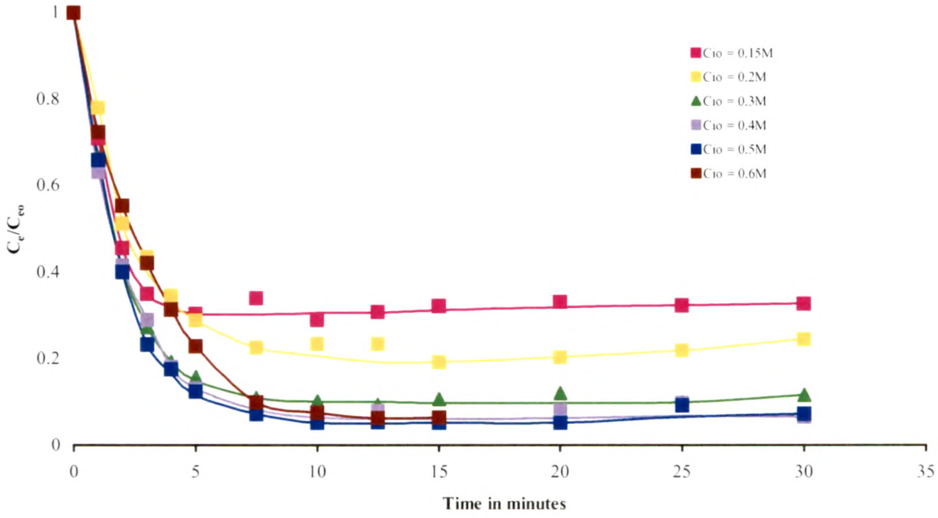

Fig. 4.34 (a): Effect of C_{io} on extraction of o-cresol

(N = 155 rpm, $\phi = 0.45$, Span80 = 3%, TR = 1:15)

The curve for $C_{io} = 0.15$ M plateau out the earliest at C_e/C_{eo} values of 0.3 at about 5 minutes. The other curves plateau after 7.5 minutes, when $C_{io} = 0.2$ M almost 80% extraction is achieved while for higher C_{io} values close to 90 % extraction is achieved.

For C_{io} =0.6 M, data could be collected only for the first 15 minutes of the run in view of the disintegration of the ELM due to high NaOH concentration. Although this curve attained plateau by 12.5 minutes, it showed a different initial rate, marginally lower than other runs. This may be attributed to a decrease in both the internal and external surface areas on account of large sized globules and also larger internal droplets within the emulsion as a consequence of higher NaOH concentrations. The data obtained in these runs once again indicate that the dominant parameter governing ELM extractions in batch processes is the molar ratio M of NaOH to solute. A brief summary of these runs with C_{io} variation is listed below.

C_{io} (M)	C_{eo} (mg/dm^3)	M	% Recovery of o-cresol	% NaOH utilization
0.15	498.66	0.98	70.85	71.97
0.20	507.24	1.29	80.65	62.50
0.30	508.90	1.93	90.49	46.91
0.40	500.81	2.61	93.75	35.51
0.50	503.81	3.25	94.65	29.14
0.60	499.53	3.93	93.56	23.80

Case II $\phi = 0.5$

Extraction runs with emulsions having internal phase volume fraction $\phi = 0.5$ were performed varying C_{io} from 0.2 M to 0.5 M while keeping all other membrane and process parameters identical. Results of these extractions are shown in the Fig. 4.34 (b). Nature of these plots is remarkably similar to the plots seen in Fig. 4.22 (b) for extraction of phenol under identical conditions. In both the Figs. mentioned above it was found that the extraction curve for emulsion with 0.3 M NaOH registered a greater recovery at 7.5 minutes and attained plateau before C_{io}= 0.4 M as well as 0.5 M. A brief summary of these runs with C_{io} variation is listed below.

C_{io} (M)	C_{eo} (mg/dm^3)	M	% Recovery of o-cresol	% NaOH utilization
0.20	484.08	1.49	87.20	58.956
0.30	495.66	2.18	93.17	42.758
0.40	487.52	2.95	94.90	32.128
0.50	499.96	3.60	94.61	26.270

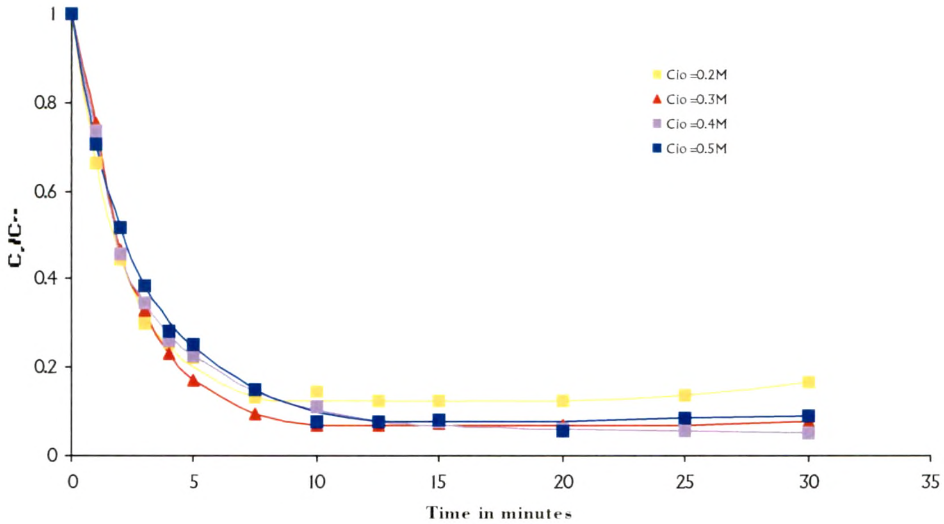

Fig. 4.34 (b): Effect of C_{io} on extraction of o-cresol

(N = 155 rpm, $\phi = 0.5$, Span80 = 3%, TR = 1:15)

4.6.5 Effect of Treat ratio (TR)

Increase in Treat ratio always leads to an increase in solute removal because increase in Treat ratio means addition of more emulsion to the system that leads to an increase in the molar ratio *M*. Treat ratio variations in the range 1:20 to 1:6 were studied using ELMs having $\phi = 0.45$ and $\phi = 0.5$. Further for emulsions having $\phi = 0.45$, the Treat ratios were varied but the molar ratio for each variation was maintained at a constant value of 2. Results of these extraction runs are shown in Figs. 4.35 (a) and (b) and Fig. 4.36 for case of $\phi = 0.45$, $\phi = 0.5$ and $\phi = 0.45$ at molar ratio 2 respectively. All other emulsion and process parameters were kept constant at $C_{io} = 0.3$ M, $W_{surf} = 3$ %, $C_{eo} \approx 500$ mg/dm^3 and stirring speed 155 rpm.

Fig. 4.35 (a) shows significant and orderly difference in the extraction profiles at different treat ratios with $\phi = 0.45$. In terms of initial rates and also the amount of o-cresol extracted, the curves for Treat ratio of 1:10, 1:7.5 and 1:6 all cluster together indicating no significant advantage gained by increasing the Treat ratio and correspondingly the molar ratio beyond a certain value. Fig. 4.35 (b) also shows similar trend with reasonably well resolved curves showing extraction profiles at different Treat ratios using ELMs having $\phi = 0.5$. Larger extent of solute removal was observed when $\phi = 0.5$ in view of larger molar ratio.

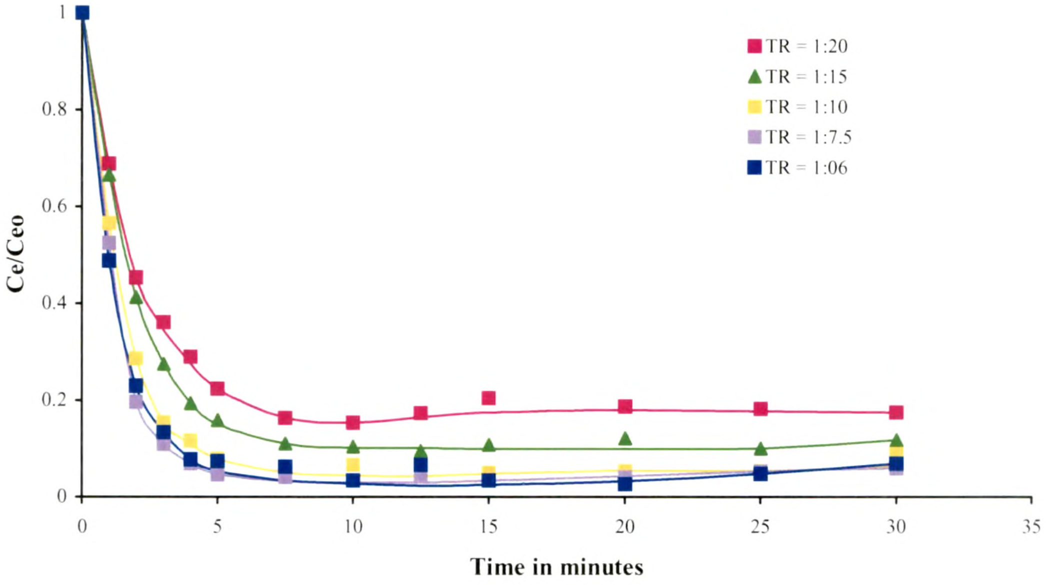

Fig. 4.35 (a): Effect of TR on extraction of o-cresol

(N = 155 rpm, $\phi = 0.45$, Span80 = 3%, $C_{io} = 0.3M$)

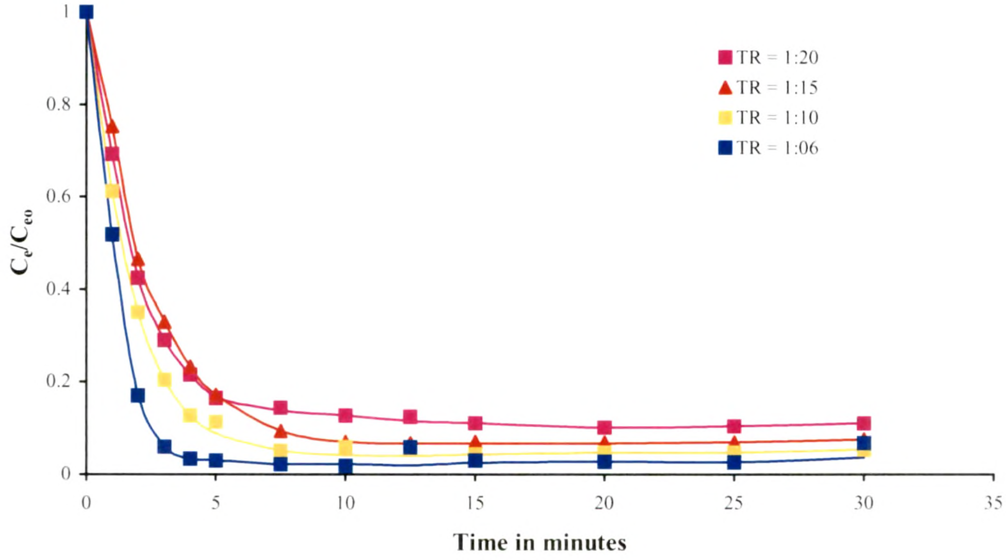

Fig. 4.35 (b): Effect of TR on extraction of o-cresol

(N = 155 rpm, $\phi = 0.45$, Span80 = 3%, $C_{io} = 0.3M$)

However, when Treat ratios were varied keeping molar ratio $M = 2$ it was observed that the curves tended to come together. Variation of Treat ratio, keeping M constant implies that only the mass transfer surface area is increased. One finds in Fig. 4.36 that this does not really have much influence on the extraction profile. Increase in TR from 1:20 to 1:6 leads to just 10 % more extraction and that too in the first 5 minutes of the run. It is interesting to observe in Fig. 4.36 that curves representing different Treat ratios at M =2, all converge after a duration of about 15 minutes indicating that extraction capacity in the internal phase dominates ELM separations.

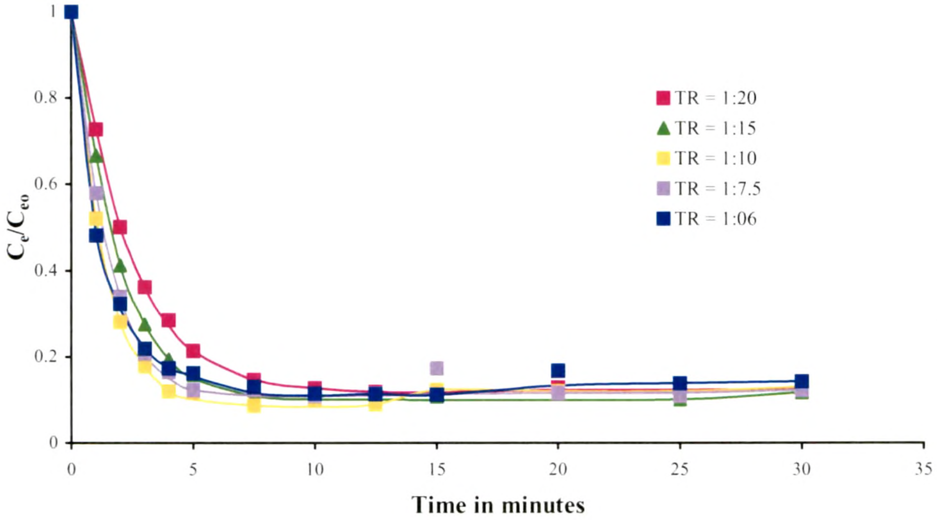

Fig. 4.36: Effect of TR on extraction of o-cresol at $M = 2$

(N = 155 rpm, $\phi = 0.45$, Span80 = 3%)

4.6.6 Effect of initial o-cresol concentration (C_{eo})

Effect of external phase solute concentration (C_{eo}) keeping membrane and process parameters constant, is a manifestation of change in molar ratio M. ELMs having ϕ = 0.45, C_{io} = 0.3 M, TR = 1:15, were dispersed in continuous phase at 155 rpm. The solute concentration in the continuous phase was varied from 101 mg/dm^3 to almost 625 mg/dm^3. Results of these extraction runs are presented in Fig. 4.37. The run with C_{eo} = 101 mg/dm^3 shows 80 % recovery that is attained in just 5 minutes duration .For this particular case, in spite of very favorable molar ratio of 9.67, further recovery was not possible due to depletion of the driving force both in the external phase as well within the emulsion globule.

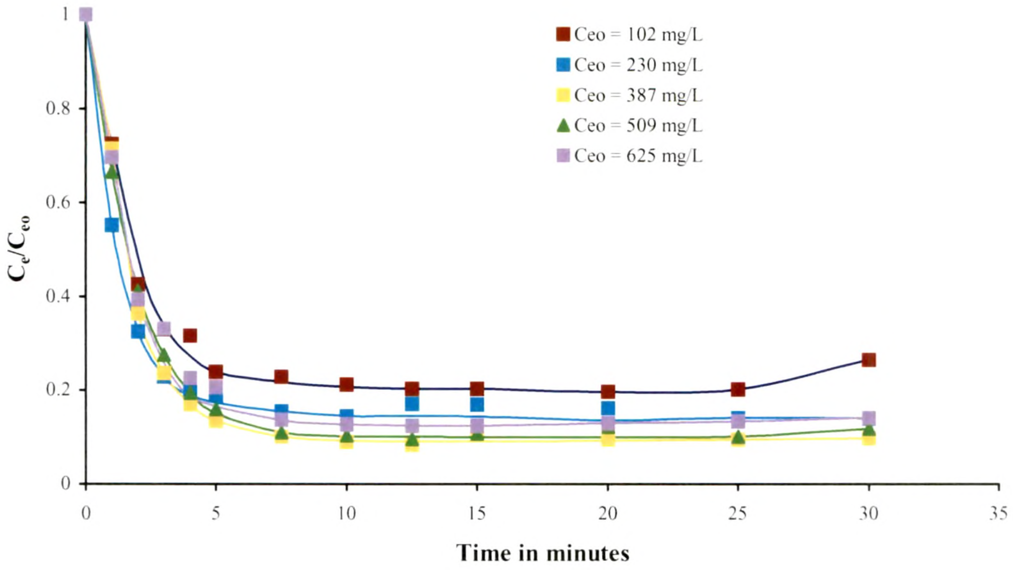

Fig. 4.37: Effect of initial o-cresol concentration on extraction

(N = 155 rpm, ϕ = 0.45, Span80 = 3%, C_{io} = 0.3M, TR = 1:15)

Increasing C_{eo} results in greater recoveries of o-cresol. When solute concentrations increase to 230 mg/dm^3 the recoveries are better than that obtained for 101 mg/dm^3 but in this case also driving force rapidly diminishes thereby restricting further recoveries. Best results are observed for C_{eo} of 388 mg/dm^3 and 509 mg/dm^3. With further increase in concentration the molar ratios tend to become unfavorable resulting in less recovery.

Effect of C_{eo} maintaining molar ratio M = 2 is shown in Fig. 4.38. Influence of the driving force is more clearly visible in this case. Low C_{eo} values require low C_{io} in order to balance the molar ratio. This means that greater solute penetration within the globule is necessary in these cases for solute recovery in comparison with situations with high $C_{io.}$ Having high C_{io} in the emulsion necessitates the diffusing species to just move a small distance before getting reacted and entrapped within the globules. When C_{eo} is less, both the external as well as the internal driving forces are quite low hence rates of extraction as well as the extent of extraction are less.

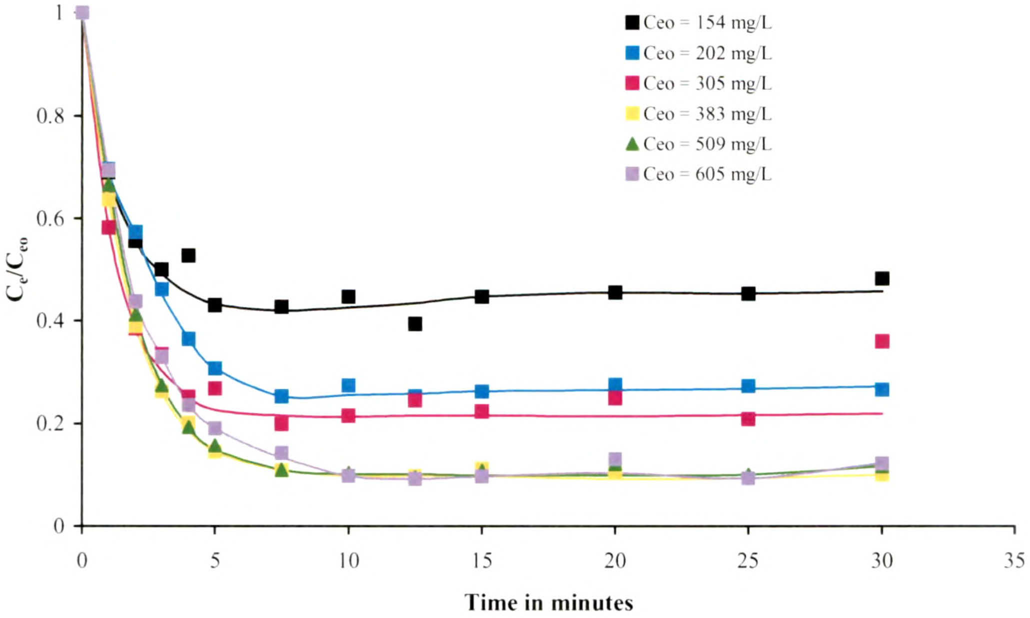

Fig. 4.38 Effect of initial o-cresol concentration on extraction at $M = 2$ (N = 155 rpm, $\phi = 0.45$, Span80 = 3%, TR = 1:15)

4.6.7 *Effect of temperature*

Extractions were performed at temperature other than the usual 30°C to assess the influence of temperature effect on ELM extraction. Fig. 4.39 shows results of two experimental runs conducted at different temperatures i.e. at 24°C and 30°C using identical emulsion compositions ($\phi = 0.45$, $W_{surf} = 3\%$ (wt), $C_{io} = 0.3$ M) and process conditions ($C_{eo} \approx 500$ mg/dm^3, TR = 1:15 and N = 155 rpm). It was observed that there was just no change in the extraction profiles in the specified range of temperature difference and both the curves superimpose on one another. Similar behavior was observed for phenol extraction as seen in Fig. 4.27.

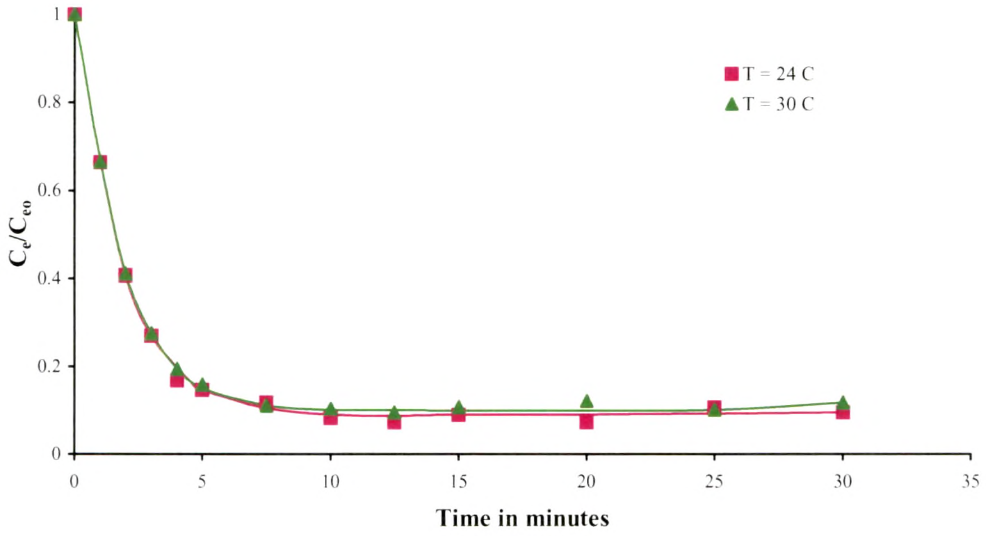

Fig. 4.39 Effect of temperature on extraction of o-cresol

(N = 155 rpm, $\phi = 0.45$, Span80 = 3%, $C_{io} = 0.3M$, TR = 1:15)

4.6.8 *Effect of membrane material*

A number of membrane materials were tried out to prepare the ELMs with the idea to identify potential membrane material as an alternative to kerosene. In total four petroleum fractions: light naphtha, aviation turbine fuel, kerosene and hydrocracker white diesel were tried out. Experiments were carried out also with toluene as the membrane material. The results are presented in Fig. 4.40, all emulsion and process conditions were identical i.e. $\phi = 0.45$, $W_{surf} = 3\%$ (wt), $C_{io} = 0.3$ M, $C_{eo} \approx 500$ mg/dm^3, TR = 1:15 and N = 155 rpm.

The composition and relevant properties of the petroleum fractions used are detailed below:

Composition	Light naphtha	Kerosene	ATF	Diesel (white)
Boiling range (°C)	40 to 125	152 to 271	150 to 260	144 to382
Density (15°C) kg/m^3	690	821.3	800	829.7
% Paraffin	54	27	39	46
% Aromatic	29	16	6	11

Gu, Ho and Li (1992) suggested that superior W/O emulsions could be prepared using largely paraffinic solvents. The desired membrane properties listed in Section 2.4.1 are largely satisfied by them. There are pointers, which suggest that aromatic content is also important for rapid extraction in both Type I and Type II transport, since presence of aromatics induces greater solubility of aromatic compounds in the ELMs. It can be made out from Fig. 4.40 that kerosene as membrane material yields the best results comparable with toluene and ATF. ELMs using diesel show gradual extraction on account of their higher viscosity.

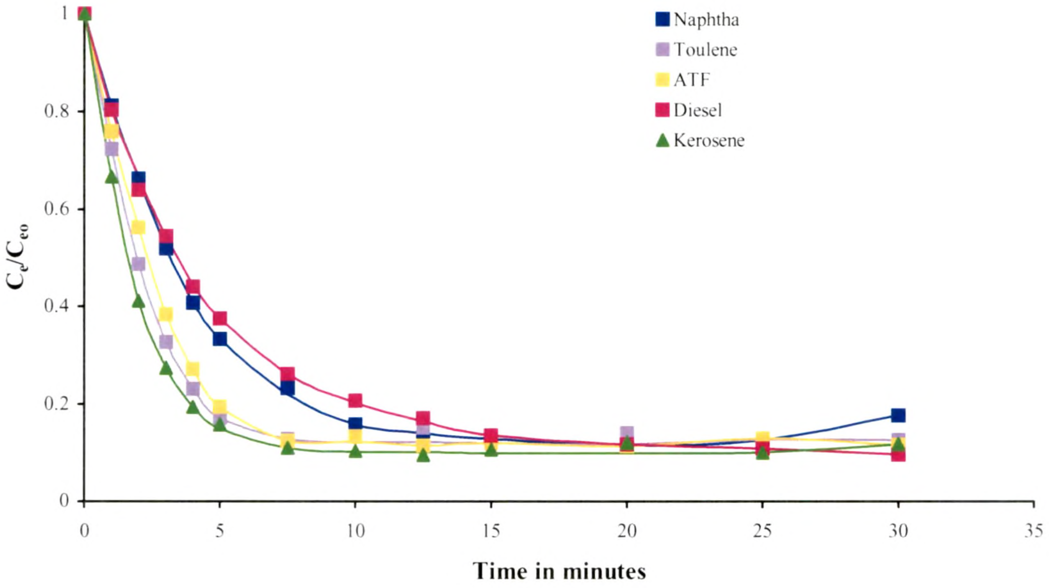

Fig. 4.40: Effect of membrane material on extraction of o-cresol

(N = 155 rpm, $\phi = 0.45$, Span80 = 3%, $C_{io} = 0.3M$, TR = 1:15)

Broad conclusions regarding various membrane materials studied in this investigation are listed below:

- Kerosene is by far the best membrane material to work with and hence it is being so widely used in ELM extractions and also in solvent extraction of metals.
- Light naphtha is a difficult material to handle in view of its high volatility. Even during emulsion preparation due to local rise in temperature during blending process, some vaporization takes place inspite of the fact that emulsions were always prepared keeping the contents in a chilled water bath.
- Aviation turbine fuel in a way is very close to kerosene but its low aromatic content may be a hindrance during extraction of aromatic compounds, which are usually facilitated by the presence of aromatics in the membrane phase.
- Hydrocracker diesel fraction, which has substantial paraffin content in it yields W/O emulsions that are more viscous than the emulsions obtained with other

fractions. These emulsions have good dispersion characteristics and are reasonably stable. Hence, hydrocracker diesel can be considered potential membrane material for ELM extractions. The only drawback with this fraction is its availability and the W/O emulsions prepared using them are quite viscous that may require to be dispersed at high stirring speeds

4.6.9 Extraction using Acrylate resin 505 emulsifier

A proprietary surfactant, essentially a polymeric acrylate emulsifier was also tried out for the extraction of o-cresol from its aqueous solutions. This surfactant had excellent tolerance for NaOH in comparison with Span 80 and it was possible to prepare reasonably stable W/O emulsions even with C_{io} = 1 M. It was observed that the interfacial tension using acrylate emulsifier in the membrane was just 5 mN/m, between the standard composition of W/O emulsion used in this work and the aqueous phenol solution, while it was 20.6 mN/m when Span 80 was used as the emulsifier. However, no significant change in the globule sizes was observed. Fig. 4.41 shows the extraction curves for o-cresol extraction using ELMs prepared using the acrylate emulsifier having C_{io}= 0.3 M, and C_{io}=1M.

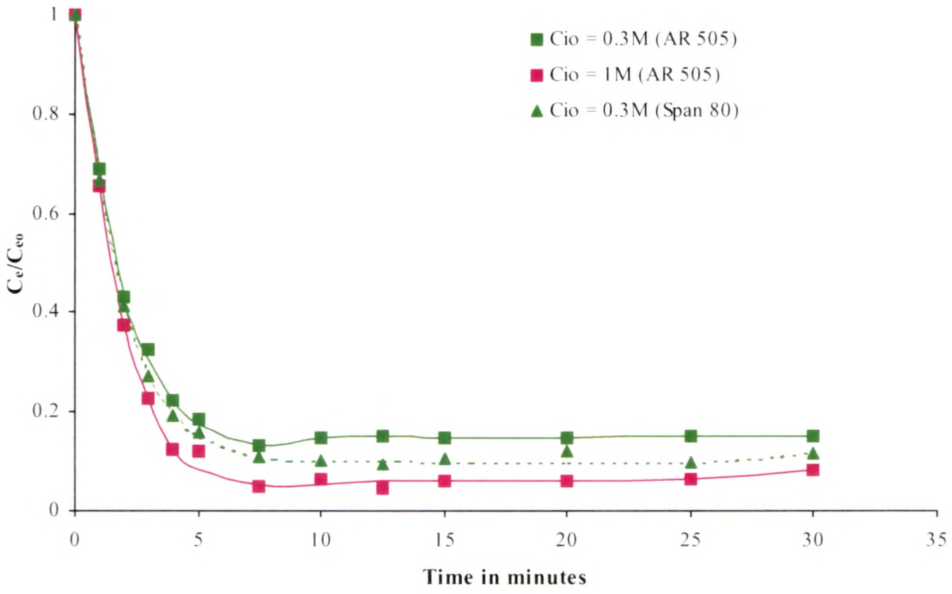

Fig. 4.41: Effect of C_{io} on extraction of o-cresol using AR 505 emulsifier (N = 155 rpm, ϕ = 0.45, AR 505 = 3%, TR = 1:15)

Other emulsion and process parameters were the following:- ϕ = 0.45, W_{surf} = 3% (wt), $C_{eo} \approx$ 500 mg/dm^3, TR = 1:15 and N = 155 rpm. Comparing these two curves show that initial rates of extraction are same, after 3 minutes the curve containing 0.3 M NaOH attains plateau while when C_{io} = 1M a larger amount of solute is extracted and plateau reached after 7.5 minutes.

The results for extraction at C_{io} = 0.3 M are also compared with those obtained using Span 80 under identical conditions. It was found that although initial rates were same but with Span 80 there was slightly more extent of extraction. Fig. 4.42 shows the influence of ϕ on extraction of o-cresol .As expected, increase in ϕ results in greater extraction although the initial rates are all the same.

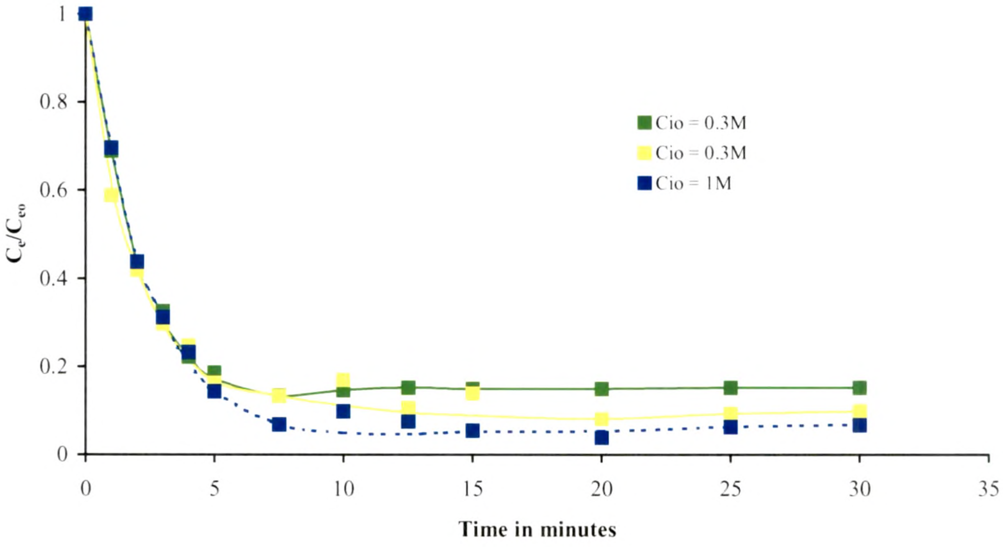

Fig. 4.42: Effect of ϕ on extraction of o-cresol using AR 505 emulsifier (N = 155 rpm, AR 505 = 3%, TR = 1:15)

4.7 EXTRACTION OF p-CRESOL

Extraction of p-cresol using ELMs is almost uninvestigated, the only literature citation that could be pointed is the work of Terry, Li and Ho (1982) where they mentioned of a single run using p-cresol. In this Study, p-cresol extraction from its dilute aqueous solutions using ELMs was considered. Since emulsion compositions were identical with the emulsions used for o-cresol extraction it was expected that the dispersion behavior would remain unchanged. Hence, the effect of stirring speeds was not studied. All dispersions were stirred at 155 rpm. Further, variation of surfactant concentration was also not investigated due to the same reasons mentioned above. The surfactant concentration was $W_{surf} = 3$ % wt for all cases. Attempt has been made to study the effect of the main factors influencing p-cresol extraction. The results are presented in the following sections:

4.7.1 *Effect of internal phase volume fraction* (ϕ)

Extraction of p-cresol with varying emulsion internal phase volume in the range of $\phi = 0.4$ to $\phi = 0.69$ was studied. In all these runs the p-cresol concentration in the continuous phase was maintained nearly 500 mg/dm^3. The W/O emulsions were prepared using kerosene as the external membrane phase and NaOH solution as the inner phase. Span 80 was the surfactant used and its concentration in the kerosene phase was 3 % (wt) of the kerosene phase. Treat ratio of 1:15 was maintained. The emulsions were dispersed at stirring speed of 155 rpm. The results of these extractions are presented in Fig. 4.43 and Fig. 4.44.

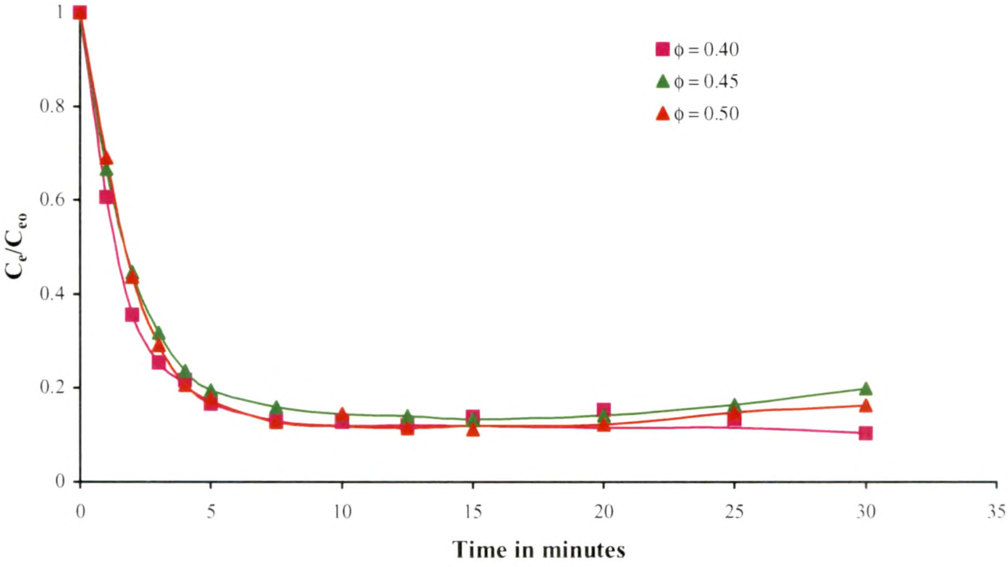

Fig. 4.43: Effect of ϕ on extraction of p-cresol

(N = 155 rpm, Span 80 = 3%,Coi = 0.3M, TR = 1:15)

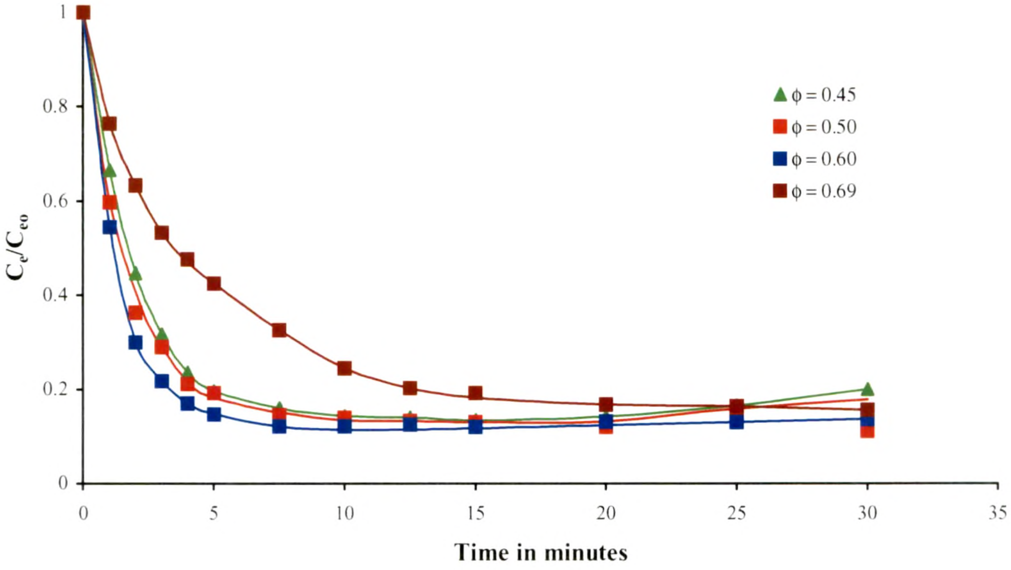

Fig. 4.44: Effect of ϕ on extraction of p-cresol at M = 2
(N = 155 rpm, Span 80 = 3%, TR = 1:15)

In Fig. 4.43 the internal phase concentration of NaOH was maintained at C_{io} = 0.3M, although the curves are very close to each other but still it is surprising to find that the extraction curve for ϕ = 0.4 passes below the curve for ϕ = 0.45 through out the duration of the run and also below ϕ = 0.5 during the initial period of the run. Looking carefully in Fig. 4.31 for o-cresol extraction, the same trend was observed under identical conditions. This trend however is not observed with phenol extraction in Fig. 4.20.

Many reasons could be attributed to this behavior. Increased ϕ leads to increase in both globule size as well as inner drop sizes, increase in viscosity etc. resulting in lower extraction in initial period with increased ϕ. It could also be a manifestation of the relatively large distribution coefficient of cresols in kerosene to that of water, in comparison to that of phenol in kerosene, that caused greater extraction in the initial stages when oil fraction of globules was more. However, nothing conclusively can be said without further investigation.

Fig. 4.44 shows the extraction profiles of p-cresol at constant molar ratio M = 2, it is seen that when internal phase volume fraction increases from 0.45 to 0.6 there is a small but definite increase in the initial extraction rates and also in the extent of p-cresol extraction. Further increase in ϕ to 0.69 leads to a sharp decrease in initial extraction rates and a more gradual decay of the extraction curve.

Behavior at $\phi = 0.69$ is explainable in view of large globule sizes ($d_{32} = 1.312$ mm), large internal drop sizes and much larger viscosity ($\eta = 296$ mPa.s at 38.4 s^{-1}) in comparison with the standard ELMs having $\phi = 0.45$ where $d_{32} = 1.128$ mm and $\eta = 13.32$ mPa.s. Due to these factors, it is likely that that diffusion within the globules will be considerably slowed down. Moreover, to maintain molar ratio $M = 2$ it is also necessary to reduce C_{io} values from 0.3 M to 0.2 M in this specific case. Therefore, the solute would require moving deeper inside the globules to react with NaOH and get entrapped. Increase in diffusion path lengths leads to slower rate of extraction at any particular sampling time.

The extraction curves for $\phi = 0.5$ and $\phi = 0.6$ lie almost superimposed on each other through out the experimental run. The nature of the extraction curve for $\phi = 0.6$ with $M = 2$ is unexplainable.

4.7.2 Effect of internal phase reagent concentration(C_{io})

Fig. 4.45 shows the effect of C_{io} variation on rates of extraction. The trend of extraction is identical to that observed for o-cresol in Fig. 4.33(a).

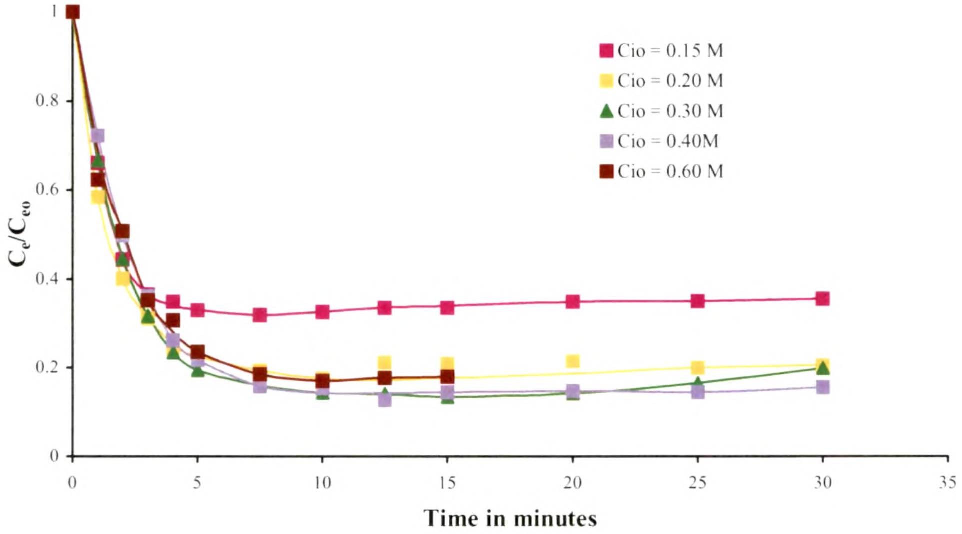

Fig 4.45: Effect of C_{io} on extraction of p-cresol

(N = 155 rpm, $\phi = 0.45$, Span 80 = 3%, TR = 1:15)

The point of departure is that, under identical conditions o-cresol is extracted to a greater extent than p-cresol, which is evident by comparing these two plots. Increase in C_{io} manifests in increased molar ratio M leading to greater extraction This is evident by comparing the curves obtained for $C_{io} = 0.15$ M with $C_{io} = 0.3$ M. Same is the case when curves for 0.2 M and 0.3 M are compared. Increase in C_{io} beyond a certain value results in situation where the advantage gained by increase in molar ratio is offset by morphological changes in the inner droplets and also increase in emulsion globule sizes. This aspect is visualized comparing curves for $C_{io} = 0.3$ and $C_{io} = 0.4$ which remain almost merged together through out the progression of the run.

Further increase in C_{io} to 0.6 M had a deleterious effect on the extraction since the emulsion became unstable and the experimental run had to be discontinued after 15 minutes sampling time. The initial rates of extraction were identical for all cases except for $C_{io} = 0.6$. This is understandable in view of the morphological changes in the emulsion as well as the increase in globule sizes and emulsion viscosity that lead to less amount of extraction in the initial period of the run.

4.7.3 Effect of Treat ratio

Treat ratio is an operational parameter parallel to solvent to feed ratio frequently used in liquid-liquid extraction. With reference to ELMs, variation in Treat ratios is also manifestation of variation in molar ratios. Since addition of more emulsion to the system also results in addition of more amount of internal reactive phase to the system thereby resulting in increased capacity of the ELM system to extract more solute.

Fig. 4.46 shows the results obtained for p-cresol extraction using standard membrane formulations with treat ratio varied in the range of TR = 1:20 to TR = 1:6. As expected with increase in Treat ratio both the rates of extraction as well as the amount extracted increase.

Fig. 4.47 shows the effect of Treat ratio at molar ratio $M = 2$. Maintaining constant molar ratio in a way fixes the extracting capability of the ELMs. Thus any difference observed at constant molar ratio could be attributed to physical factors. It is observed in Fig. 4.47 the profiles of curves are very different from those observed in Fig.

4.46,but at the same time they all converge at almost same amount extracted because all have same capacity to extract.

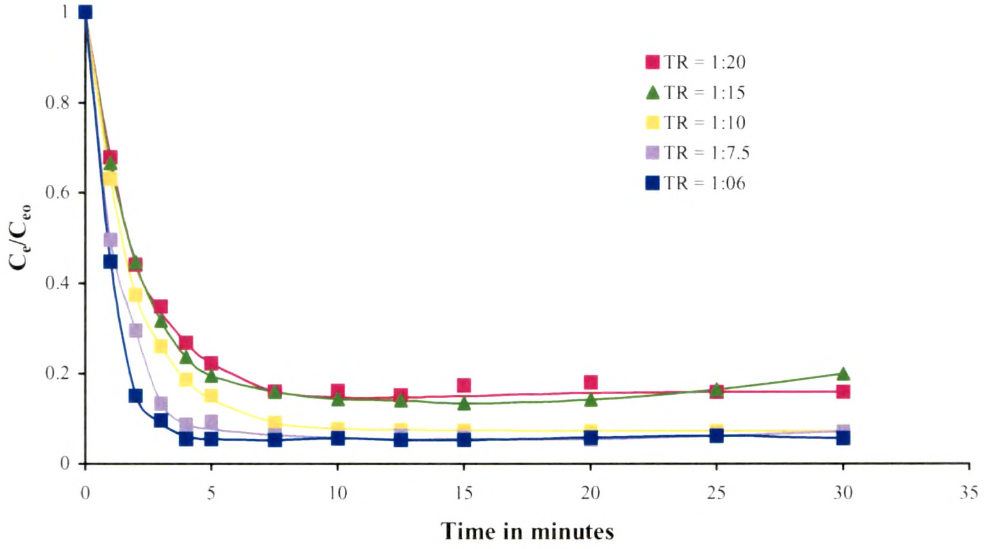

Fig. 4.46: Effect of TR on extraction of p-cresol

(N = 155 rpm, $\phi = 0.45$, Span 80 = 3%, $C_{io} = 0.3M$)

The gradual decrease of the TR = 1:20 curve in comparison with the other curves seen in Fig. 4.47 is largely due to formation of less number of globules in the dispersed phase since less volume of emulsion was added. This caused a corresponding decrease in the external globule surface area. Moreover to maintain $M = 2$, in this particular case the internal NaOH concentration was increased resulting in increased internal droplet sizes leading to decreased internal surface areas. When Treat ratio is less, same level of recovery of solute necessitates deeper penetration of solute inside the globules. Deeper penetration corresponds to thicker membranes and correspondingly more resistance to transport and eventually resulting in the nature of the extraction observed in this case.

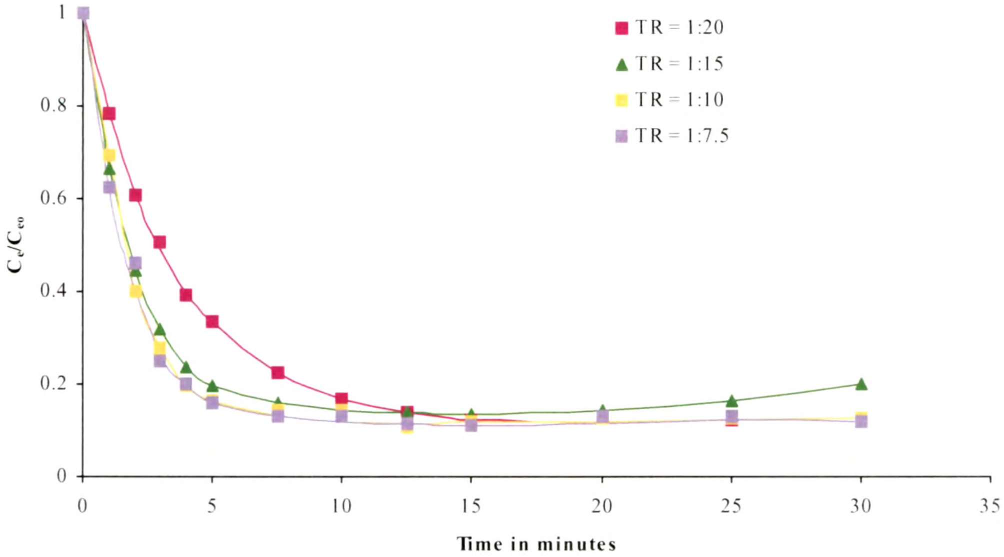

Fig. 4.47: Effect of TR on extraction of p-cresol at $M = 2$

(N = 155 rpm, $\phi = 0.45$, Span 80 = 3%)

4.7.4 Effect of initial p-cresol concentration (C_{eo})

Fig. 4.48 represents the effect of continuous phase p-cresol concentration ranging from 103 mg/dm^3 to 591 mg/dm^3 using ELMs having C_{io} = 0.3 M. Fig. 4.49 shows the effect of C_{eo} variation ranging from 200 mg/dm^3 to 800 mg/dm^3 at molar ratio 2. The trend in both these Figures are similar to the trend observed in Fig. 4.36 and Fig. 4.37 respectively for o-cresol extraction.

Fig. 4.48 can be explained in terms of the extracting capacity of the ELMs and the driving force available for transport. This is particularly true at lowest C_{eo} value (103 mg/dm^3). It was found that after the initial spurt of removal in 3 minutes no further removal occurs due to depletion of driving force in the external phase. While for C_{eo} values ranging between 201 mg/dm^3 and 591 mg/dm^3 all the curves lump together. This behavior appears to be quite generalized with cresols since it was visible in o-cresol extractions as well.

Even at molar ratio M = 2 identical trend is observed in Fig. 4.49. Exception is the case with C_{eo} = 800 mg/dm^3 which showed exponential decay behavior. Such nature of the curve is prompted by large globule size, large internal drop size and also deep penetration of solute within globules. In this case it originated from the requirement to increase inner phase NaOH concentration C_{io} to 0.48 M in order to balance the molar ratio to 2.

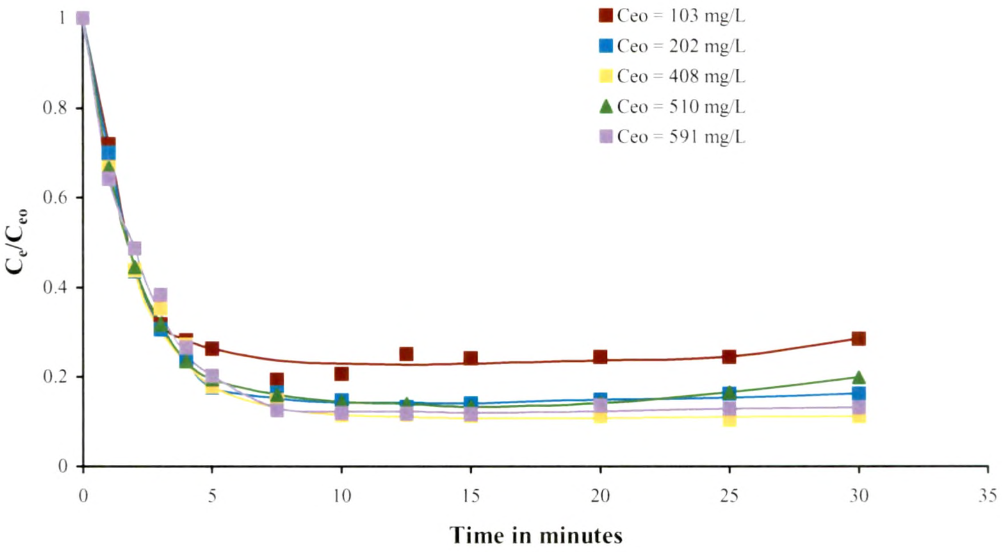

Fig. 4.48: Effect of initial p-cresol concentration on extraction (N = 155 rpm, ϕ = 0.45, Span 80 = 3%, Cio = 0.3M, TR = 1:15)

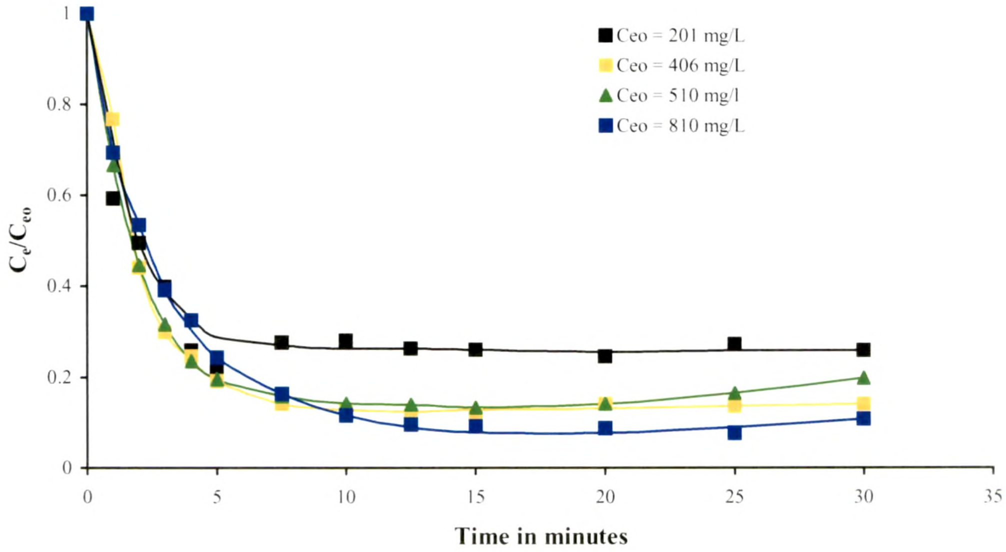

Fig. 4.49: Effect of initial p-cresol concentration on extraction at *M* = 2 (N = 155 rpm, ϕ = 0.45, Span 80 = 3%, TR = 1:15)

Looking closely at figures representing C_{eo} variations in p-cresol extraction as well as o-cresol extraction (i.e. Fig. 4.48, 4.36 and 4.37) a curious behavior is noticed. In all these figures the experimental run with $C_{eo} \approx 400$ mg/dm^3 showed maximum extraction of solute. The reason for this behavior could not be figured out and needs to be investigated.

4.8EXTRACTION OF 2-CHLOROPHENOL

2-Chlorophenol is a very toxic substance which makes its presence felt even in concentrations of μg/dm^3, has wide ranging influence on marine life and is potentially dangerous to human health. Recently Correia and Carvalho (2000) studied extraction of o-chlorophenol in ELMs, they used Shellsol as membrane phase, ECA 4360 as the surfactant and 0.5 M NaOH as the internal reagent phase. In this investigation taking their investigation as a starting point the behavior of o-chlorophenol extraction into emulsion liquid membranes is explored.

The ELM formulation was the standard one, that was used throughout this investigation. It contained kerosene as the membrane phase Span 80 as the surfactant (3 % wt), internal reagent phase was 0.3 M NaOH solution and internal phase fraction $\phi = 0.45$. The emulsion was dispersed at 155 rpm in the continuous phase that contained ≈ 500 mg/dm^3 of o-chlorophenol to give a Treat ratio = 1:15.

Effect of stirring speed was not explored, since dispersion properties are not likely to change with any change of solute. The effect of surfactant concentration was also not investigated since surfactant concentration variations did not affect ELM extractions significantly in the other systems studied. The effect of other emulsion parameters such as ϕ, C_{io} and process parameters such as TR and C_{eo} were investigated in detail

4.8.1 Effect of internal phase volume fraction (ϕ)

The effect of variation of ϕ was studied in the range of 0.45 to 0.55, effect of ϕ was also investigated while maintaining constant molar ratio $M = 2$. One aspect that is unique with extraction of o-chlorophenol is that the amount extracted is much larger in comparison to phenol and cresols under identical conditions. This behavior stems out from the fact that o-chlorophenol has a very favorable distribution coefficient towards kerosene over water. The distribution coefficient was experimentally obtained as 4.4659.

Fig. 4.50 shows the effect of ϕ on extraction. Almost 94 to 97 % removal was seen in all cases. Although all the curves are very close but it is observed that for $\phi = 0.45$ the amount of extraction in the first five minutes is the largest indicating higher initial rates. As ϕ is increased there is marginal decline in amount extracted. Since the oil component in globules is highest when $\phi = 0.45$ in comparison to other cases, this behavior is perhaps due to favorable distribution coefficients.

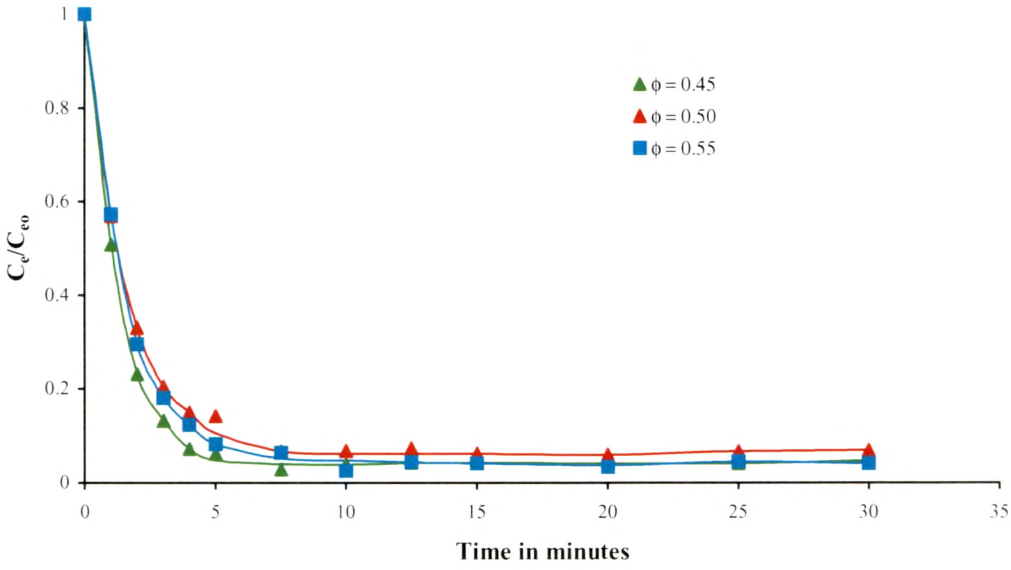

Fig. 4.50 Effect of ϕ on extraction of 2-chlorophenol

(N = 155 rpm, Span 80 = 3%, C_{io} = 0.3M, TR = 1:15)

Comparing the curves for $\phi = 0.5$ and $\phi = 0.55$, it is observed that the extraction curve for $\phi = 0.5$ passes above that for $\phi = 0.55$. This may be explained in terms of molar ratio but since both curves pass above $\phi = 0.45$, it is difficult to reason out the behavior in terms of single parameter variation. In all the systems studied so far increase in ϕ always showed an increase in extraction because of increase in the molar ratio (*M)* hence the capacity of ELMs to extract. This behavior is also seen in this case for $\phi = 0.50$ and $\phi = 0.55$ but not for $\phi = 0.45$.

At molar ratio $M = 2$, the curves for $\phi = 0.45, 0.5$ and 0.6 all merge together as seen in Fig.4.51. There is some resolution between sampling times of 3 minutes to 7.5 minutes, it was found that the curve for $\phi = 0.5$ at this stage passed below all other curves, but that could occur also due to some minor fluctuations during the experiments or in the analysis. One thing that stands out from these experiments is that the molar ratio *M* that is otherwise a dominant parameter in ELM extractions may not be so important if the distribution coefficient for solute towards membrane phase is very large.

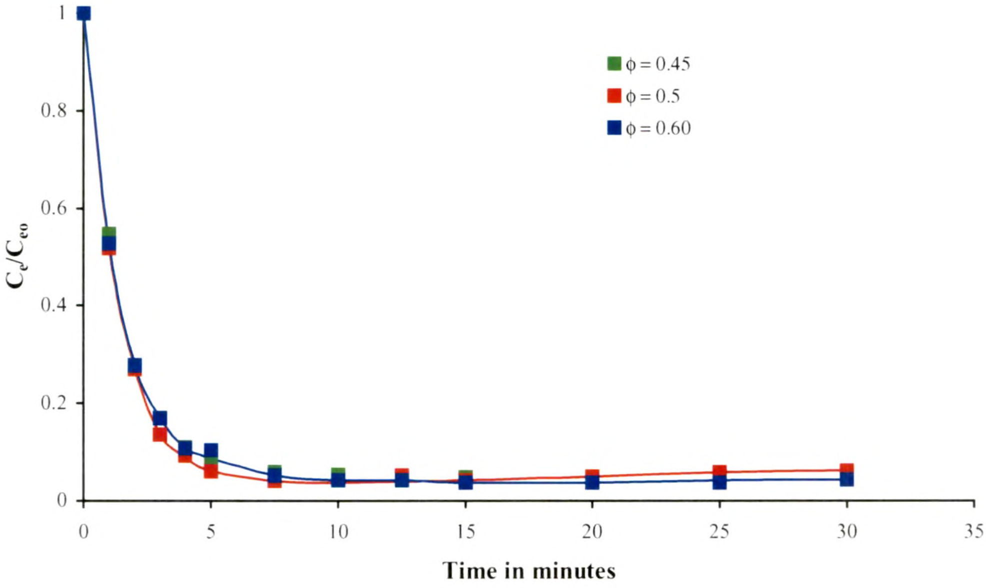

Fig. 4.51 Effect of ϕ on extraction of 2-chlorophenol at M = 2
(N = 155 rpm, Span 80 = 3%, TR = 1:15)

4.8.2 Effect of internal phase reagent concentration (C_{io})

The effect of C_{io} variation was studied using W/O emulsions having internal phase fraction of 0.45 and other parameters corresponding to our standard run as mentioned earlier. In Fig. 4.52 the extraction curves at three different values of C_{io} 0.13 M, 0.3 M and 0.5 M respectively are presented.

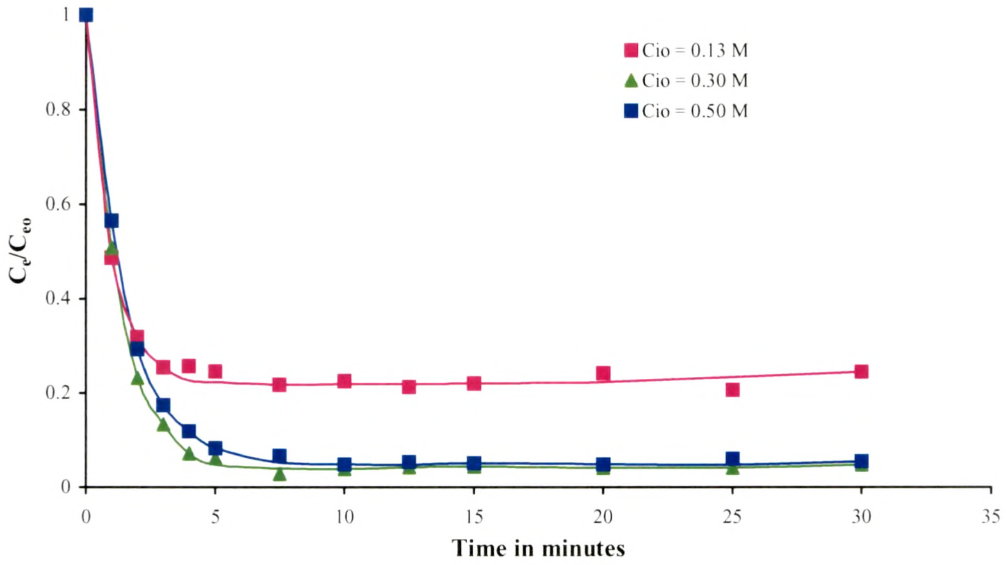

Fig. 4.52: Effect of C_{io} on extraction of 2-chlorophenol

(N = 155 rpm, $\phi = 0.45$, Span 80 = 3%, TR = 1:15)

It was observed that, at C_{io} of 0.3 M, around 80 % removal is achieved, with C_{io} of 0.3 M and 0.5 M about 95 % removal is achieved from initial o-chlorophenol concentration of ≈ 500 mg/dm^3. Up to 2 minutes the curves remain merged after two minutes they spread out and plateau in accordance to their extraction capacity. The relevant details of these three runs are listed below.

C_{io} M	C_{eo} mg/dm^3	M	% recovery 2-chlorophenol	% NaOH utilization
0.13	487.4	1.048	79.4	75.77
0.30	498.5	2.343	97.18	41.46
0.50	484.9	4.014	95.07	23.76

It is seen in Fig. 4.52 that extraction curve for C_{io} = 0.5 M moves above the curve for C_{io} = 0.3 M. One possible reason for this behavior is the reduced surface area of both external globules as well as internal drops due to an increase in globule size also internal drop size with an increase in the concentration C_{io} of the system.

4.8.3 Effect of Treat ratio

The effect of treat ratio at molar ratio M ≈ 2 was investigated at three different Treat ratio of TR = 1:15, TR = 1:10 and TR = 1:6 using ELMs having internal phase volume fraction ϕ = 0.45 and other emulsion parameters corresponding to the standard run mentioned earlier. Since molar ratio was same in each case, the extractive capacity of the inner phase was same in all the three cases. However, because amount of emulsion added was different in the three cases, the surface area of mass transfer as well as the extraction capacity of the membrane phase increased with an increase in treat ratio. This effect is observed in Fig. 4.53, which shows that o-chlorophenol extraction in all cases is nearly the same but larger Treat ratio leads to more rapid extraction in the initial period of the run.

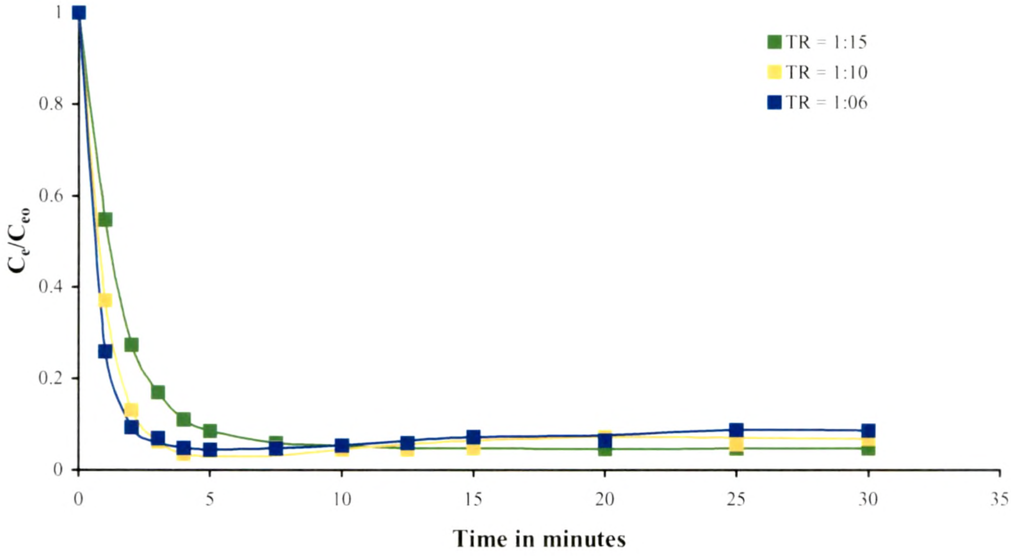

Fig. 4.53: Effect of TR on extraction of 2-chlorophenol at $M = 2$ (N = 155 rpm, ϕ = 0.45, Span 80 = 3%)

4.8.4 *Effect of 2-chlorophenol concentration (C_{eo})*

Fig. 4.54 shows the effect of o-chlorophenol concentration in the continuous phase on the nature of extraction. In all these runs membrane formulation was the standard one used earlier i.e. ϕ = 0.45, C_{io} = 0.3 M, W_{surf} = 3%, TR = 1:15 and N = 155 rpm. It is seen in Fig. 4.54 that with C_{eo} = 95 mg/dm^3, although M = 12.25 the removal of o-chlorophenol is 84 %. Increasing C_{eo} progressively decreases the molar ratios in view of the constant C_{io} values but there is corresponding increase in removal of chlorophenol. It would be erroneous to generalize this behavior that increase in M causes a decrease in % removal of the solute.

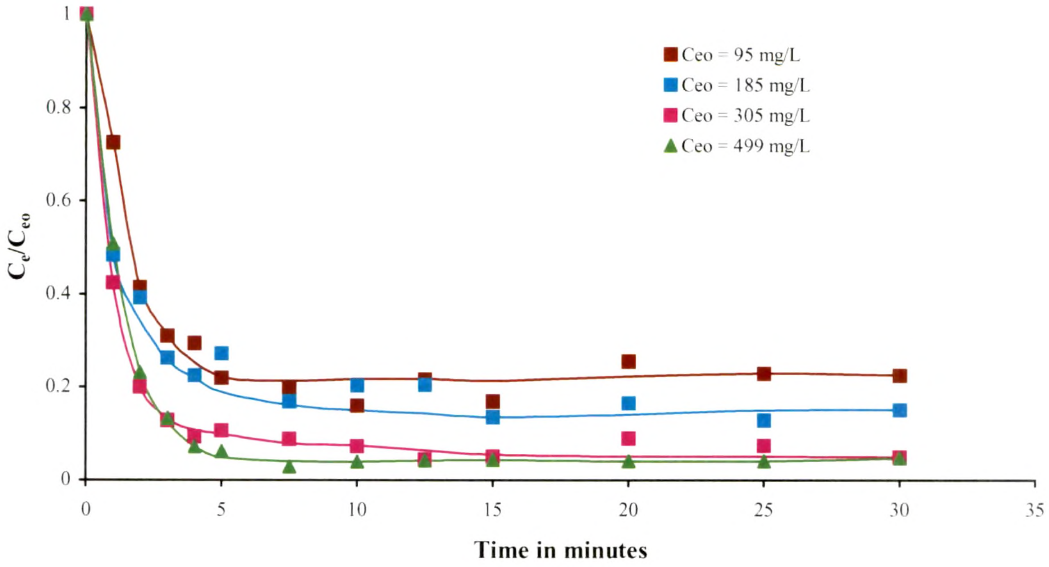

Fig. 4.54: Effect of initial 2-chlorophenol concentration on extraction (N = 155 rpm, $\phi = 0.45$, Span 80 = 3%, $C_{io} = 0.3M$ TR = 1:15)

Lower recoveries at low C_{eo} values are observed because of the rapid depletion of the solute concentration in the external phase resulting in lack of driving force to push the solute inside the globules. The data below gives an assessment of the runs with C_{eo} variation.

C_{eo} mg/dm^3	*M*	C_e mg/dm^3	% Recovery 2-chlorophenol	% utilization NaOH
95.3	12.25	15.29	83.97	6.85
185	6.314	23.92	87.07	13.78
305.4	3.825	13.65	95.53	24.97
498.5	2.343	14.06	97.18	41.46

It is apparent from the above data that one cannot expect to extract below a certain residual solute concentration C_e, in single stage extraction. This is understandable in terms of lack of driving force and the membrane morphology. In single stage systems, once the ELMs extracts the solute the peripheral internal drops inside the globules get saturated. Further extraction is possible only when solutes diffuse deeper inside the globules, which is possible when large driving forces are present. If extraction were carried out in more than one stage using fresh emulsion in each stage, inspite of low concentrations in the second and subsequent stages, large driving force coupled with short diffusion path lengths would lead to greater removals. However, this necessitates the optimization of various process and system parameters and requires to be taken up for further investigation.

4.9 FEATURES OF EMULSION SWELLING AND BREAKAGE

Emulsion swelling and breakage/ leakage are inevitable in ELM separations. Emulsion breakage has a deleterious effect on ELM separations and requires to be addressed before commercialization of the ELM technique. It is necessary to formulate ELMs and select operational conditions such that breakage/leakage is minimized if not totally eliminated. Aspects of emulsion swelling and emulsion leakage were discussed in literature survey in Section 4.6 and 4.7 respectively.

In order to get a better understanding of the process of swelling and emulsion breakage/leakage, it is necessary to quantify these two processes. A tracer technique could be conveniently used to quantify breakage/leakage while swelling could be measured by accounting for the change in emulsion volume or emulsion density. Change in inner droplet sizes of the W/O emulsion could also be a measure of the emulsion swelling. Ramaseder *et al.* (1993) discussed the advantages and shortcomings of the various methods to quantify emulsion swelling and breakage.

4.9.1 Swelling of emulsions

In this Study, the emulsion swelling was measured after each run. The influence of various parameters on swelling are listed in Table 4.10. The data reported were with reference to the standard emulsion formulation and operating conditions that include the following when not specifically varied:- $\phi = 0.45$, $C_{io} = 0.3$ M, $W_{surf} = 3$ % (wt), Treat ratio = 1:15, N = 155 rpm and $C_{eo} \approx 500$ mg/dm^3. Swelling is expressed as % swelling that is defined as % swelling = $(\Delta V_{em}/ V_{em0}) \times 100$. Swelling was measured for standard emulsion configuration also with respect to time.

Time in minutes	5	10	20	30
% Swelling	0.5	5	7.5	10

Table 4.9 Effect of various parameters on emulsion swelling

$\phi = 0.45$, $W_{surf} = 3\%$ $C_{io} = 0.3$ M TR = 1: 15		N = 155 rpm $\phi = 0.45$ $C_{io} = 0.3$ M, TR = 1: 15		N = 155 rpm $\phi = 0.45$ $W_{surf} = 3\%$ $C_{io} = 0.3$ M		N =155 rpm $W_{surf} = 3\%$ $C_{io} = 0.3$ M TR = 1: 15	
N (rpm)	% Swelling	W_{surf} (wt %)	% Swelling	Treat ratio	% Swelling	ϕ	% Swelling
135	5	1	- ve	20:1	6.66	0.4	10
155	10	2	- ve	15:1	10	0.5	10
185	22.5	3	10	10:1	11.66	0.6	10
200	30	4.7	12.5	7.5:1	15	0.625	5
		7.5	30	6:1	20	0.69	0

Data shows that swelling is linear with time. Swelling is often a prelude to drop breakage. Due to swelling the internal size distribution changes and the droplets grow in size. This behavior was observed by measuring the internal drop size of emulsion before and after the extraction run using Malvern 2000 particle size analyzer. It was found that the internal drop size d_{32} increased from 3.998 μm to 7.11 μm as a consequence of swelling.

Due to swelling the interfacial film of surfactant molecules has to expand more and more over the water droplets resulting in a decrease in its density and compactness. The interfacial film that acts as a barrier against the internal phase droplet coalescence will now no longer be immune against droplet coalescence and hence rate of coalescence will be higher. If this process continues the dispersed phase will separate and emulsion will break. Such behavior is observed in Fig. 4.55.

In the course of investigations on emulsion swelling some unique features that were observed are:

- Swelling is independent of the solutes extracted, at least in the concentration range of the experiments in this work.
- There was no emulsion swelling when Acrylate resin 505 surfactant was used for emulsion preparation in spite of the fact that up to 1 M NaOH solution was used in the inner phase.
- There was no swelling observed when W/O emulsion with internal phase fraction $\phi = 0.69$ was used.

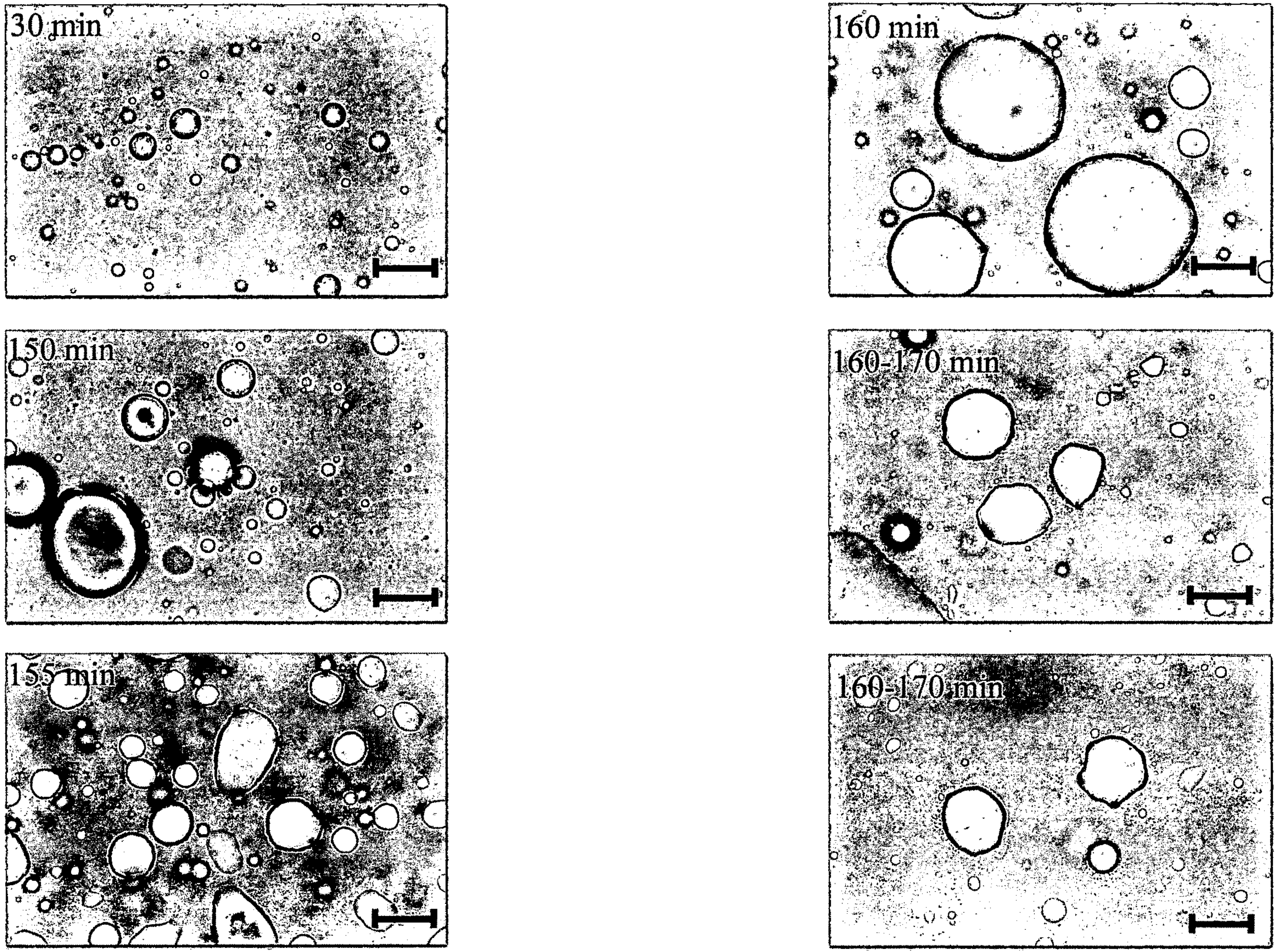

Fig. 4.55: Photomicrographs showing the morphological change of W/O emulsion with time.
(Ø= 0.45, Span 80=3%, Cio=0.3M, Bar = 10 µm)

- There is significant increase in swelling with increase in Span 80 concentration.

4.9.2 Emulsion breakage / leakage

Emulsion breakage was studied using tracer technique. The tracer chosen was lithium hydroxide, selection of this tracer was based on the consideration that lithium is not present in water and lithium hydroxide had similar properties like that of sodium hydroxide with respect to emulsion stability.

Emulsions were prepared using kerosene as membrane phase containing 3 % (wt) Span 80, LiOH concentration in the inner phase was 0.5 M, internal phase volume fraction ϕ was 0.45. The emulsions were dispersed in water at stirring speeds of 155 rpm and the Treat ratio was maintained at 1:15. Effects of stirring speed, surfactant concentration and internal phase volume fraction were studied. Effect of redispersion was also studied by allowing the emulsion to settle after sample withdrawal by stopping the agitation and again starting the agitation to redisperse the emulsion.

Assessment of the breakage was done using material balance with the basis that if the emulsion completely broke down and all the lithium present in the internal phase of the emulsion was down loaded in the continuous external phase, the concentration of lithium in the external phase would be 91 mg/dm^3. Table 4.11 presents the relevant data on emulsion breakage as studied by tracer technique.

Table 4.11 Effect of parametric variations on emulsion breakage

Time in minutes	Parametric variations					
	ϕ variation			N variation	W_{surf} Variation	Redispersion ($\phi = 0.45$ N = 155 rpm, $W_{surf} = 3$ %)
	0.45	0.50	0.60	185 rpm	1 % (wt)	
	(N = 155 rpm, $W_{surf} = 3$ %)			($\phi = 0.45$, $W_{surf} = 3$ %)	(N = 185 rpm $\phi = 0.45$)	
	% Breakage of emulsion					
5	0.44	2.1	4.08	1.32	2.09	1.87
10	0.55	2.1	4.08	2.20	2.75	1.98
15	0.77	2.6	4.08	3.52	4.07	2.53
20	1.1	2.8	6.0	4.84	5.28	3.19
25	1.43	2.8	6.0	5.06	7.82	4.07
30	2.09	4.2	6.0	7.15	7.82	4.62

Analyzing the data presented in Table 4.11 the following can be inferred.

- Higher stirring speeds lead to greater emulsion breakage.
- Increase in the surfactant concentration stabilizes the ELM hence breakage is considerably reduced.
- Increase in ϕ leads to an increase in emulsion breakage that appears to be rather discrete and not continual.
- Redispersion leads to a progressive increase in emulsion breakage.
- Minimum breakage is observed in the standard emulsion formulation.

Emulsions prepared with 3 % (wt) acrylate surfactant instead of Span 80 under other wise identical conditions registered a breakage of 13% in the first 5 minutes that remained constant throughout the duration of the run.

4.9.3 Some aspects of emulsion stability

Emulsions are essentially unstable constructs that are stabilized by the use of surfactants. The aspects of emulsion breakage discussed in Section 4.9.2 are essentially with respect to emulsion globule breakage under agitated conditions. In the absence of stirred environments also emulsions tend to split up to their constituent phases. Splitting of emulsions is inevitable in view of their inherent instability. What is actually of interest is how long an emulsion would sustain itself. There are certain environmental factors, which actually tend to accelerate the emulsion splitting process. One such factor is the presence of a strong electrolyte like NaOH inside the inner phase of the W/O emulsion.

Since NaOH solution was used in the inner phase of the W/O emulsions that were used as ELMs in all the solute extractions discussed earlier, it is necessary to be alert to the unstable behavior of such emulsions. This resulted in gathering of substantial amount of data from which some very interesting aspects of ELMs could be inferred. It is observed that the emulsions split with clockwork precision. In fact, the efficacy of an emulsion could be judged with its time taken to split up.

The data gathered for the time of splitting of emulsion with various parameters when analyzed critically revealed that it all related to the amount of NaOH present in the inner phase. Fig. 4.56 shows the time taken by emulsions to split versus NaOH concentration in the internal phase of the emulsion having ϕ = 0.45 and Span 80 concentration of 3 %(wt). This curve shows an exponential nature, where small increase in NaOH concentration leads to sharp decrease in emulsion stability.

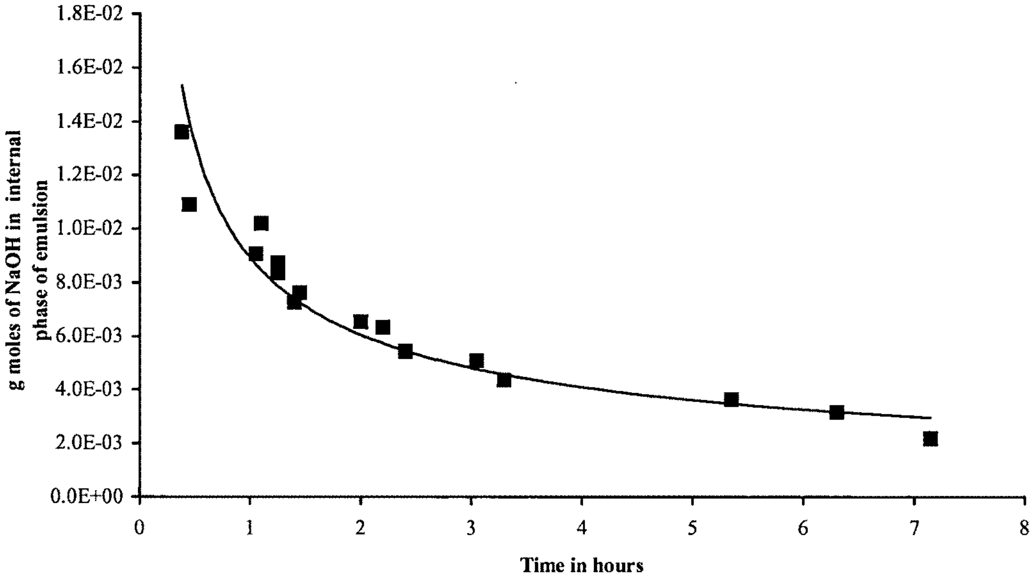

Fig. 4.56: Effect of internal phase reagent concentration on emulsion stability

A very interesting consequence observed of this behavior was the relatively longer stability of emulsions used in the extraction runs vis-à-vis those that were of the same lot but were not used for extraction. The emulsion introduced in the system for extraction depleted a substantial part of its NaOH content and hence remained stable for longer period of time, while the other fraction of the lot split up quickly because of its larger NaOH content.

Increase in surfactant concentration leads to greater longevity of emulsions. Fig. 4.57 shows the stability behavior of emulsion having ϕ =0.5 as a function of surfactant concentrations. It is seen that with increase in surfactant concentration the emulsion becomes stable for longer period of time.

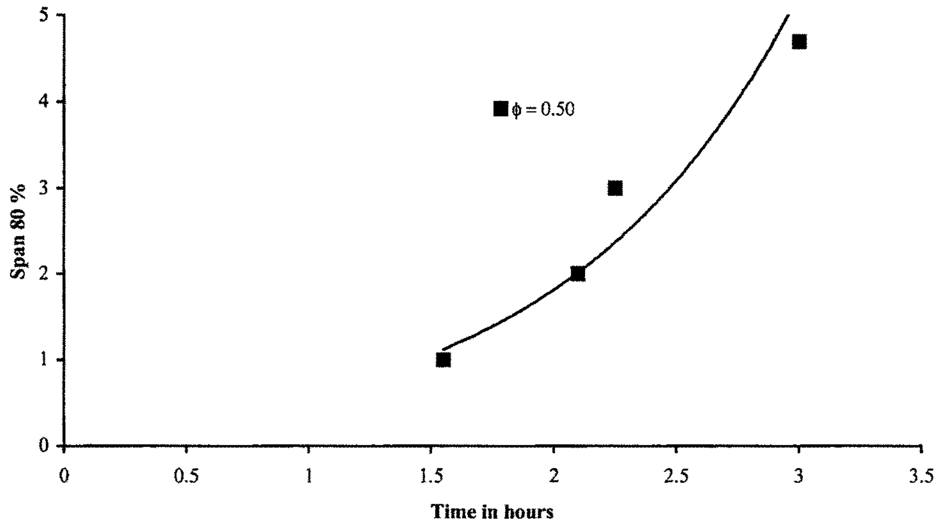

Fig. 4.57: Effect of surfactant concentration on emulsion stability

Fig. 4.55 shows the morphological changes that take place in the internal phase droplet behavior with time. Increase in the internal drop size with time due to drop coalescence is observed. Thinning of surfactant films prior to drop rupture is observed in these photomicrographs and all these events take place just before splitting of the emulsion.

4.10 AN INTEGRAL VIEW OF SEPARATION OF PHENOLS

Extraction of the four phenols from their aqueous solutions using ELMs revealed many points of similarities and also differences between the extraction behaviors of these solutes. Since extraction of phenol is typical representative of Type I transport mechanism, an integrated view of these extractions could be formulated to be applicable to all Type I transport.

In all the experiments performed with the four solutes, it was noticed that the amount extracted with time varied considerably when any of the following four parameters varied. These parameters were the emulsion parameters, ϕ and $C_{io,}$ and the operational parameters, Treat ratio and C_{eo}. Effects of these variations were reported for all the solutes in Sections 4.6 to 4.9. Critical analysis of these parameters reveal that variation of any one of these parameters amounts to variation in the molar ratio of

NaOH/solute i.e. change in the extraction capacity of the ELMs. Hence, it was inferred that the molar ratio *M* was the dominant parameter influencing the extraction behavior of emulsions.

Comparison of the extraction behavior of the four phenols would make sense only when the extracting capacities of the emulsions were the same. Hence, comparison between the four solutes were made at molar ratio $M = 2$. Data at $M = 2$ was available for extractions other than phenol. Therefore, experimental data were generated at $M = 2$ under different sets of conditions i.e. with variation in ϕ, TR and $C_{eo.}$ These data was utilized for comparison with other solutes. The comparative results are presented and discussed below:

4.10.1 Effect of ϕ on extraction of phenols at $M = 2$

Fig. 4.58 shows the extraction behavior of solutes at the standard operating conditions i.e. with emulsions with $\phi = 0.45$ and $C_{io} = 0.3$ M, $W_{surf} = 3$ %(wt), TR = 1:15, $C_{eo} \approx$ 500 mg/dm^3 and N = 155 rpm. This figure sets the base line for comparisons between the solutes, when the extracting capacities of the ELMs are held constant by maintaining molar ratio $M = 2$.

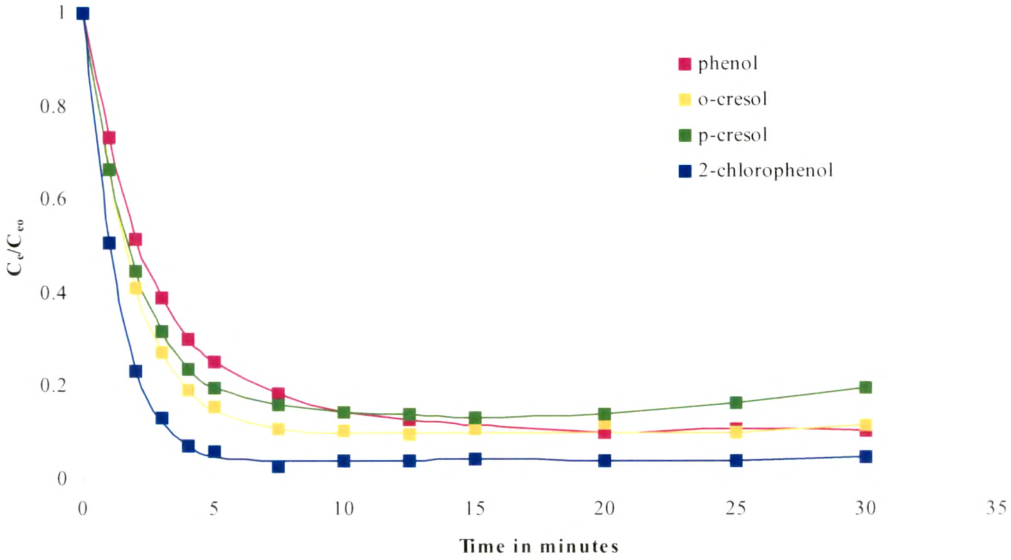

Fig. 4.58: Comparative extraction of phenols

(N = 155 rpm, $\phi = 0.45$, Span 80 = 3%, $C_{io} = 0.3$M TR = 1:15)

The standard configuration results in $M = 2$ for o-cresol and p-cresol. For the other two solutes in order to maintain $M = 2$ the C_{io} values require to be suitably altered. Thus, for phenol with standard ELM configuration to get M = 2 the $C_{io} = 0.351$ M and for 2-chlorophenol the $C_{io} = 0.257$ M. These values are with reference to $C_{eo} = 500$ mg/dm^3. In case there is some fluctuation in C_{eo} values the C_{io} can be appropriately modified to get $M = 2$ for all cases.

In order to assess the influence of ϕ on extraction of phenols with ELMs having identical extraction capacity, the molar ratio was maintained at $M = 2$ by varying the C_{io} values appropriately. For all these cases the ELMs were made with kerosene containing 3 %(wt) Span 80, TR = 1:15, N = 155 rpm, and the external phase concentration of the phenols were about 500 mg/dm^3.

The results are presented in Figs.4.59 (a) to (d) for cases of $\phi = 0.45$, $\phi = 0.5$, $\phi = 0.6$ and for $\phi = 0.69$ respectively. It is interesting to compare Fig. 4.58 with Fig. 4.59 (a) both are for $\phi = 0.45$. In Fig. 4.58, it is found that the phenol curve eventually merges with o-cresol curve and one could conclude that extent of extraction in both cases are the same but then one requires to note that the molar ratio $M = 2$ for o-cresol while it is $M = 1.70$ for phenol.

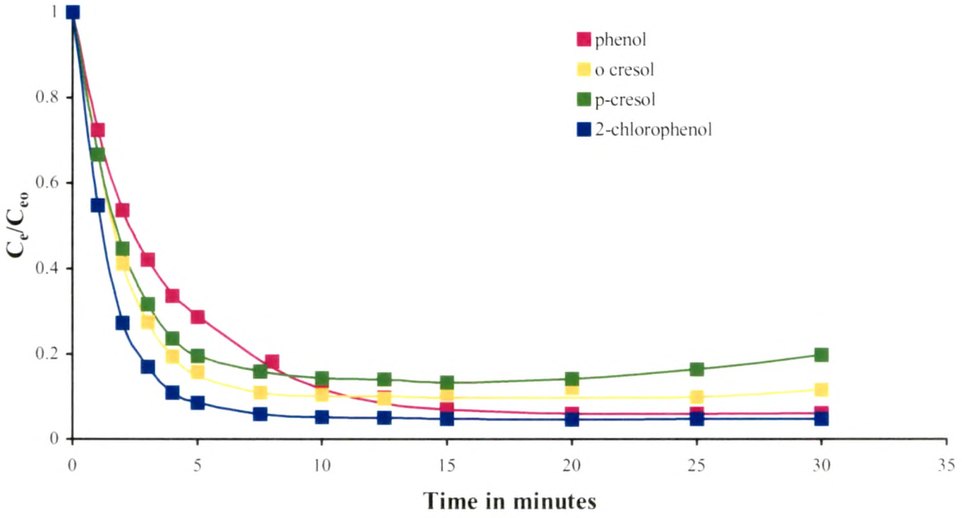

Fig. 4.59 (a) Effect of ϕ on extraction of phenols at $M = 2$

(N = 155 rpm, $\phi = 0.45$, Span 80 = 3%, $C_{io} = 0.3$M TR = 1:15)

Solute	$K_a \times 10^{10}$ 25°C
phenol	1.1
o-cresol	0.63
p-cresol	0.67
2-chorophenol	77

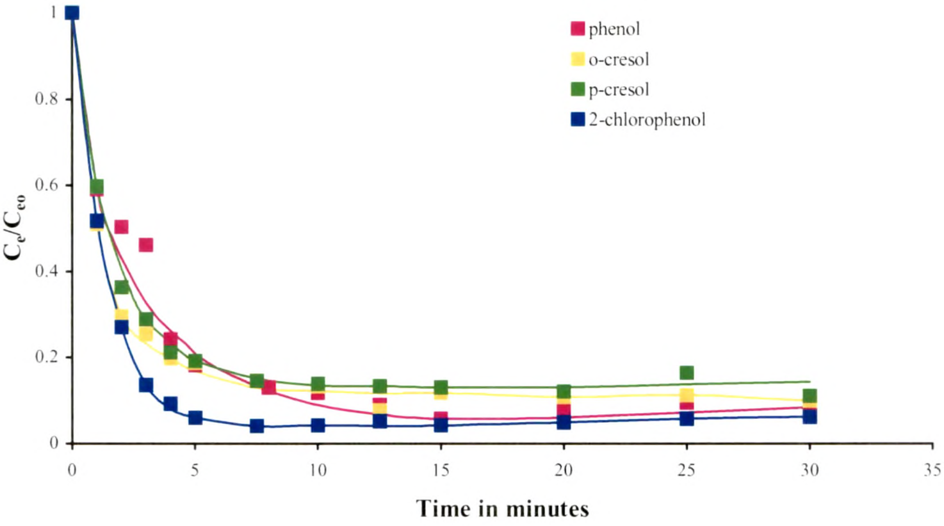

Fig. 4.59 (b) Effect of ϕ on extraction of phenols at $M = 2$

(N = 155 rpm, ϕ = 0.5, Span 80 = 3%, C_{io} = 0.3M TR = 1:15)

In Fig. 4.59 (a) the pattern is changed when extraction curves for all solutes are plotted at *M* = 2. It is found that the phenol curve now crosses the curve for o-cresol and almost merges with the 2–chlorophenol curve after 20 minutes of extraction. Comparison of the extraction rates of phenol and cresol indicate that cresol is extracted more rapidly than phenol in the early stages of the experiment because the distribution coefficient K for cresol is much larger than that for phenol. However, at later stages, the degree of extraction of phenol is higher because of its larger acid dissociation constant, K_a. On the same lines it is observed that for 2-chlorophenol the distribution coefficient K is largest among all the solutes studied and the acid dissociation constant, K_a is also the largest, this results in the 2-chlorophenol extraction curve displaying not only the largest rate of extraction but also the largest extent of extraction. On similar lines one can reason the nature of o-cresol and p-cresol curves. o-Cresol having larger value of K in comparison with p-cresol showed greater extent of extraction.

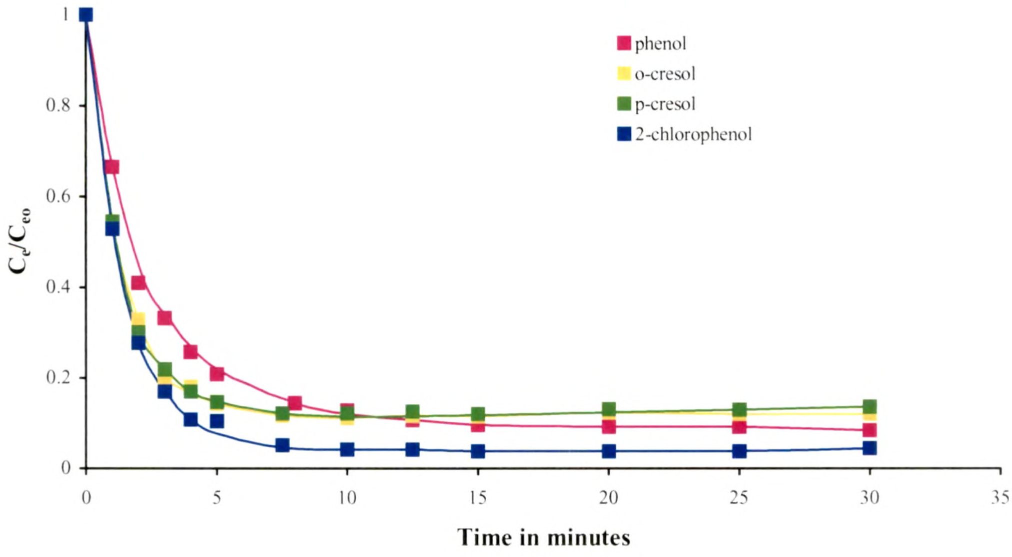

Fig. 4.59 (c) Effect of ϕ on extraction of phenols at *M* = 2

(N = 155 rpm, ϕ = 0.6, Span 80 = 3%, C_{io} = 0.3M TR = 1:15)

Comparing extraction curves for solutes at *M* = 2 and various ϕ,it is found that the behavior becomes even more intriguing. When ϕ = 0.5, the resolution of individual curves in the initial period of the run vanishes, the two cresol curves come quite close and phenol curve intersects the cresol curve at lower sampling times. Each solute also registers greater extent of extraction at all time scales. One possible explanation of this behavior is that with increased ϕ, at each spherical plane within globules more number of internal droplets are encountered and hence more rapid extraction occurred for all cases this led to merger of o-cresol and 2-chlorophenol curves in earlier stages, o-cresol and p-cresol curves at later stages and phenol intersection with cresol curves at shorter time spans.

Further increase in ϕ to 0.6 led to complete merger of the cresol curves. There is considerable reduction in the gap between cresols and 2-chlorophenol. There is also a distinct shift of the phenol curve from cresol curves that results in a late intersection of these curves at about 12 minutes. The amount of phenol extracted appeares to decline with increasing ϕ and the curve for phenol moved away from 2-chlorophenol. This behavior possibly results from the fact that increasing ϕ also results in a decline in C_{io}. Therefore, to get converted, the solute has to move deep within the globules causing a slow down in extraction rates and also the amount extracted at specified time interval. A close look at the phenol profile in Fig. 4.59 (c) indicates that phenol curve has not reached plateau at 30 minutes.

Fig. 4.59 (d) represents the situation when $\phi = 0.69$. It is observed that phenol passes below p-cresol through out the time span of the extraction run.

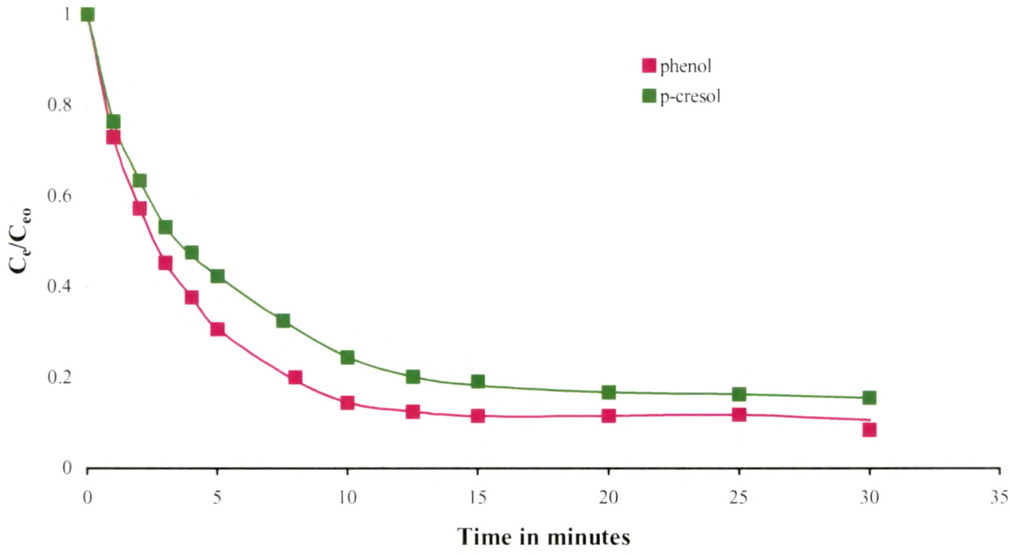

Fig. 4.59 (d) Effect of ϕ on extraction of phenols

(N = 155 rpm, Span 80 = 3%, C_{io} = 0.3M TR = 1:15)

The extraction rate and the extent of extraction of p-cresol get substantially reduced, while the rate of extraction gets reduced for phenol. In the absence of a very convincing argument to rationalize such reversal of behavior one could forward the following reasons that may have caused the change.

- Decline in kerosene phase. p-cresol has substantially larger distribution coefficient K in comparison to phenol that helps in the initial stages of the run but increase in ϕ reduces that advantage.
- Reduction of C_{io} in order to maintain $M = 2$, required relatively deep penetration of solutes inside globules.
- Further changes in membrane morphology that lead to formation of larger size internal drops cause a decline in the internal area of drops. Changes in the dispersion behavior on account of increase in interfacial tension and viscosity,

causes formation of larger globule sizes. Hence it results in an overall decline in mass transfer area.

4.10.2 Effect of Treat ratio on extraction of phenols at M = 2

Increase in the Treat ratio, while maintaining constant molar ratio *M*, should lead to an increase in the rates of solute extraction, without any significant increase in the extent of separation. Since, adding more amount emulsion to the system lead to formation of more globules ,hence results in an increase in surface area.

This behavior is observed in Fig. 4.59 (a) and Fig. 4.60 (a) to (c) where it is found that increase in Treat ratios progressively from 1:20 to 1:6 increases the rates of extraction of all solutes. However, the relative increases in rates are not identical. Comparing the Figs 4.59 (a) and 4.62 (a) to (c) one finds that the relative increase in rates of phenol extraction is less than that observed for cresol extraction. This is largely due to the favorable distribution coefficient for cresol in comparison with phenol. It can be observed in all the figures that extent of extraction of phenol is more than cresols due to reasons discussed earlier.

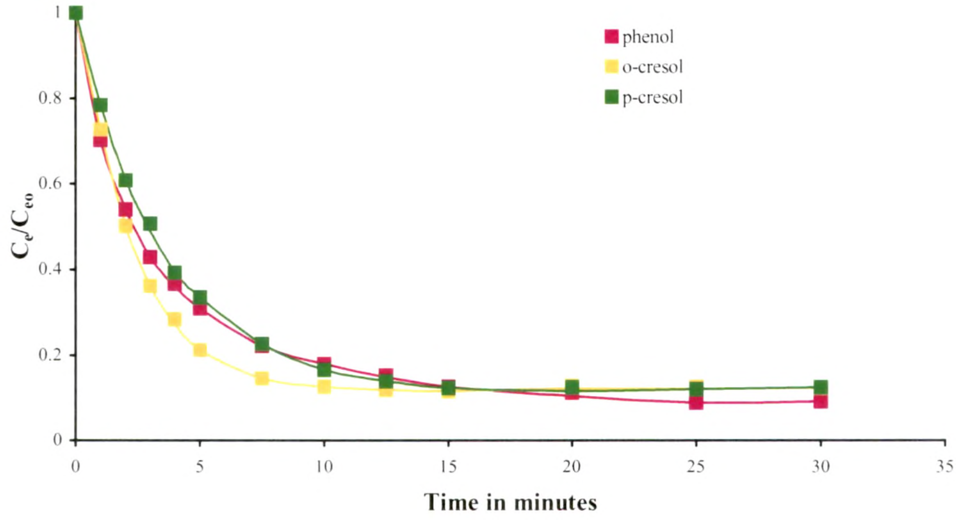

Fig.4.60 (a): Effect of TR on extraction of phenols at *M* = 2

(N = 155 rpm, ϕ = 0.45, Span 80 = 3%, TR = 1:20)

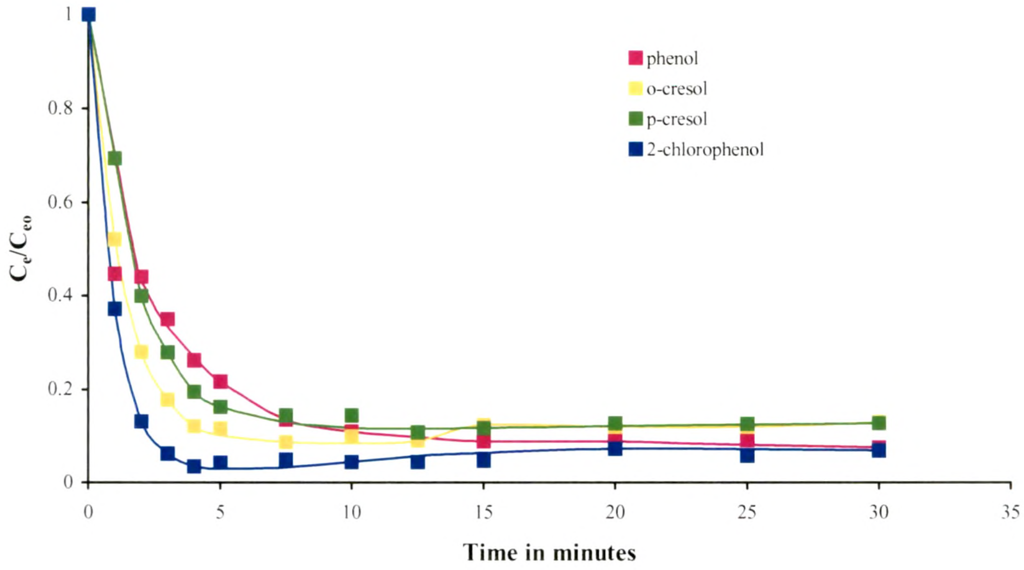

Fig.4.60 (b) Effect of TR on extraction of phenols at *M* = 2

(N = 155 rpm, ϕ = 0.45, Span 80 = 3%, TR = 1:10)

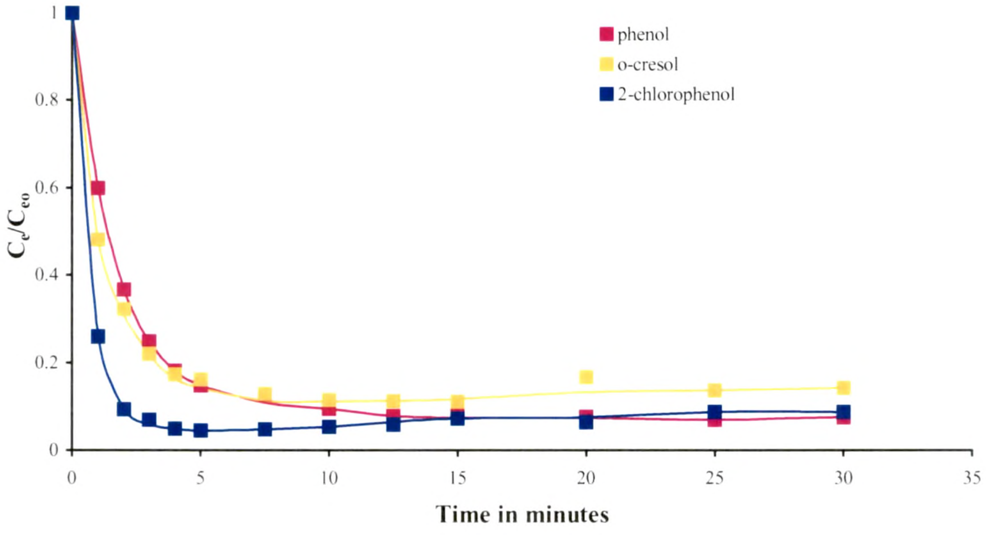

Fig.4.60 (c) Effect of TR on extraction of phenols at *M* = 2

(N = 155 rpm, ϕ = 0.45, Span 80 = 3%, TR = 1:6)

Behavior of 2-chlorophenol is a class apart. The very large distribution coefficient of 2-chlorophenol coupled with very large acid dissociation constant K_a makes its removal almost quantitative. Experience with 2-chlorophenol extractions brings in the realization that the distribution coefficient after the molar ratio is the most dominant parameter. The ELMs almost behave as a 2-chlorophenol sink that is evident from all the extraction curves of 2-chlorophenol. The increase in treat ratio also leads to a further increase in 2-chlorophenol extracted due to increase in the organic content in the system. The rates of extraction also increase because of an increase in the mass transfer surface area.

There is strong evidence of globule breakage when Treat ratios are large, particularly for TR = 1:10 and TR = 1:6, but that is expected in view of the increased ELM globule number density which would cause greater collision between globules.

4.10.3 Effect of C_{eo} on extraction of phenols at $M = 2$.

At constant molar ratio the effect of any change in extraction pattern due to a change in initial solute concentration C_{eo} is mostly a manifestation of the influence that distribution coefficient exercises on the extraction. Some times the influence of diffusion of solutes within the membranes also comes to play, particularly so at high solute concentrations.

These effects are seen when Fig 4.59 (a) is compared with Fig. 4.61 (a) and (b). Focusing on the phenol extraction curves in these Figs. it is observed that with increase in phenol concentration from 400 mg/dm^3 (Fig.4.62 (a)) to 500 mg/dm^3 (Fig. 4.59(a)) there is significant increase in initial rates that appears to be driven by distribution coefficients. Further increase in phenol concentration to 600 mg/dm^3 does not significantly change the rates, but there is a definite decrease in the rates of extraction when phenol concentration is further increased to 800 mg/dm^3 as seen in Fig 4.61 (b). Such decrease in rates is caused by two factors 1). Relative increase in C_{io} (0.56 M) causes a corresponding increase in globule sizes also internal drop sizes as discussed in Section 4.3 causing an overall decrease in mass transfer surface area hence the rates of mass transfer. 2) The necessity of phenol to penetrate deeper inside the globules to get entrapped within droplets because of rapid saturation of the peripheral layer of internal drops.

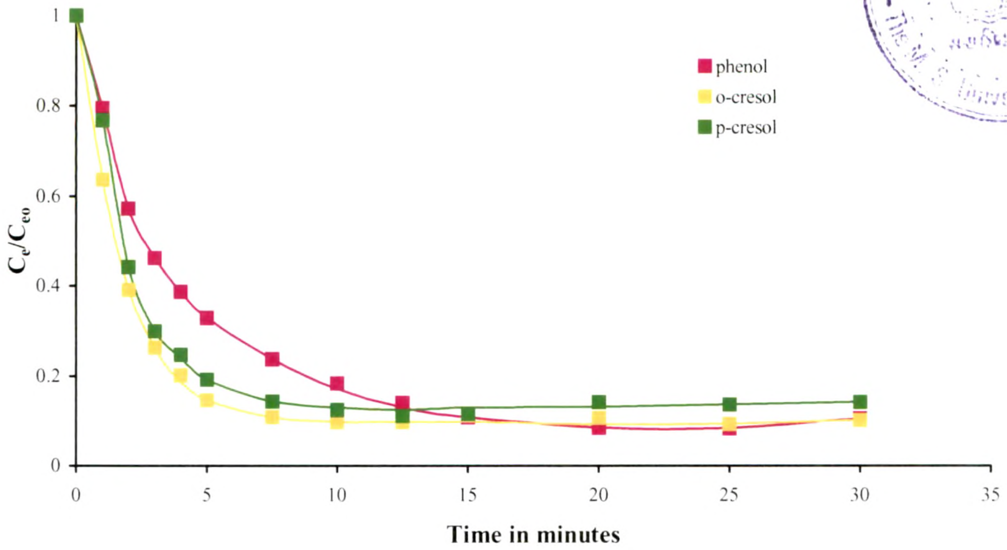

Fig. 4.61(a): Effect of initial concentration of phenols on extraction at *M* = 2 (N = 155 rpm, ϕ = 0.45, Span 80 = 3%, TR = 1:15, Ceo = 400mg/dm^3)

In the case of cresol extractions because of favorable distribution coefficients no significant change is noticed with change in C_{eo} at *M* = 2, except for the case of p-cresol in Fig. 4.61 (b) where at 800 mg/dm^3 concentration there is slight decline in noted which could be attributed to the reasons stated above.

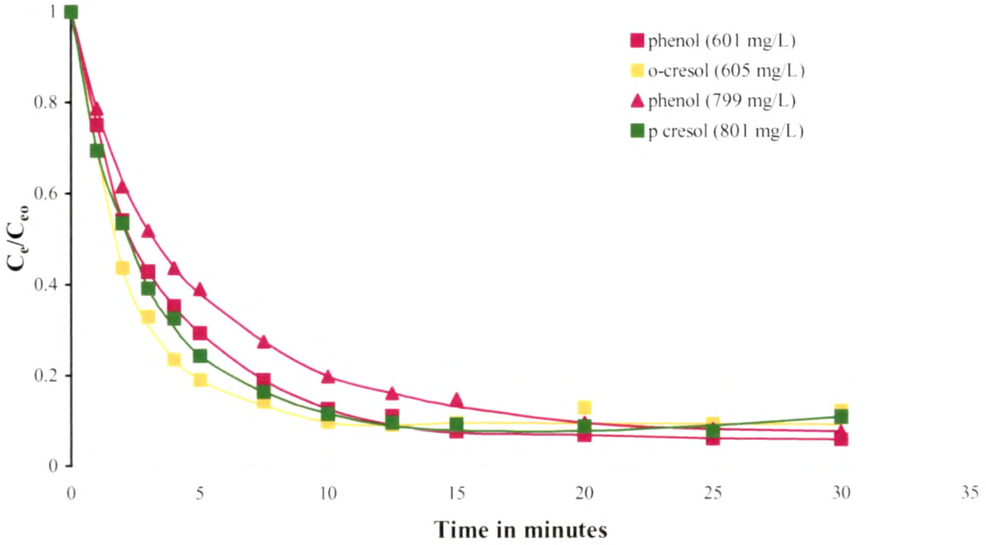

Fig. 4.61(b) Effect of initial concentration of phenols on extraction at *M* = 2 (N = 155 rpm, ϕ = 0.45, Span 80 = 3%, TR = 1:15, Ceo = 600mg/dm^3 ,800mg/dm^3)

It can be concluded that for Type I separations, the dominant parameters are the molar ratio M and distribution coefficient of solute between membrane and water phase. Maximization of these two parameters would certainly be very effective in removal of solutes. Stage operations may turn out to be an economic and effective way of removing even trace amount of solutes. Insight into the dynamics of separation could be gained with the use of properly characterized membranes. Therefore, one can sum up that the W/O emulsion is the key to ELM separations.